CAPITAL UNIVERSITY OF SCIENCE AND TECHNOLOGY, ISLAMABAD

Combating Antimicrobial Resistance: Design, Synthesis and Characterization of Fluoroquinolone Derivatives

by

Waqar Ahmad

A thesis submitted in partial fulfillment for the degree of Master of Philosophy

in the

Faculty of Pharmacy
Department of Pharmaceutical Chemistry

2026

CERTIFICATE OF APPROVAL

Combating Antimicrobial Resistance: Design, Synthesis and Characterization of Fluoroquinolone Derivatives

by

Waqar Ahmad

(MPH241002)

THESIS EXAMINING COMMITTEE

S. No.	Examiner	Name	Organization
(a)	External Examiner	Dr. Munir Ullah Khan	Iqra Uni., Islamabad
(b)	Internal Examiner	Dr. Reem	CUST, Islamabad

Dr. Siraj Khan
Thesis Supervisor
April, 2026

Dr. Reem
Head
Dept. of Pharmaceutical Chemistry
April, 2026

Dr. Muzaffar Abbas
Dean
Faculty of Pharmacy
April, 2026

Author's Declaration

I, **Waqar Ahmad** hereby state that my MPhil thesis titled "**Combating Antimicrobial Resistance: Design, Synthesis and Characterization of Fluoroquinolone Derivatives**" is my own work and has not been submitted previously by me for taking any degree from Capital University of Science and Technology, Islamabad or anywhere else in the country/abroad.

At any time if my statement is found to be incorrect even after my graduation, the University has the right to withdraw my MPhil Degree.

(Waqar Ahmad)

Registration No: MPH241002

Plagiarism Undertaking

I solemnly declare that research work presented in this thesis titled "**Combating Antimicrobial Resistance: Design, Synthesis and Characterization of Fluoroquinolone Derivatives**" is solely my research work with no significant contribution from any other person. Small contribution/help wherever taken has been duly acknowledged and that complete thesis has been written by me.

I understand the zero tolerance policy of the HEC and Capital University of Science and Technology towards plagiarism. Therefore, I as an author of the above titled thesis declare that no portion of my thesis has been plagiarized and any material used as reference is properly referred/cited.

I undertake that if I am found guilty of any formal plagiarism in the above titled thesis even after award of MPhil Degree, the University reserves the right to withdraw/revoke my MPhil degree and that HEC and the University have the right to publish my name on the HEC/University website on which names of students are placed who submitted plagiarized work.

(Waqar Ahmad)
Registration No: MPH241002

Acknowledgement

In the name of **Allah**, the most gracious and the most merciful; and prayers and peace be upon **Muhammad**, His servant and messenger. First and foremost, I would like to acknowledge my limitless thanks to **Allah Almighty** and to his last **Prophet Muhammad (S.A.W)**. Without their guidance, this work would never have been completed. I owe deep gratitude to our University, **Capital University of Science & Technology (CUST)**, for giving me the opportunity to complete this work. Special thanks to **Dean Dr. Muzaffar Abbas** for his encouragement throughout the entire process.

I would like to acknowledge and am very grateful to my **Supervisor Dr. Siraj Khan**, who has been generous during all phases of the research and for all the valuable lessons that I learned during this period; I thank him from the bottom of my heart.

Finally, I want to express my heartfelt gratitude to my **family**, especially **my parents**, who have provided me with generous support throughout my life and especially in conducting my research. Because of their unconditional love, support, and prayers, I have completed this thesis.

(Waqar Ahmad)

Abstract

Fluoroquinolone is an important class of antibiotics, and ciprofloxacin is a representative drug with broad antibacterial activity. This study aimed to design and synthesize novel ciprofloxacin derivatives (CW1-CW5). The antimicrobial potential of the derivatives was evaluated using experimental, and *in silico* approaches. These compounds were characterized using thin-layer chromatography (TLC) and Fourier-transform infrared (FTIR) spectroscopy to confirm their chemical structures.

FTIR confirmed the characteristic peaks of hydroxyl group (3000 cm^{-1} 3300 cm^{-1}), amide carbonyl group (1650 cm^{-1} 1750 cm^{-1}), and -CH stretching (2800 cm-1 3300 cm^{-1}), which validated the successful incorporation of pharmacophores. Molecular docking studies of OmpF, Topoisomerase II, and a multidrug efflux pump revealed stronger binding affinities for the synthesized derivatives than ciprofloxacin. The docking scores of the synthesized compounds against OmpF (-8.8 to -9.8 kcal/mol), topoisomerase II (-8.5 to -10.3 kcal/mol), and multidrug efflux pump (-8.0 to -10.0 kcal/mol) were higher than those of the standard ciprofloxacin. However, CW3 showed the highest binding affinity against multiple targets. SwissADME analysis revealed satisfactory drug-likeness and physicochemical properties for most compounds, with moderate lipophilicity (iLogP 2.64-3.66) and TPSA values ranging from 94.88 $Å^2$ to 175.21 $Å^2$. Toxicity prediction by ProTox-II 3.0 classified the compounds into GHS toxicity cclasses4 and c, with predicted LD50 values ranging from 4000 to 4336 mg/kg, representing low to moderate acute toxicity.

The synthesized compounds exhibited notable antibacterial activity against non-resistant bacterial strains, with zones of inhibition ranging from 19.70 ± 1.98 mm to 31.51 ± 1.34 mm against *E. coli*. Among the derivatives, CW5 demonstrated strong activity against *B. subtilis* (37.16 ± 1.78 mm), while CW3 showed the highest inhibition against *S. abony* (33.25 ± 0.95 mm). The antibacterial activity against *P. aeruginosa* was comparatively lower across all compounds.

Furthermore, evaluation against resistant bacterial strains revealed that the synthesized derivatives retained significant antibacterial activity, with several compounds demonstrating comparable or superior efficacy relative to ciprofloxacin. In particular, CW5 exhibited the highest activity across resistant strains, followed by CW3 and CW1. In addition, antifungal activity assessed by the disk diffusion method against *C. albicans, A. niger*, and *A. flavus* showed no observable zones of inhibition, indicating a lack of antifungal potential under the tested conditions.

In conclusion, this study demonstrates that structural modification of the ciprofloxacin scaffold significantly influences molecular binding affinity, drug-likeness, and antibacterial activity in a compound-dependent manner. The synthesized derivatives exhibited variable efficacy, with CW5 showing superior and consistent antibacterial activity against both non-resistant and resistant bacterial strains, while CW3 displayed strong binding affinity in molecular docking studies, supporting its potential as a lead compound. Importantly, several derivatives exhibited comparable or enhanced activity relative to ciprofloxacin against resistant strains, highlighting their potential in combating antimicrobial resistance. The combined synthetic, in silico, and biological findings suggest that these derivatives provide valuable lead structures for further optimization toward the development of effective antibacterial agents against resistant pathogens.

Keywords: Ciprofloxacin derivatives, Fluoroquinolones, Antibacterial activity, Molecular docking, SwissADME, Toxicity prediction, Anti-microbial resistance

Contents

List of Figures

List of Tables

Abbreviations

AMR	Antimicrobial Resistance
ADME	Absorption, Distribution, Metabolism, and Excretion
AUC	Area Under the Curve
CADD	Computer-Aided Drug Design
CW	Ciprofloxacin with
DCM	Dichloromethane
DNA	Deoxyribonucleic Acid
DMSO	Dimethyl Sulfoxide
FTIR	Fourier Transform Infrared Spectroscopy
GHS	Globally Harmonized System
KI	Potassium Iodide
LBDD	Ligand-Based Drug Design
MD	Molecular Dynamics
MIC	Minimum Inhibitory Concentration
PMQR	Plasmid-Mediated Quinolone Resistance
QSAR	Quantitative Structure Activity Relationship
QRDR	Quinolone Resistance-Determining Region
SAR	Structure Activity Relationship
SBDD	Structure-Based Drug Design
SD	Standard Deviation
TEA	Triethylamine
TLC	Thin-Layer Chromatography
WHO	World Health Organization
ZOI	Zone of Inhibition

Chapter 1

Introduction

1.1 Background

The global evolution of antibiotic therapy in the 20th century was a revolutionary advancement in the treatment of infectious diseases. Infections that consistently lead to death or lifelong disability are now frequently treated, resulting in notable advances in surgery, cancer therapy, and intensive care medicine. However, in the early 21^{st} century, antimicrobial resistance (AMR) appeared as a new calamity. The World Health Organization (WHO) projects that by 2050, there will be 10 million casualties annually [1, 2]. Multidrug - resistant bacteria are becoming common in community and hospital settings, undermining the efficacy of medications and placing a significant burden on healthcare systems [3].

The synthetic fluoroquinolone class of antibiotics has led to the development of antibacterial treatments. Fluoroquinolones emerged from nalidixic acid, which was established in 1962; This drug was enhanced by adding a fluorine atom at the C-6 site and a piperazinyl moiety at the C-7 position of the quinolone core, thereby improving their antimicrobial activity and pharmacokinetic properties [4, 5]. Ciprofloxacin, a revolutionary drug of the fluoroquinolone class, is widely used for urinary tract infections, respiratory infections, gastrointestinal infections, soft tissue infections, and prophylaxis in high-risk patients [6]. Its broad spectrum,

good oral bioavailability, and favorable tissue distribution make it the preferred choice for clinicians worldwide [7].

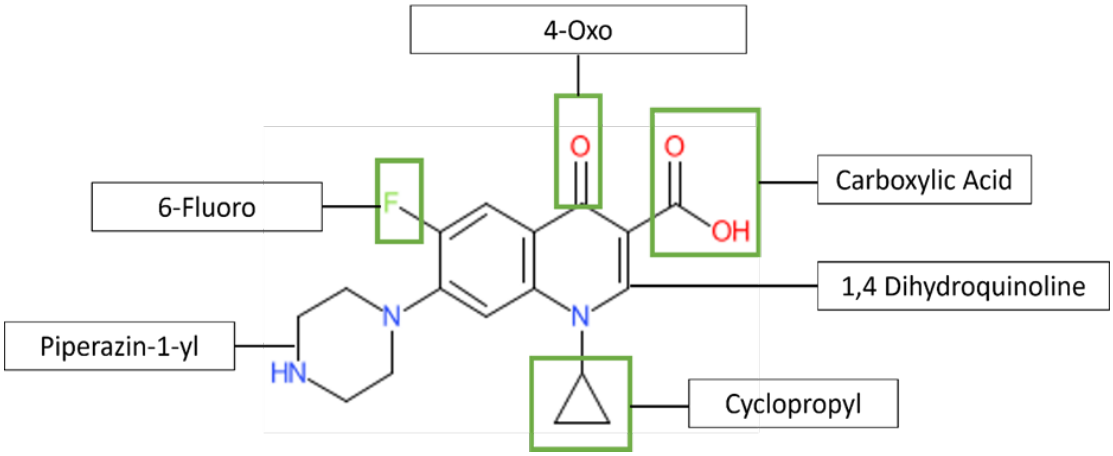

FIGURE 1.1: Chemical structure of ciprofloxacin

Ciprofloxacin has well-defined and highly flexible chemical structure. The addition of a fluorine atom at C-6 increases lipophilicity and cellular penetration, whereas the piperazine ring at the C-7 position makes it a broad-spectrum drug and improves gram-negative activity. The keto group at the C-4 position, together with the carboxylic acid at the C-3 site, coordinates with Mg^{2+} and facilitates enzyme interaction [8, 9]. The structural profile of ciprofloxacin allows it to stabilize the cleavage complex formed by bacterial topoisomerase IV and DNA gyrase. This action blocks the reannealing of DNA strands, causing double-strand breaks and rapidly triggering bacterial cell death [10, 11].

However, the success of ciprofloxacin has contributed to the current challenge; the widespread and sometimes non-selective use of fluoroquinolones has put notable pressure on bacterial populations [12]. Consequently, resistance to ciprofloxacin has emerged and increased significantly. Studies have shown that resistance rates among clinical isolates of *Escherichia coli* (*E. coli*) vary from 30% to 60% in specific settings [13]. Bacteria evade ciprofloxacin in various ways; alterations in the quinolone resistance determining region (QRDR) of the gyrA and parC genes decrease drug binding. Overexpression of efflux systems (e.g., AcrAB-TolC in *E. coli* and MexAB-OprM in *Pseudomonas aeruginosa*) lowers intracellular drug concentrations [14, 15]. Changes in outer membrane porins limit drug entry,

whereas plasmid-mediated quinolone resistance (PMQR) elements, such as *qnr* genes and *aac(6')-Ib-cr*, enable the horizontal distribution of resistant traits [16]. These mechanisms significantly weaken the effectiveness of ciprofloxacin and limit its empirical use.

The presence of a piperazine moiety at the C-7 position allows chemical derivatization to decrease efflux susceptibility, improve enzyme binding, and enhance pharmacokinetic properties [17]. Despite dual-site modification approaches that alter both the C-3 and C-7 positions within the same molecule, they may yield synergistic benefits in antibacterial activity [18, 19]. Furthermore, computer-aided drug design (CADD) tools, including molecular docking, pharmacophore modeling, and molecular dynamics simulations, provide crucial predictive insights [20]. A gap persists between *in silico* design and experimental synthesis. Many compounds predicted to be promising remain unpublished or unevaluated in biological systems, and few studies have comprehensively correlated structure-activity relationships (SAR) with resistance-modulating outcomes [21].

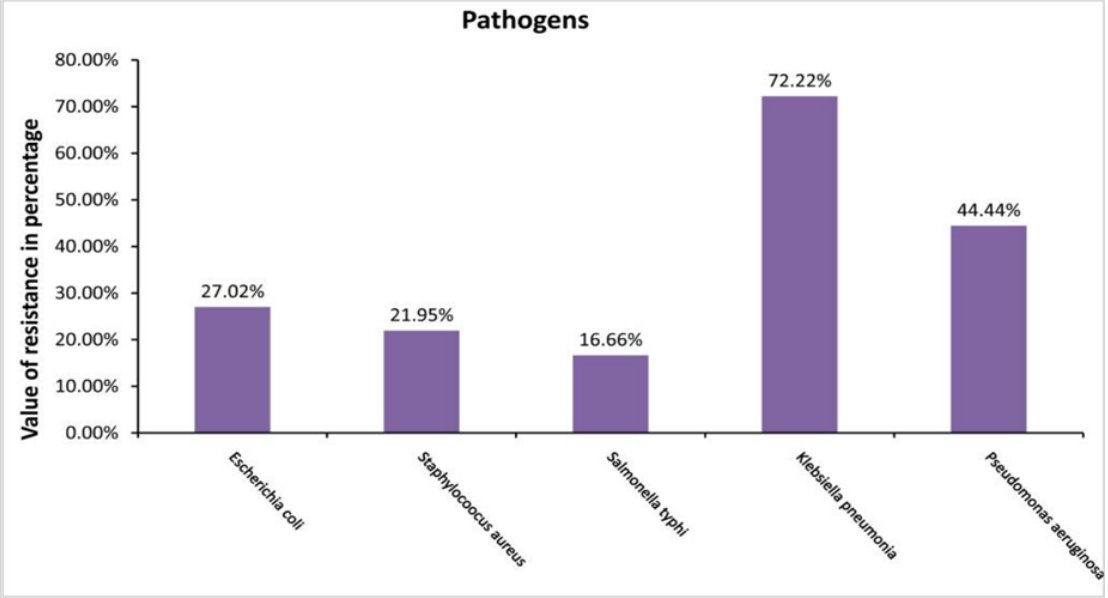

FIGURE 1.2: Trends in ciprofloxacin resistance

Source: Reproduced from [22]

In addition to antimicrobial and resistance dimensions, the pharmacokinetic and pharmacodynamic properties of ciprofloxacin must be considered. For instance,

clinical efficacy correlates strongly with the C_{max}/MIC and AUC/MIC ratios, and suboptimal dosing can foster resistance rather than suppress it [23]. Additionally, pressure of sub-therapeutic dosing and over-the-counter antibiotic use aggravate AMR and reduce the efficacy of established drugs [24, 25]. This emphasizes the necessity for advanced and targeted strategies that extend beyond the discovery of novel antibiotics. As a substitute, designing more potent derivatives of existing compounds, such as ciprofloxacin, offers a faster and more cost-effective solution.

1.2 Research Gap

Despite the abundance of ciprofloxacin derivatives, there is a need for structurally improved compounds with better antibacterial efficacy against resistant bacterial strains. Although many studies have documented single-site modifications of ciprofloxacin, they are frequently limited in scope and mostly concentrate on synthesis and initial antibacterial screening. Most investigations lack comprehensive structural characterization, molecular docking with *in silico* drug-likeness and toxicity evaluation, and comparison with conventional ciprofloxacin. Furthermore, the study did not properly examine the structural alterations at established modification sites and potentially helpful functional groups. These drawbacks highlight the need for carefully planned ciprofloxacin derivatives that are synthesized, comprehensively described, and evaluated using computational and experimental techniques to better understand their antibacterial potential.

1.3 Rationale of the Study

Owing to its chemical flexibility, ciprofloxacin serves as a suitable scaffold for structural modifications, particularly at functionally important sites, such as the C-7 piperazine moiety, influencing pharmacokinetics and antibacterial activity. This study aimed to design, synthesize, and evaluate novel ciprofloxacin derivatives using integrated experimental and *in silico* approaches to better understand the structure-activity relationships and contribute to ongoing efforts to overcome antimicrobial infections.

1.4 Aim and Objectives

1.4.1 Aim

The main goal of the present study was to design, synthesize, characterize, and evaluate ciprofloxacin derivatives to enhance their antibacterial efficacy against gram-negative and gram-positive bacterial strains.

1.4.2 Objectives

i. Novel ciprofloxacin derivatives were synthesized by modifying the C-7 piperazine group.

ii. The synthesized derivatives were purified by recrystallization and column chromatography.

iii. The synthesized derivatives were characterized using spectroscopic techniques.

iv. *In silico* studies of synthesized derivatives targeting bacterial proteins.

v. Evaluation of the antimicrobial potential of the synthesized derivatives against gram-negative and gram-positive bacterial strains.

Chapter 2

Review of Literature

2.1 Historical Development and Evolution of Fluoroquinolones

The evolution of fluoroquinolones is intrinsically linked to the scientific goal of overcoming bacterial resistance. In 1962, nalidixic acid was discovered as a synthetic alternative to target bacterial DNA replication mechanisms following the emergence of antimicrobial resistance to β-lactams and aminoglycosides [26, 27]. Nalidixic acid, a byproduct of chloroquine production, marked the beginning of quinolone class antibiotics. It has selective efficacy against gram-negative bacteria, particularly *E. coli* and Proteus species, by inhibiting DNA gyrase, an enzyme required for supercoiling and maintaining the bacterial DNA structure [28]. However, its limited tissue distribution, rapid development of resistance, and narrow antibacterial range limit its therapeutic applicability, necessitating further structural improvements [29].

Fluorine substitution at the C-6 position and alteration of the C-7 piperazine ring in the 1980s resulted in the discovery of fluoroquinolones, which marked a significant advance in antibiotic therapy [4]. These alterations improve lipophilicity, bacterial cell penetration, and the antibacterial spectrum against both gram-positive and gram-negative bacteria [30]. The resultant compounds, including

norfloxacin, ciprofloxacin, and ofloxacin, are second-generation quinolones with increased potency, good pharmacokinetics, and enhanced therapeutic characteristics [31]. Ciprofloxacin has emerged as the most effective agent, primarily because of its high activity against *P. aeruginosa*, *S. aureus*, and *E. Coli* species, as well as its good tissue distribution and oral absorption [32]. Structural changes have been made to combat the increasing resistance and pharmacological challenges. Third-generation fluoroquinolones, such as levofloxacin and sparfloxacin, are more effective against gram-positive bacteria, including Streptococcus pneumoniae [33, 34]. Fourth-generation antibiotics, such as moxifloxacin and gemifloxacin, have shown superior efficacy against anaerobes and atypical respiratory infections [35]. Each subsequent generation has been guided by an improved understanding of the structure-activity relationship (SAR) of the fluoroquinolone core, indicating that small alterations in key molecular regions can drastically affect pharmacological effects [5, 36].

The effectiveness of ciprofloxacin has led to the optimization of the quinolone framework to augment target affinity, enhance stability, and diminish toxicity. Researchers have discovered that changes to the C-3 carboxylic acid group influence cooperation with magnesium ions and enzyme-DNA interactions [8]. In contrast, C-7 substituents affect the bacterial spectrum and efflux susceptibility [37].

For example, adding bulky heterocyclic groups at C-7 reduces efflux pump recognition while increasing intracellular retention [38]. Similarly, substitution at the N-1 position with aromatic or heteroaromatic moieties improved the action against gram-positive organisms while decreasing resistance [39].

Despite these advances, fluoroquinolone resistance has spread rapidly in clinical practice owing to misuse and bacterial adaptation. Early-generation drugs, such as ciprofloxacin, were originally highly effective but were gradually limited by mutations in the *gyrA* and *parC* genes, as well as plasmid-mediated mechanisms that protect topoisomerases [40, 41]. These advances have driven the scientific community to use CADD and rational drug design methodologies to prevent resistance through *in silico* optimization before laboratory synthesis [42].

The evolution of fluoroquinolones not only demonstrates the synthetic creativity of medicinal chemists but also highlights the constant conflict between bacterial resistance and medication innovation [43]. Each generation of fluoroquinolones has increased our understanding of how molecular modifications can improve pharmacological efficacy.

The present strategy of combining computational design, synthesis, and biological testing continues this trend, especially focusing on ciprofloxacin derivatives with dual-site alterations to overcome resistance while maintaining safety and effectiveness [44, 45].

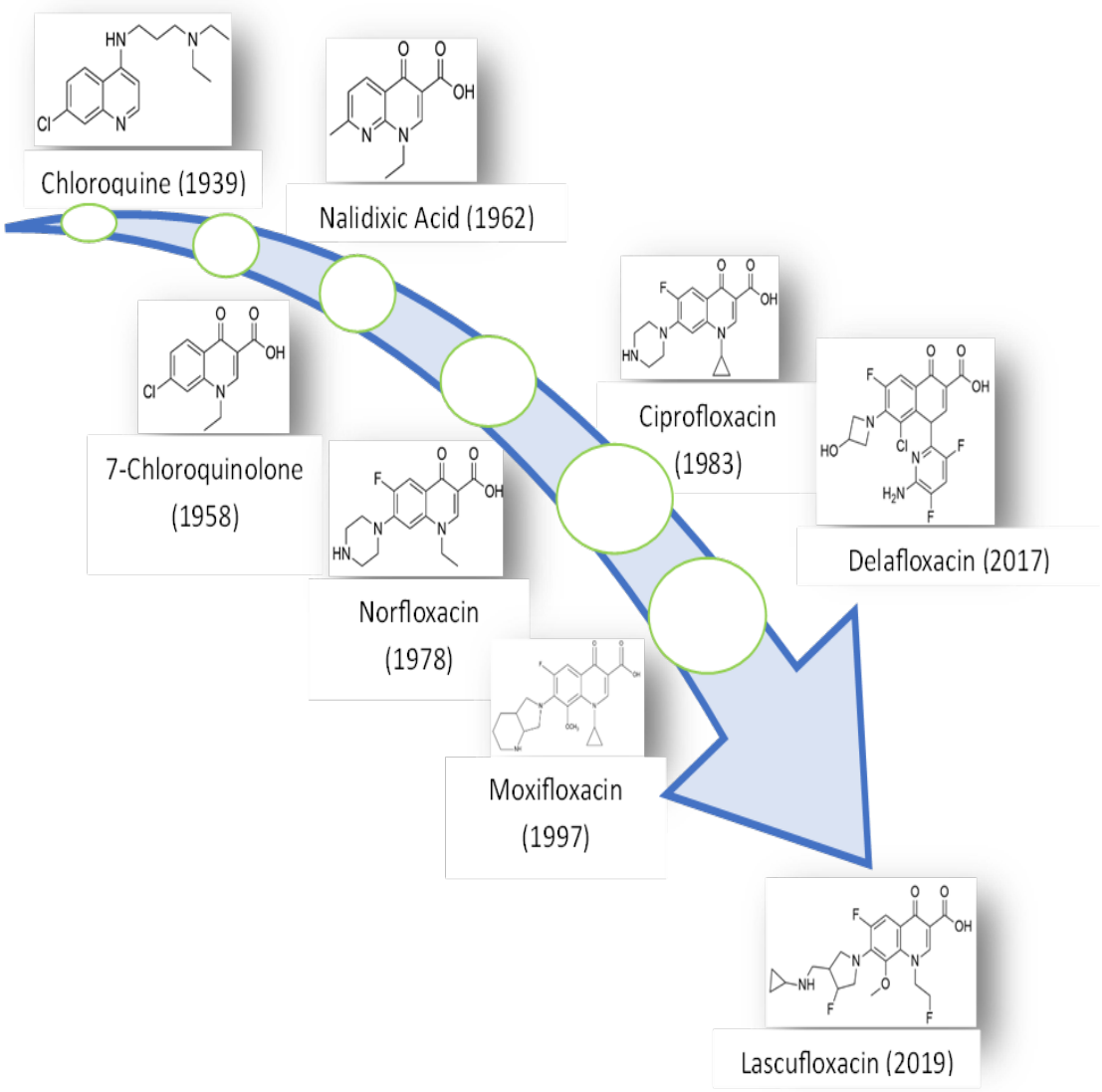

FIGURE 2.1: Evolution of fluoroquinolones from nalidixic acid to modern derivatives

2.2 Antimicrobial Resistance

AMR has become a major health crisis in the 21st century, threatening the efficacy of nearly all major classes of antibiotics. AMR refers to the ability of microorganisms, particularly bacteria, to survive exposure to antimicrobial agents that would normally inhibit or kill them [25]. The growing incidence of resistant infections causes serious clinical challenges, leading to higher treatment costs, prolonged hospital stays, and increased mortality [46].

According to the Global Research on Antimicrobial Resistance (GRAM) report, resistant bacterial infections were responsible for approximately 1.27 million deaths worldwide in 2019, and this estimate suggests that the number could rise to 10 million by 2050 if the current trends continue [47]. These alarming patterns highlight the need for innovative drug discovery approaches and targeted structural modifications of existing antibiotics to combat AMR.

The primary mechanisms that initiate AMR include genetic mutations, horizontal gene transfer, and enzymatic degradation of antibiotics. These actions lead to reduced drug permeability, enhanced efflux, and alterations in target binding sites [48]. The misuse or overuse of antibiotics in clinical settings further accelerates the spread of resistant strains [49]. Multidrug-resistant (MDR) pathogens, such as *P. aeruginosa*, *Klebsiella pneumoniae*, *Acinetobacter baumannii*, and methicillin-resistant Staphylococcus aureus (MRSA), have been recognized by the WHO as critical or high-priority organisms for new drug development. The urgent need for effective antibacterial agents that can target these resistant pathogens has renewed the scientific focus on fluoroquinolones, a class of synthetic agents that once served as a cornerstone in the management of bacterial infections [50, 51].

Fluoroquinolones mainly work by blocking the topoisomerase IV and DNA gyrase bacterial enzymes which are required for DNA replication and supercoiling. This dual mode of action makes it effective against both gram-negative and gram-positive bacteria [51–53]. However, during the last few decades, the widespread use of fluoroquinolones has led to growing resistance, particularly to ciprofloxacin, one of the most commonly prescribed members of this class. Resistance is caused

by alterations in the activation of efflux pumps, quinolone resistance-determining regions (QRDRs) of *gyrA* and *parC*, and plasmid-mediated mechanisms that shield bacterial topoisomerases from inhibition [51, 54]. These multifaceted resistance routes have severely reduced the clinical utility of ciprofloxacin, necessitating the exploration of new derivatives with enhanced efficacy.

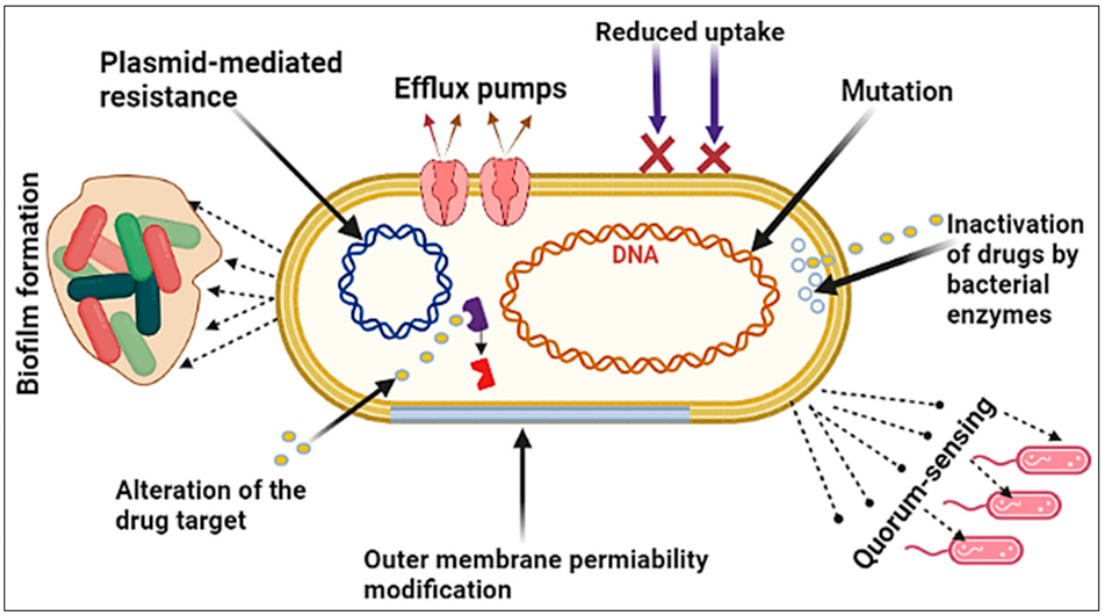

FIGURE 2.2: Different mechanisms of antimicrobial resistance

Source: Reproduced from [55]

Ciprofloxacin is an ideal candidate for structural alterations because of its well-versed pharmacophore, safety profile, and synthetic flexibility [56]. Modifications of the C-7 piperazine group have been widely explored to enhance antibacterial effectiveness, improve pharmacokinetics, and overcome efflux-mediated resistance [14]. Substituting the piperazine group at the C-7 position with bulky heterocycles or aromatic amines could enhance drug binding and reduce efflux susceptibility [51, 57].

In recent years, researchers have increasingly turned to CADD to predict the effects of structural modifications on binding to target enzymes and to identify potential leads prior to synthesis. Molecular docking and pharmacophore modeling techniques enable the evaluation of novel fluoroquinolone derivatives based on their predicted interactions with DNA *gyrA*se and topoisomerase IV, thereby

accelerating drug development [20, 58]. Studies by [59] and [57] reported that computational modeling of ciprofloxacin analogs effectively identified promising derivatives with enhanced *in vitro* antibacterial activity.

2.3 Chemistry, Pharmacology and Mechanism of Action of Ciprofloxacin

Ciprofloxacin is one of the most clinically important fluoroquinolones and serves as the foundation for current antibacterial chemotherapies. It was developed in the early 1980s as a second-generation fluoroquinolone derived from norfloxacin and represents a significant advancement in potency, pharmacokinetics, and safety [4]. The IUPAC name of ciprofloxacin is 1-cyclopropyl - 6-fluoro-1, 4-dihydro-4-oxo-7-(1-piperazinyl) -3-quinoline carboxylic acid and molecular formula is $C_{17}H_{18}FN_3O_3$ [60]. At C-6 position presence of a fluorine atom enhances cellular penetration and activity against gram-negative organisms. Concurrently, at C-7 site presence of piperazine ring expands the spectrum of activity, especially against *Pseudomonas aeruginosa* and other resistant pathogens [56].

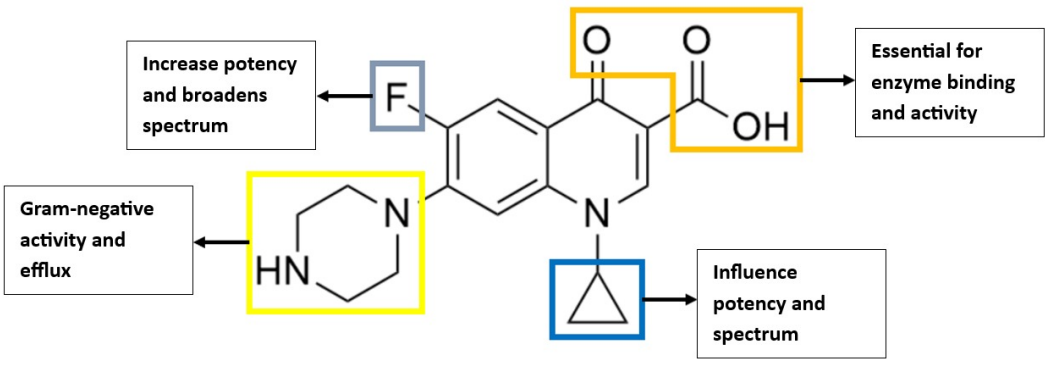

FIGURE 2.3: Key substitution sites in ciprofloxacin structure

The quinolone core of ciprofloxacin has key positions like C-3 and C-4, which are crucial in drug target interactions because they form chelation complexes with magnesium ions [61]. For replication and transcription these enzymes are vital for managing the supercoiling and relaxation of bacterial DNA [8, 39]. The cyclopropyl group at N-1 position improves the antibacterial activity, whereas

piperazine group at C-7 site influences the antibacterial activity, lipophilicity, and efflux resistance [39]. Pharmacologically, by inhibiting type II topoisomerases, specifically DNA *gyrA*se and topoisomerase IV ciprofloxacin exhibits bactericidal activity. Topoisomerase IV handles the decatenation of daughter DNA molecules after replication, whereas DNA gyrase induct negative supercoils into chromosomal DNA, a process vital for replication and gene expression [62, 63]. Ciprofloxacin prevent the re-ligation of DNA strands by stabilizing the DNA cleavage complex formed during these reactions, result in double-stranded DNA breaks, chromosome fragmentation, and ultimately bacterial cell death [64].

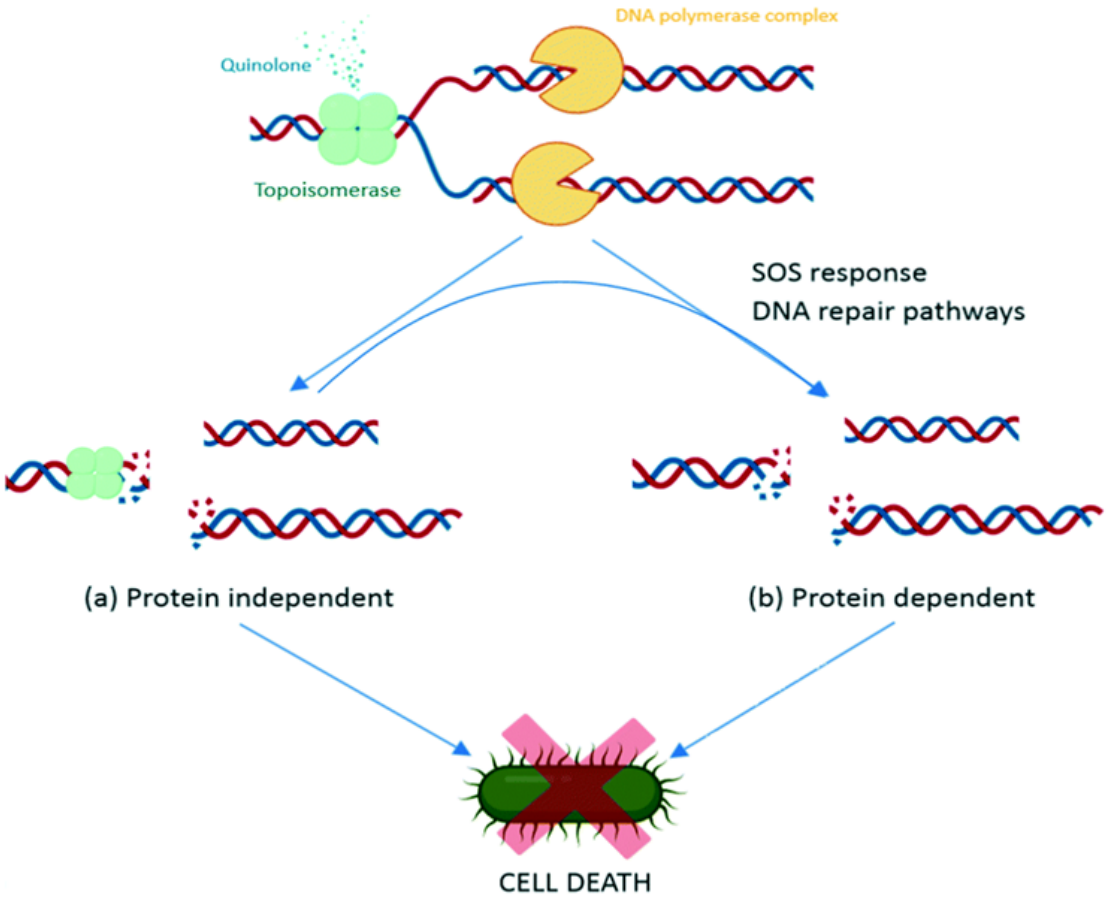

FIGURE 2.4: Ciprofloxacin binding to DNA *gyrA*se and formation of a ternary complex

Source: Reproduced from [31]

Pharmacokinetics of ciprofloxacin exhibit high oral bioavailability (∼70%), rapid absorption, and extensive tissue distribution, reaching therapeutic concentrations in the lungs, kidneys, and the urinary tract [12]. It shows moderate plasma protein

binding (∼30%) and is mainly excreted unchanged in the urine, making it effective for treating urinary tract infections. It short half-life (∼4 hrs) supports twice daily dosing [65]. Hence strong antibacterial properties, good pharmacokinetics, and broad-spectrum activity make ciprofloxacin a valuable antibiotic in clinical practice. However, the rise in resistance has encouraged structural modifications in ciprofloxacin to preserve its effectiveness against multidrug-resistant strains [66].

2.4 Mechanisms of Ciprofloxacin Resistance

Ciprofloxacin is becoming less effective against multi - drug - resistant bacterial strains. Resistance appeared soon after their introduction of ciprofloxacin and has since developed through multiple molecular mechanisms that collectively impair target binding, reduce drug accumulation, and lower overall antibacterial efficacy [52].

These mechanisms can generally be grouped into (i) target-site mutations, (ii) efflux pump activation, (iii) decreased outer membrane permeability, and (iv) plasmid-mediated resistance, all of which often coexist in resistant clinical isolates.

2.4.1 Target Site Mutations

The most common and well-established mechanism of ciprofloxacin resistance includes point mutations in the genes *gyrA* and *gyrB* and *parC* and *parE*. Mutations like these occur within specific amino acid residues known as quinolone resistance-determining regions (QRDRs), which directly interact with ciprofloxacin during enzyme–DNA complex formation [51].

Substitution of serine at position 83 and aspartate at position 87 of *gyrA*, along with similar mutations in *parC*, have been frequently linked to high-level resistance in *E. coli*, *P. aeruginosa*, and *K. pneumoniae* [67].

These alterations lowers the binding affinity of ciprofloxacin to its enzymatic targets, permitting the bacteria to continue DNA replication and repair even when the drug is present [68].

2.4.2 Efflux Pump Overexpression

Efflux pumps a major resistance pathway that actively removes ciprofloxacin from the bacterial cytoplasm, bringing intracellular levels below the therapeutic threshold [69]. The AcrAB-TolC system in *E. coli* and the MexAB - OprM system in *P. aeruginosa* are two of the most extensively researched pumps responsible for fluoroquinolone resistance [70]. Overproduction of these efflux systems not only results in ciprofloxacin resistance, but additionally contributes to multidrug resistance. These systems are regulated by complicated transcriptional regulatory networks, such as the MarA, SoxS, and Rob regulons, which activate in response to environmental stresses and sub-inhibitory drug doses [71].

2.4.3 Reduced Outer Membrane Permeability

Reduced outer membrane permeability is another factor that causes ciprofloxacin resistance, especially in gram-negative bacteria. Changes in porin proteins, such as OmpF and OmpC in *E. coli* and *OprD* in *P. aeruginosa*, decrease ciprofloxacin penetration into bacterial cells [72]. Mutations that inhibit porin expression or produce structural changes efficiently diminish intracellular drug accumulation. In clinical isolates of *K. pneumoniae*, the cumulative impact of porin loss and efflux overexpression has been shown to considerably enhance the MIC values for ciprofloxacin, often exceeding serum levels [73]. These findings emphasize that alterations to the outer membrane and target mutations play an essential role in promoting resistance [74].

2.4.4 Plasmid Mediated Quinolone Resistance

In addition to chromosomal mechanisms, PMQR contributes significantly to the dissemination of ciprofloxacin resistance genes across bacterial populations. The first PMQR determinant, qnrA, was found in *K. pneumoniae* in 1998 [75]. The DNA *gyrA*se and topoisomerase IV from quinolone inhibition are protect by qnr proteins, acting as DNA mimic proteins that prevent drug enzyme binding [76]. Other PMQR mechanisms include acetylation of ciprofloxacin by the *aac(6')-Ib-cr* enzyme and active efflux mediated by plasmid-encoded transporters such as

qepA and *oqxAB* [16]. The coexistence of PMQR genes with β-lactamase or carbapenemase genes on the identical plasmids further accelerates the spread of multidrug resistance through horizontal gene transfer [51].

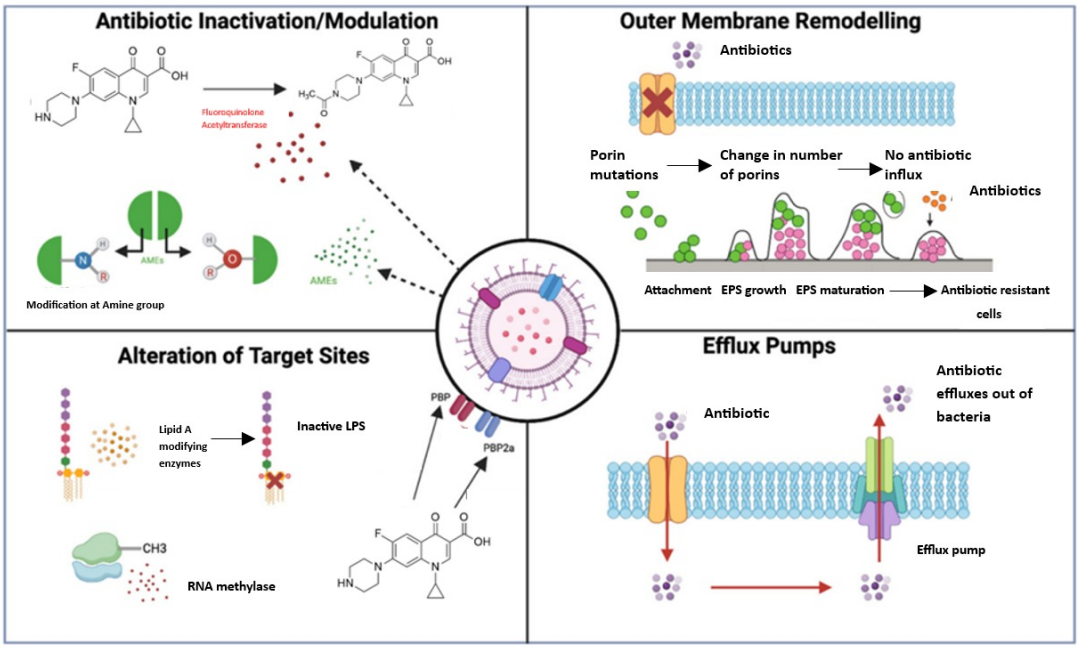

FIGURE 2.5: Combined effects of target modification, efflux, and biofilm formation in conferring high-level ciprofloxacin resistance

Source: Adapted from [77]

2.5 Strategies to Overcome Ciprofloxacin Resistance

2.5.1 Structural Modification of Ciprofloxacin

One of the most widely adopted strategies to overcome resistance involves rational structural modification at key sites of the ciprofloxacin molecule. Studies have identified the C-3 carboxylic acid and C-7 piperazine positions as the most influential for altering the antibacterial spectrum, target affinity, and pharmacokinetic behavior [18]. The C-3 carboxyl and C-4 keto groups form chelation bridges with magnesium ions at the drug DNA enzyme complex, while the C-7 piperazine ring influences bacterial cell penetration and efflux recognition [52, 78]. Substituting

the C-7 piperazine with bulky heterocyclic or aromatic moieties has been shown to enhance lipophilicity, reduce efflux susceptibility, and broaden antibacterial activity [12]. For example, [79] synthesized ciprofloxacin derivatives bearing substituted benzimidazole and triazole groups at the C-7 position, which exhibited improved docking scores against DNA *gyrA*se and enhanced inhibition zones compared to parent ciprofloxacin. In the same way, modifications at the C-3 site, like esterification or amide formation, can improve binding stability by providing electrostatic interactions and additional hydrogen bonding with topoisomerase IV [80].

The addition of electron-withdrawing or hydrophobic groups into the fluoroquinolone scaffold can alter drug permeability and diminish efflux pump recognition. For example, an investigation by [81] found that C-7 modified ciprofloxacin analogues with halogen or nitrogen substituents have improved intracellular retention and bactericidal action against overexpressing *E. coli* bacteria. These findings highlight the necessity of chemical modification in overcoming resistance while retaining critical physiological factors responsible for enzyme inhibition.

2.5.2 Hybrid and Conjugate Design

Hybridization is another promising approach to develop dual-acting compounds by combining ciprofloxacin with other pharmacophores or biologically active scaffolds. Hybrid compounds can target numerous metabolic pathways at once, minimizing the risk of resistance formation [82]. For example, hybrid compounds including ciprofloxacin-Schiff base conjugates and ciprofloxacin azoles have demonstrated exceptional antibacterial and antifungal activity [83]. These compounds combine the fluoroquinolone core with imine or triazole linkers, producing synergistic interactions with bacterial enzymes and cell walls. Metal ciprofloxacin complexes are novel hybrid derivatives. ciprofloxacin bind to transition metals like Cu(II), Zn(II), and Fe(III) using C-3 and C-4 functional groups, resulting in complexes with increased lipophilicity and membrane permeability [84].

Copper ciprofloxacin complexes have been shown to exhibit higher antibacterial activity against *S. aureus* and *P. aeruginosa*, presumably due to increased oxidative stress and improved drug absorption [85]. These type alterations enhance

the antibacterial effectiveness of ciprofloxacin and extend its therapeutic potential and pharmacological properties, such as antioxidant or anticancer effects, thereby expanding its therapeutic potential [86].

2.6 Computer Aided Drug Design in Fluoroquinolone Optimization

Traditional trial-and-error drug development techniques are slow and ineffective in the age of antimicrobial resistance. To solve this challenge, CADD emerged as a significant method in medicinal chemistry, enabling the rational design and optimization of novel antibacterial compounds with superior pharmacological properties.

CADD combines computational chemistry, bioinformatics, and molecular modelling to predict how structural changes influence biological activity, binding affinity, and pharmacokinetics [87]. For fluoroquinolones like ciprofloxacin, CADD serves as an effective tool for identifying structural analogues that overcome resistance while maintaining the important pharmacophoric properties required for enzyme inhibition.

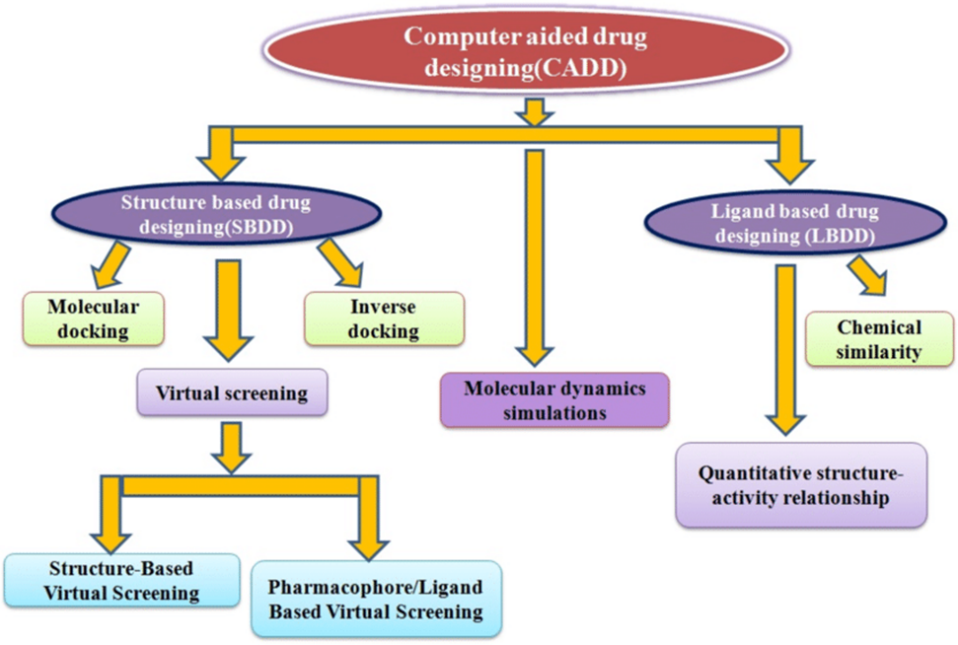

FIGURE 2.6: Overview of the Computer Aided Drug Design workflow

Source: Reproduced from [88]

2.6.1 Structure-Based Drug Design

SBDD simulates how candidate compounds interact at the active site by using high resolution crystallographic data from target enzymes such as bacterial DNA *gyrA*se and topoisomerase IV. These models provide data on the important residues involved in ligand binding, assisting in the rational modification of ciprofloxacin scaffolds [89].

Docking simulations assesses the incorporation of derivatives into the enzyme's active site, estimating binding free energy and identifying significant hydrogen bonds, electrostatic interactions, and hydrophobic contacts [90].

For example, [91] use molecular docking and dynamics simulations to analyse newly synthesized ciprofloxacin triazole derivatives. Their findings showed increased binding stability within the DNA *gyrA*se pocket, which was consistent with computational data and experimental inhibition results. Similarly, recent research using cocrystal structures of *E. coli gyrA* and *gyrB* subunits found unique binding conformations that allow fluoroquinolone analogues to avoid resistance-associated mutations [51, 52].

2.6.2 Ligand-Based Drug Design

When the target protein's 3D structure is either unavailable or only partially determined, LBDD works in combination with SBDD. In LBDD, pharmacophore models that specify structural elements responsible for activity are created by analysing molecular characteristics from well-known active substances including ciprofloxacin, levofloxacin, and moxifloxacin [92].

These characteristics usually consist of hydrophobic areas, aromatic ring cores, and hydrogen bond donors and acceptors. By virtually screening chemical libraries for novel compounds that fit these essential characteristics, pharmacophore modelling enables *in silico* prediction of possible antimicrobial activity [93].

For instance, [94] searched databases for structurally varied analogues with better binding characteristics using a pharmacophore model developed from known fluoroquinolones. The predictive power of the ligand-based technique was confirmed when several hits showed high pharmacophore fit scores and were then verified using docking simulations [95].

2.7 Organic Synthesis and Characterization of Ciprofloxacin Derivatives

The synthesis of new ciprofloxacin derivatives requires a solid foundation in organic synthesis and structural characterization. Altering ciprofloxacin's molecular structure, particularly at the C-7 piperazine position, becomes an effective method to synthesize derivatives with enhanced antimicrobial activity and resistance evasion. The method includes planning the synthetic route, carrying out reactions, purifying the products, and via spectroscopic methods verify structural integrity and purity.

2.7.1 Synthetic Strategy and Reaction Design

Ciprofloxacin contains carboxylic acid, a ketone, an amine, and a fluorine - substituted aromatic ring as functional groups which offer several reactive sites for structural modifications. The most common positions for structural modifications are the C-3, which can be converted into esters or amides, and the C-7, which can be replaced with different aromatic or heterocyclic groups [96, 97].

At C-3 site, reactions typically start by activating the carboxylic acid to an acid chloride via reagents such as, thionyl chloride ($SOCl_2$) or oxalyl chloride. This is followed by nucleophilic substitution with amines or alcohols to produce amide or ester derivatives [98]. This approach facilitates the incorporation of pharmacologically significant groups that can enhance lipophilicity and target affinity. At C-7 site, substitution is commonly done via nucleophilic aromatic substitution or N-alkylation; ciprofloxacin reacts with various alkyl halides, acyl chlorides, or aldehydes under basic conditions [99].

For instance, [100] synthesized ciprofloxacin triazole compounds through click chemistry by coupling azide linked ciprofloxacin intermediates with alkyne bearing heterocycles in the presence of Cu(I) catalysts. This reaction exhibited regioselectivity and also improved yield and purity. Similarly, [101] synthesized amide linked ciprofloxacin compounds by utilizing chloroacetyl chloride and substituted amines, showing enhanced antibacterial efficacy against multidrug resistant strains.

2.7.2 Purification and Isolation Techniques

Upon synthesizing ciprofloxacin derivatives, the reaction mixture often comprises unreacted starting materials, intermediates, and undesirable byproducts. Consequently, purification is crucial for isolating the target chemicals in a pure form appropriate for structural investigation and biological testing. TLC, recrystallization, and column chromatography are common purification techniques that offer unique benefits for reaching high purity.

2.7.2.1 Thin Layer Chromatography

TLC is primarily employed as a fast, efficient analytical method for monitoring reaction progress and determining product purity. In this technique, a tiny sample is placed on a TLC plate covered with a thin covering of silica gel, which acts as the stationary phase. The plate is then placed in a developing chamber with the suitable solvent system. varying compounds travel at varying speeds as the solvent goes up the plate due to capillary action, depending on their polarity and affinity to the stationary phase. Each spot's position is specified by an Rf (retention factor), which gives comparative data on compound identity and polarity [102]. TLC is thus an important tool for validating reaction completeness and selecting appropriate solvent systems for column chromatography.

2.7.2.2 Recrystallization

Recrystallization is a simple and effective process for purifying organic molecules, particularly crystalline derivatives. The approach works on the differential solubility principle, which states that the target compound dissolves in a hot solvent

but crystallizes when cooled. Ciprofloxacin derivatives are typically formulated with solvents such as ethanol, methanol, or ethyl acetate due to their low polarity and volatility. Impurities are either left in the solvent or filtered out during the process, while the pure result forms well-defined crystals. The recrystallized compound is then filtered, washed, and dried, producing a product with higher purity and a more uniform structure [103].

2.7.2.3 Column Chromatography

Column chromatography is an important purification technique for separating mixtures of substances with comparable physical and chemical characteristics. It works on the basis of adsorption and the polarity difference between the stationary and mobile phases [104].

Silica gel is typically utilized as the stationary phase, with binary solvent solutions as the mobile phase. When the crude sample is added to the column, components of varying polarity flow through the silica at different rates, with less polar compounds eluting first and more polar compounds following later. By carefully monitoring the eluent polarity, high-resolution separation of ciprofloxacin derivatives and their by-products is possible [105].

2.7.3 Characterization of Synthesized Derivatives

Thorough characterisation is necessary to confirm successful synthesis and structural changes. Standard analytical procedures include melting point determination, Fourier Transform Infrared (FTIR) spectroscopy, and Nuclear Magnetic Resonance (NMR) spectroscopy.

2.7.3.1 Melting Point Determination

Melting point measurement is a fundamental analytical technique used to evaluate the purity and preliminary identity of organic compounds. In general, pure substances have a sharp and well-defined melting point range, indicating a homogeneous crystal structure. Impurities, on the other hand, disrupt this lattice, resulting in melting point ranges that are either expanded or reduced. Thus,

changes from the intended melting point serve as an early signal of contamination or inadequate purification [106].

2.7.3.2 Fourier Transform Infrared Spectroscopy

FTIR an important analytical approach for detecting functional groups and validating structural changes in synthesised ciprofloxacin derivatives. It works on the idea that different bonds absorb infrared radiation at specific frequencies, resulting in a unique spectrum that reflects the structure of the molecule.

Ciprofloxacin derivatives show a carbonyl (C=O) stretching vibration of the carboxylic group between 1650-1740 cm^{-1} and a C-F stretching vibration of the fluoroquinolone core around 1250 cm^{-1}.

The removal of N-H stretching bands (typically about 3200-3500 cm^{-1}) indicates that these groups have reacted or been replaced. The formation of new amide (-CONH) peak reveals successful derivatization at the intended sites. Therefore, FTIR gives direct proof of structural changes and is critical for verifying the efficacy of synthetic modifications in ciprofloxacin-based drugs [107].

2.8 Antimicrobial Evaluation

The antimicrobial evaluation of ciprofloxacin derivatives remains a major emphasis in fluoroquinolone research, as it provides a clear indication of how structural alterations affect biological effectiveness. Ciprofloxacin primarily inhibits bacterial DNA *gyrA*se and topoisomerase IV, two enzymes required for DNA replication and transcription [52].

However, the worldwide spread of fluoroquinolone-resistant bacterial species has significantly diminished its clinical efficacy.

As a result, structural changes to ciprofloxacin, particularly C-7 piperazine ring, have become essential techniques to improve its antimicrobial strength, expand its antibacterial range, and counteract drug resistance mechanisms [80, 108].

2.8.1 *In vitro* Antimicrobial Evaluation Techniques

Ciprofloxacin derivatives' antibacterial efficacy is typically assessed using *in vitro* microbiological techniques. The most often used procedures are agar well diffusion, disc diffusion, and broth microdilution. These approaches assist determine both qualitative and quantitative antibacterial parameters, such as the ZOI, MIC, and MBC [109, 110]. The broth microdilution assay is regarded the most consistent method for measuring MIC values, which are the lowest concentrations of a compound that inhibits apparent bacterial growth. Meanwhile, MBC is defined as the concentration needed to kill 99.9% of bacterial cells [111, 112].

The ratio of MBC to MIC readings frequently reflects whether a substance has bacteriostatic or bactericidal activity. These characteristics, combined, provide a reliable basis for assessing the potency of ciprofloxacin derivatives [113].

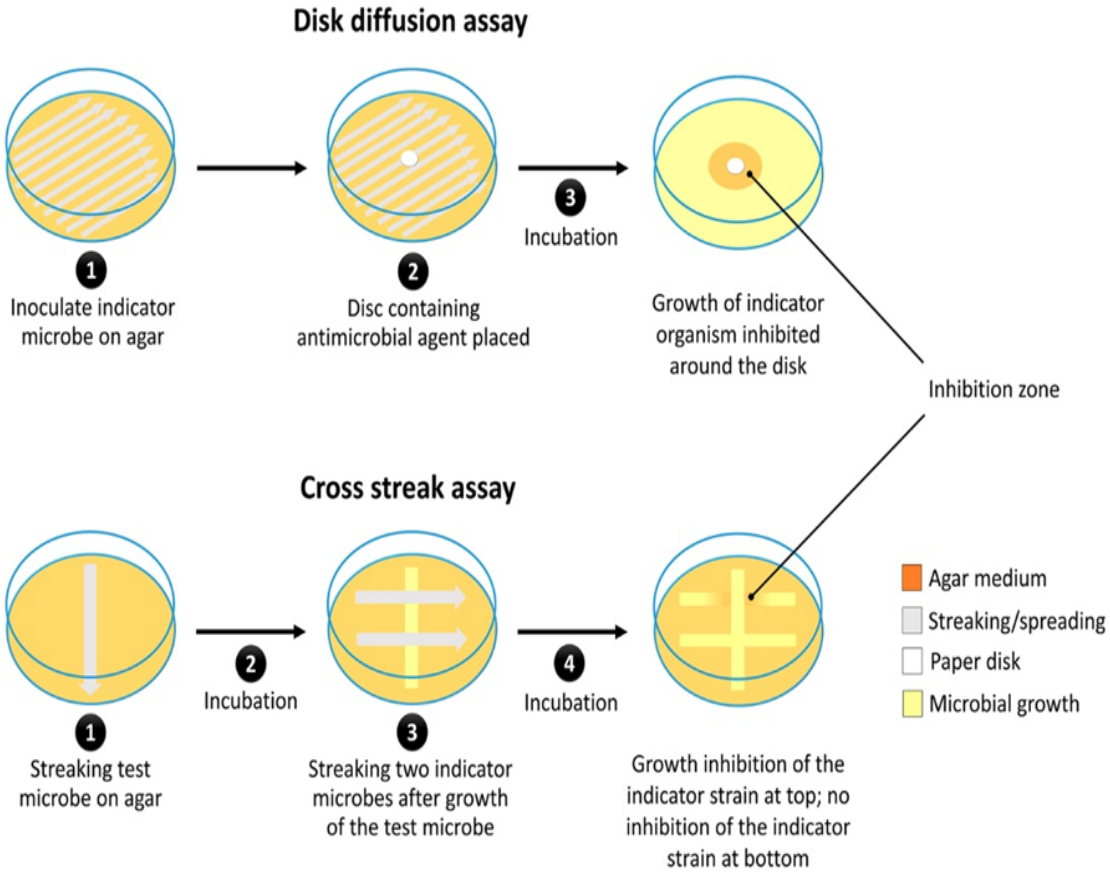

FIGURE 2.7: Visual illustration of antimicrobial techniques

Source: Reproduced from [114]

2.8.2 Activity Against Gram-positive and Gram-negative Pathogens

The spectrum of antibacterial activity of ciprofloxacin derivatives is commonly evaluated against both gram-positive and gram-negative bacteria. This testing is critical because resistance mechanisms often differ between these bacterial classes. Gram-negative bacteria such as *E. coli* and *P. aeruginosa* have a dense outer membrane and active efflux systems that limit drug entry. In contrast, gram-positive organisms such as *S. aureus* and *B. subtilis* might develop resistance via mutations in target enzymes [115].

C-3 amide linked ciprofloxacin derivatives exhibited higher antibacterial activity than ciprofloxacin itself, with MIC values reduced by approximately 50% against *E. coli* and *S. aureus* [108]. Similarly, C-7 triazole substituted ciprofloxacin derivatives that exhibited wider inhibition zones and high bactericidal activity against multidrug-resistant *P. aeruginosa* [116]. The observed improvements were attributed to enhanced hydrogen bonding between the modified side chains and the enzyme's active sites, resulting in stronger stabilization of the drug target.

2.8.3 Bacteriostatic and Bactericidal Profiles

Fluoroquinolones are commonly regarded as bactericidal drugs, as they destroy bacterial cells by causing double-stranded DNA breaks via the stabilization of enzyme DNA complexes. However, changes to the ciprofloxacin structure may affect the killing kinetics. [117] synthesized Schiff base-linked ciprofloxacin analogues that had both bacteriostatic and bactericidal properties depending on the concentration employed. The presence of aromatic imine linkages was discovered to promote lipophilicity and permit better contact with bacterial membranes, hence increasing overall antibacterial efficacy [118].

Halogen-substituted C-7 derivatives not only reduced MIC values but also exhibited quicker bactericidal kinetics against *S. aureus* and *E. coli*. The better performance was related to higher drug absorption and lower efflux recognition

[119]. These findings demonstrate that the bactericidal profile of ciprofloxacin derivatives can be modified through precise structural modifications.

2.9 Bridging the Gap in Drug Discovery

Despite substantial advances in antimicrobial agent discovery and optimization, the rise of multidrug-resistant (MDR) bacteria continues to jeopardize the clinical efficacy of even the most effective medicines. Fluoroquinolones, particularly ciprofloxacin, have transformed the treatment of bacterial infections due to their broad-spectrum action, excellent pharmacokinetics, and oral absorption. However, bacterial adaptation through target site mutations, efflux pump overexpression, and reduced membrane permeability has drastically limited the efficiency of ciprofloxacin [12, 52]. Therefore, recent drug discovery efforts have turned from inventing totally new antibiotic classes to re-engineering existing scaffolds, such as fluoroquinolones, in order to maintain efficacy and delay the emergence of resistance [120].

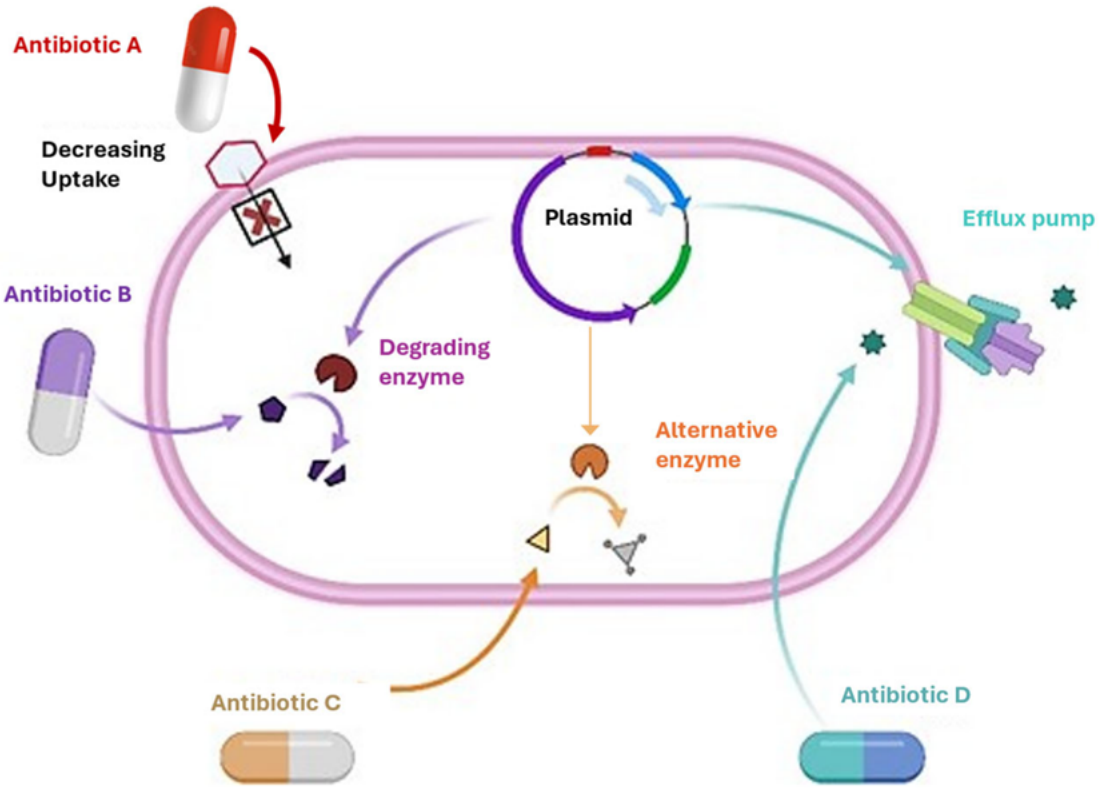

FIGURE 2.8: Illustration of drug discovery methods for combating antimicrobial resistance

Source: Reproduced from [121]

2.9.1 Challenges in Conventional Antibiotic Discovery

Traditional antibiotic discovery pipelines have slowed down significantly in recent years, largely because of rising research and development costs, a shortage of novel biological targets, and the fast adaptive mechanisms shown by bacteria. As a result, most of the antibiotics developed in recent decades are not entirely new entities but rather modified versions or structural derivatives of existing drug scaffolds, reflecting an ongoing reliance on established chemical frameworks instead of the discovery of first in-class agents [120].

Moreover, bacteria develop resistance to new agents within a few years of clinical introduction, reflecting the adaptability of microbial genomes and their ability to acquire resistance genes through horizontal transfer. This situation has created an urgent need for rational, mechanism based modifications of existing antimicrobial molecules rather than relying solely on random screening [122].

2.9.2 Role of Structural Modification and Rational Drug Design

Ciprofloxacin, a valuable scaffold for rational drug design due to its well-defined structure activity relationships (SARs) and known binding interactions with bacterial enzymes. Rational modification of C-7 functional group provides an opportunity to enhance drug target interactions, improve lipophilicity, and reduce efflux susceptibility [49, 123].

Structural optimization through computational drug design, molecular docking, and *in silico* ADMET profiling further accelerates the discovery of derivatives with improved pharmacological profiles [109]. These strategies not only predict the binding efficiency of novel compounds but also identify physicochemical properties influencing absorption, distribution, metabolism, and toxicity critical for successful translation from bench to bedside.

Recent studies demonstrate that hybrid fluoroquinolones and metal drug complexes can achieve synergistic effects by combining antibacterial and pharmacokinetic advantages [124]. The integration of such molecular design principles exemplifies the potential of medicinal chemistry to close the gap between discovery and clinical utility.

2.9.3 Emerging Perspective in Ciprofloxacin Based Antimicrobial Development

Although fluoroquinolone derivatives have shown promising results *in vitro*, few have advanced to clinical trials due to concerns regarding toxicity and pharmacokinetic constraints. Addressing these problems necessitates ongoing research into derivatives with balanced hydrophilicity, improved target selectivity, and fewer adverse effects [125]. Ciprofloxacin's molecular structure serves as a versatile scaffold for such developments. The C-7 piperazine ring remains an ideal location for adding heterocyclic moieties that can improve drug delivery, reduce resistance, and preserve broad-spectrum efficacy [126, 127].

The continued development of ciprofloxacin modification techniques demonstrates a paradigm change from random screening to focused chemical optimization. Researchers can better anticipate activity, reduce resistance, and improve safety profiles by combining synthetic chemistry with computer modelling and biological evaluation [128]. This interdisciplinary collaboration not only lays the groundwork for new drug discovery, but it also indicates how fluoroquinolone derivatives can be used as a model for next-generation antimicrobial innovation.

Chapter 3

Materials and Methods

3.1 Materials

The materials for this experimental study were carefully selected to ensure consistency and reproducibility. Chemicals, solvents, and laboratory materials were procured from recognized providers to preserve uniformity across synthetic, analytical, and biological operations.

3.1.1 Chemicals

Chemicals utilized in this experiment were of analytical grade. The chemicals like 2-Amino Benzothiazole, 3-Indoleacetic acid, 3-Ethynylaniline, Amantadine, Ciprofloxacin HCl, Chloroacetyl Chloride, Magnesium sulfate ($MgSO_4$), Potassium Iodide (KI), Sulfamethazine, Sodium Chloride (NaCl), Sabouraud Dextrose Agar and Mueller Hinton Agar were bought directly from Sigma-Aldrich and used without further purification.

3.1.2 Solvents

The solvents used for synthesis, purification, and spectrum analysis were analytical grade. Sigma-Aldrich supplied Triethylamine (TEA), Dichloromethane (DCM), Dimethyl Sulfoxide (DMSO), Diethyl Ether, and Methanol (MeOH). All solvents were analytical grade and employed immediately in the experimental procedures,

with no further purification. For moisture sensitive processes, anhydrous solvents were used. DCM was dried on activated molecular sieves before usage.

3.1.3 Apparatus and Equipment

The compounds were synthesized, purified, and characterized using standard laboratory and analytical tools.

A separating funnel, analytical balance, magnetic stirrers, round-bottom flasks, micropipettes, heating mantles, and reflux settings for controlled reactions are all essential pieces of equipment.

IR spectra were acquired using a Shimadzu FTIR (Shimadzu Corporation, Kyoto, Japan) device. The Gallenkamp melting point apparatus was utilized to check the melting point of synthesized compounds.

Microbiological evaluations were performed using petri plates, autoclave, incubator, and a laminar flow hood to maintain sterile conditions during antimicrobial assays.

3.2 Methods

3.2.1 General Reaction for the Synthesis of Fluoroquinolone Derivatives

3.2.1.1 Regeneration of Ciprofloxacin Free Base

ciprofloxacin free base was synthesized from ciprofloxacin hydrochloride based on a previously reported method [129]. 5.0 g (13.5 mmol) of ciprofloxacin hydrochloride was dissolved in 30 ml of distilled water, and it was treated with an excess 5% Na_2CO_3 solution.

Add Na_2CO_3 solution dropwise until the pH of 7 is attained. The resulting white precipitate were filtered via a vacuum pump and allowed to dry to give 88% yield (4.4 g).

3.2.2 Synthesis of 7-(4-(2-Chloroacetyl)piperazin-1-yl)-1-cyclopropyl-6-fluoro-1,4-dihydro-4-oxoquinoline-3-carboxylicAcid

Compound 3 was synthesized from ciprofloxacin free base and chloroacetyl chloride by following a previously reported method [101]. Compound 2 (4.0 g, 12 mmol) was dissolved in 40 mL of dry DCM, and TEA (1.73 mL, 12 mmol) was added.

The reaction mixture was stirred at 0°C for 15 minutes, followed by the slow addition of chloroacetyl chloride (1.45 mL, 18.5 mmol) over 30 minutes. Stirring continued for 30 minutes at 0°C and then maintained at room temperature for an additional 4-5 hours.

The reaction mixture was filtered, and the obtained solid was thoroughly washed with water and DCM. The aqueous phase was then extracted with 3 × 30 mL portions of DCM. The organic layer was dried over anhydrous $MgSO_4$ and concentrated. The crude residue was purified by column chromatography using CH_2Cl_2: MeOH (2%) as the eluent to yield the desired product.

3.2.2.1 General Procedure for the Preparation of Derivatives of Ciprofloxacin (CW1 - CW5)

To a solution of compound 3 (407 mg, 1 mmol) in dry DCM (10 mL), TEA (139 μL, 1 mmol) was added at room temperature, and the reaction mixture was stirred for 15 mins. Then, add KI (166 mg, 1 mmol), and stir the reaction mixture for 15 more minutes at room temperature. After this activation, an equimolar amount (1 mmol) of the selected nucleophilic partner, namely the amantadine, 3-Indoleacetic acid, 3-Ethynylaniline, 2-Amino benzothiazole, and sulfamethazine was added to the reaction mixture.

The resulting mixture was stirred under the same conditions until completion, as monitored by TLC. Upon completion, the reaction was quenched with saturated brine solution. The aqueous phase was then extracted with 3 × 30 mL portions of DCM, and the organic layer was separated, dried over anhydrous $MgSO_4$, filtered,

and concentrated. The crude product was purified by silica gel chromatography using CH2Cl2: MeOH (2%) as the eluent to yield the corresponding derivatives.

3.3 General Reaction Scheme of Synthesized Derivatives

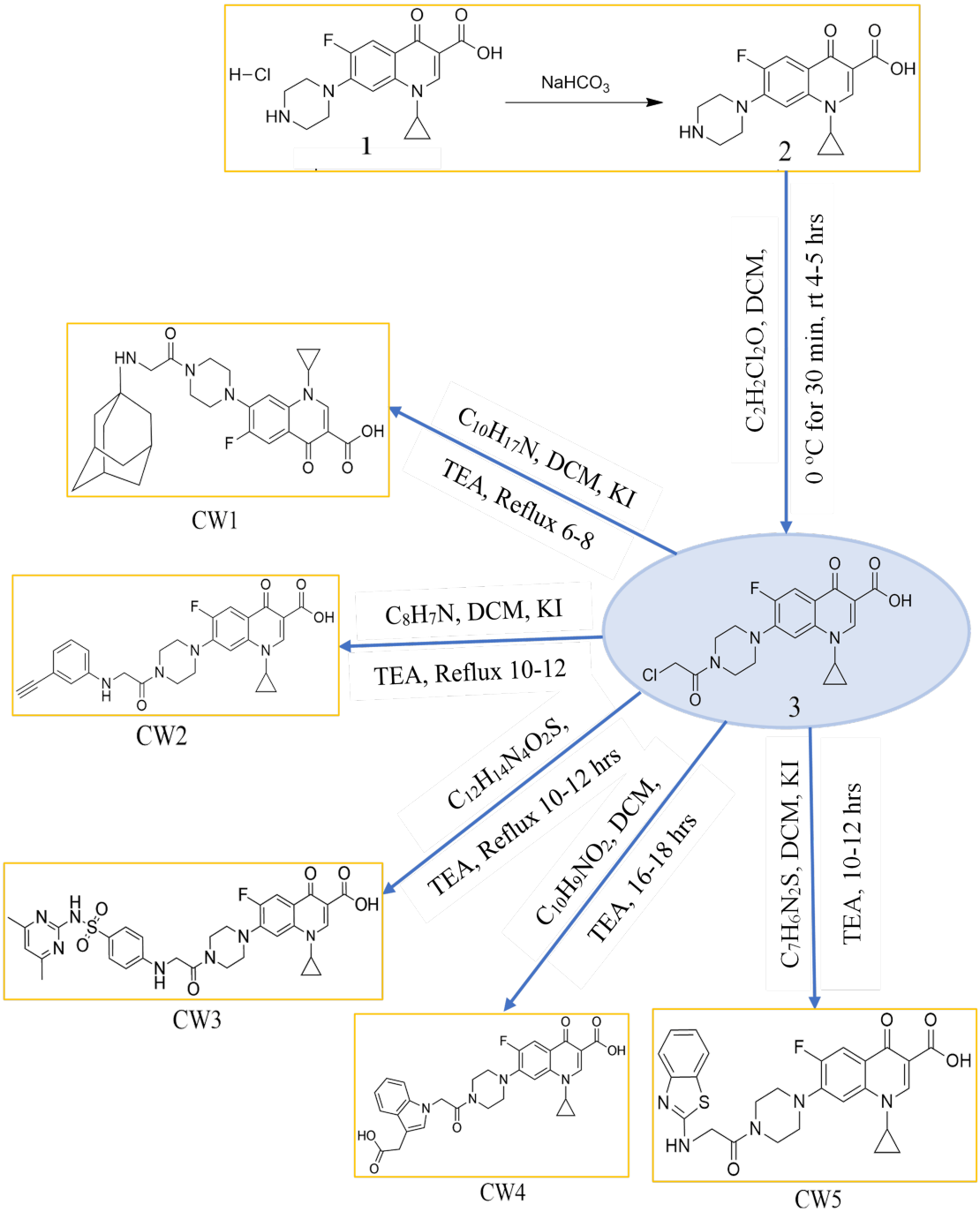

FIGURE 3.1: General reaction scheme of ciprofloxacin derivatives

3.4 Purification of Synthesized Compounds

Purification of the synthesized compounds was carried out using standard techniques to ensure high purity for subsequent characterization and biological evaluation.

3.4.1 Recrystallization

Recrystallization was accomplished by dissolving the crude product in a suitable solvent and slowly cooling it to room temperature. Filters were used to capture the crystals, which were then rinsed with a cold solvent and dried.

3.4.2 Column Chromatography

Column chromatography was utilized for substances that could not be efficiently purified via recrystallization. Silica gel served as the stationary phase, while solvent solutions were adjusted based on the polarity of the target molecules. Fractions were collected, tested using TLC, and mixed depending on chemical purity.

3.5 Characterization of Synthesized Compounds

The purity and structural integrity of all produced compounds were validated using a mix of physicochemical and spectroscopic methods. Each method offered complimentary data to validate the molecular structure and measure quality.

3.5.1 Melting Point Determination

The melting points of the synthesized compounds were determined using a Gallenkamp digital melting point instrument and the capillary tube method. The chemical was inserted into the capillary tube, with one end closed. Tap the open end lightly to confirm that the compound was packed correctly. Then, place the capillary tube and thermometer into the Gallenkamp melting point apparatus's designated slot. The complex was then monitored using a lens until it melted. Take note of the readings, repeat the practice in triplicate to reduce errors, and

determine the average. The values were checked with starting materials or published literature to ensure compound production and purity.

3.5.2 Solubility Testing

The synthesised derivatives were tested for solubility. To test the solubility of the compounds, a small amount of chemical was introduced to several Eppendorf tubes, which were subsequently filled with various solvents one at a time. Close the lid tightly, shake the Eppendorf tubes on the shaker until the compound is dissolved, then leave the tubes to stand for a while so that the settled contents may be clearly seen.

3.5.3 FTIR Spectroscopy

The produced compounds were characterized using FTIR spectroscopy, which detected important functional groups and confirmed structural alterations after derivatization. Solids were prepared by coarsely grinding 1-2 mg of the synthesized chemical and mixing it with spectroscopic grade KBr before compressing it into a clear pellet. Semi-solid materials were tested as tidy films by sandwiching a little portion of the sample between clean KBr plates. The prepared samples were scanned using a Shimadzu FTIR spectrometer in the mid-infrared band (4000-400 cm^{-1}), with a background spectra obtained before each study to exclude air influence. The resulting spectra were evaluated for typical absorption bands and aromatic vibrations, and compared with standard frequency values to confirm the existence of functional groups and assess spectrum shifts associated to effective derivatization.

3.6 *In silico* Studies

In silico studies on the synthesized derivatives were conducted to get insight into their potential interactions with the receptor's active region. The spatial orientation of the ligands within the target proteins' active pocket was determined, binding affinities were predicted, and critical amino acid residues implicated in

interactions were identified using molecular docking. These computational evaluations not only provide a solid framework for understanding the compounds' mechanisms of action, but also highlight their promise as a front-runner for future therapeutic development.

Such approaches provide a cost-effective and time-saving alternative to early-stage experimental screening, hence increasing the efficacy of structure-based drug development programs. Computational studies were conducted to supplement experimental work and forecast the binding interactions, pharmacokinetic properties, and likely biological activity of the synthesized [130].

3.6.1 Molecular Docking Investigation

Molecular docking was performed to assess the interaction of the synthesized compounds with the target proteins. The docking procedure provided insights into binding modes, energy scores, and potential active site interactions.

3.6.1.1 Recovering Protein Structure from PDB

The three-dimensional structures of *Salmonella typhi OmpF* (4KRA), Topoisomerase II (5BTC) and multi-drug efflux pump (8GJL) were retrieved from the Protein Data Bank (PDB) (https://www.rcsb.org/). Structures were selected based on relevance to the antimicrobial target and downloaded in PDB format.

3.6.1.2 Preparation of a Protein Macromolecule

The selected molecular proteins were prepared and docked for further examination using the AutoDock Tools. After that, the chosen proteins underwent addition of Gasteiger charge and energy reduction. Protein structures were stored in pdbqt format once the foundation was laid. Discovery Studio 4.1 Client (2012) used for structural validation and visualization resulted in quicker generation of Ramachandran plots and hydrophobicity profiles. In addition, the statistical distribution of physical features, such as β-helices, coils, turns, and β-sheets, was examined using the VADAR 1.8 web server [131].

3.6.1.3 Ligand Proteins Molecular Docking

The ligands were drawn using the Discovery Studio Client after energy reduction, and they were then saved as ligands in pdb format. Using AutoDock Tools most stable configuration of ligands was generated.

After adding the Gasteiger and Kolman charges, the ligands were stored in pdbqt format. An application for virtual screening that uses the Auto Dock Vina Wizard technique discussed in [132] for better conformational placement in the active region of the target protein.

The default exhaustiveness value of 100 was used to dock the chosen protein targets to individual molecules. The lowest binding energy values (kcal/mol) were used to assess the anticipated docked complexes. Discovery Studio (2.1.0) and (Discovery Studio Visualizer Software, Version 4.0 (2012)) were used to graphically depict each docked complex in three dimensions [133].

3.6.1.4 ADMET Assessment

The Swiss ADME prediction system (https://www.swissadme.ch/) was used to evaluate the pharmacokinetic parameters and physicochemical properties of the synthesized compounds. The number of hydrogen bond donors/acceptors, molecular weight, Topological polar surface area (TPSA), number of rotatable bonds, and Log P (o/w) (iLOGP) were all assessed using Swiss ADME prediction. The drugs' inhibitory potential, carcinogenicity, human intestinal absorption and plasma protein binding were estimated using the Pre ADME-T server [134, 135].

The BOILED-Egg model was developed using the Swiss ADME tool's online interface. The ProTox-II website was developed by Drwal *et al.* (2014) [136]. It was used for the in -silico study. Parameters such as genetic toxicity endpoints (specifically carcinogenicity, mutagenicity, and cytotoxicity), organ toxicity (specifically immunotoxicity and hepatotoxicity), and oral acute toxicity (specifically median lethal dose [LD_{50}] in mg/kg) were predicted for established synthetic compounds based on the protocol of [136].

3.7 Biological Evaluation of Synthesized Compounds

3.7.1 Antibacterial Activity

The antibacterial potential synthesized derivatives were evaluated using standard *in vitro* assays against resistant strains *Methicillin resistant staphylococcus aureus (MRSA) (ATCC 43300), Escherichia coli (E. coli) (ATCC 25922), Acinetobacter baumannii (A. baumannii) (ATCC 17978)* and non-resistant strain *Salmonella abony (S. abony) (ATCC 6017), Escherichia coli (E. coli) (ATCC 10536), Staphylococcus aureus (S. aureus) (ATCC 6538), Pseudomonas aeruginosa (P. aeruginosa) (ATCC 9027)* and *Bacillus subtilis (B. subtilis) (ATCC 6633).* Experiments were designed to evaluate zone of inhibition effects under controlled conditions.

3.7.2 Agar Well Diffusion Method

The antibacterial activity of the synthesized compounds was evaluated using the agar well diffusion method against resistant and non-resistant bacterial strains. Mueller–Hinton agar plates were prepared and uniformly inoculated with standardized bacterial cultures. Wells of consistent diameter were aseptically created in the agar using a sterile cork borer in each plate. Each well was then filled with 0.05 μg/mL concentration of the respective synthesized derivatives for non-resistant strains and 0.2 μg/mL used for resistant strains. The inoculated plates were incubated at 37°C for 24 hours duration. After incubation, antibacterial activity was assessed by measuring the diameter of the clear ZOI surrounding each well. The extent of these inhibition zones was used as an indicator of the antibacterial efficacy of the synthesized compounds.

3.8 Antifungal Activity

Antifungal activity of the synthesized derivatives was assessed through disc diffusion method against *C. albicans, A. flavus,* and *A. niger.* Fresh fungal cultures were prepared, and fungal concentrations were homogenously spread onto sterile

agar plates under aseptic conditions. 6 mm diameter discs were prepared with fixed 0.1 μg/ml concentrations of the synthesized compounds and placed on the agar plates, while ciprofloxacin drug was included as a reference control with same concentration. The plates were incubated for 24 hours, after which they were observed for the presence of ZOI around the disks. The diameter of inhibition zones was measured in millimeters, and all experiments were performed in triplicate; the absence of a zone was indication of no antifungal activity.

3.9 Statistical Analysis

Statistical analysis was performed in triplicate, and findings were expressed as mean ± SD. ZOI and melting point values were measured for each synthesized derivative, and descriptive statistical analysis was used. Mean and standard deviation were determined in Microsoft Excel to analyse data variability and consistency. The study did not use inferential statistical tests because it was primarily focused on the descriptive and comparative evaluation of the synthesized derivatives.

Chapter 4

Results

4.1 Chemistry

Ciprofloxacin derivatives were synthesized by following the synthesis scheme shown in Figure 3.1. The purity of the compounds was confirmed by TLC, and structures were elucidated through FTIR. The successful formation of ciprofloxacin derivatives was confirmed by changing position of the chromatogram over the TLC plate and the presence or absence of stretching frequencies in FTIR spectra, confirming the structural integrity of the synthesized compound.

The synthesis of ciprofloxacin derivatives was optimized under various reaction conditions, as summarized in Table 4.1. The optimization trials validate that basic conditions and extended reaction time were vital for product formation. Additionally, the chemical structures of all synthesized compounds are illustrated in Figure 4.1.

Table 4.1: Optimization of reaction conditions for the synthesis of compounds CW1-CW5

Compound	**Trial No.**	**Temp (°C)**	**Catalyst**	**Time (hr)**	**pH**	**Solvent**	**Molar Ratio**	**Product formed**
CW1	1	60	-	8	3	Acetonitrile	1:1	No
CW1	2	60	KI	8	3	Acetonitrile	1:1	No
CW1	3	rt	-	10	5	Acetonitrile	1:1	No
CW1	4	rt	KI	10	5	Acetonitrile	1:1	No

Table 4.1 continued from previous page

Compound	Trial No.	Tem (°C)	Catalyst	Time (hr)	pH	Solvent	Molar Ratio	Product formed
CW1	5	60	KI	10	5	Acetonitrile	1:1	No
CW1	6	rt	-	6	3	DCM	1:1	No
CW1	7	rt	KI	6	3	DCM	1:1	No
CW1	8	rt	KI	8	5	DCM	1:1	Yes
CW2	1	60	-	5	3	Acetonitrile	1:1	No
CW2	2	rt	KI	7	3	Acetonitrile	1:1	No
CW2	3	rt	KI	10	5	Acetonitrile	1:1	No
CW2	4	60	KI	8	5	Acetonitrile	1:1	No
CW2	5	rt	-	7	3	DCM	1:1	No
CW2	6	rt	KI	10	3	DCM	1:1	No
CW2	7	rt	KI	12	5	DCM	1:1	Yes
CW3	1	rt	-	8	3	DCM	1:1	No
CW3	2	rt	KI	10	3	DCM	1:1	No
CW3	3	rt	KI	12	4.5	DCM	1:1	No
CW3	4	rt	KI	10	5	Acetonitrile	1:1	No
CW3	5	60	KI	10	5	Acetonitrile	1:1	No
CW3	6	rt	KI	12	6.5	DCM	1:1	Yes
CW4	1	rt	KI	8	3	DCM	1:1	No
CW4	2	rt	KI	8	4.5	DCM	1:1	No
CW4	3	rt	KI	12	5	DCM	1:1	No
CW4	4	rt	KI	18	7	DCM	1:1	Yes
CW5	1	rt	KI	8	5	DCM	1:1	No
CW5	2	rt	KI	12	3.5	DCM	1:1	No
CW5	3	rt	KI	12	7	DCM	1:1	Yes

The physical characteristics of synthesized compounds, including molecular formula, melting point, yield, and solubility, are presented in Table 4.2.

TABLE 4.2: Physical Data of Synthesized Compounds

Compound	Molecular formula	Mol weight (g/mol)	Melting point (°C)	Physical state	Color	Percentage Yield (%)	Solubility
CW1	$C_{29}H_{35}FN_4O_4$	522.61	224	Solid	White	70	DMSO

Table 4.2 continued from previous page

Compound	Molecular formula	Mol weight (g/mol)	Melting point (°C)	Physical state	Color	Percentage Yield (%)	Solubility
CW2	$C_{27}H_{25}FN_4O_4$	488.51	192	Solid	Light Brown	69	DMSO
CW3	$C_{31}H_{32}FN_7O_6S$	649.69	212	Semi solid	Pale Yellow	62	DMSO
CW4	$C_{29}H_{27}FN_4O_6$	546.55	234	Solid	Dark Brown	51	DMSO
CW5	$C_{26}H_{24}FN_5O_4S$	521.56	174	Semi solid	Cinnamon	54	DMSO

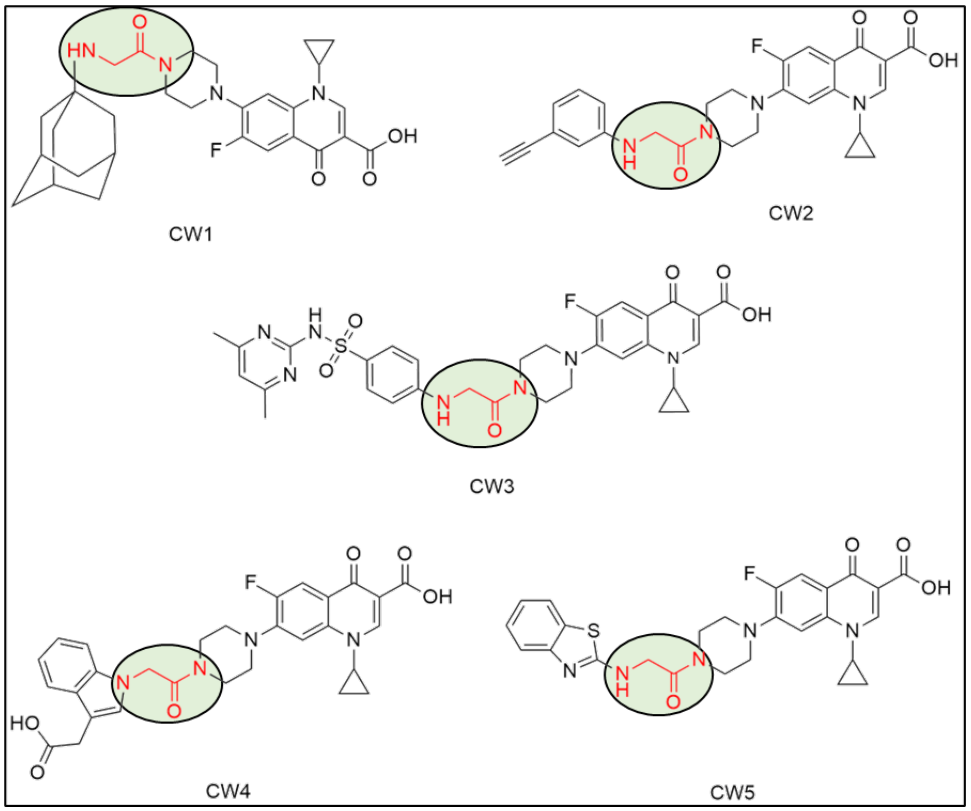

FIGURE 4.1: Structures of the synthesized derivatives of ciprofloxacin

4.2 FTIR Spectral Data

The derivatives of ciprofloxacin were synthesized according to reported procedures in the literature, and the desired compounds were attained in good yields. Fourier

Transform Infrared (FTIR) spectroscopy was employed to check the functional groups present in the synthesized compounds.

4.2.1 FTIR of 1-cyclopropyl-6-fluoro-4-oxo-7-(piperazin-1-yl)-1,4-dihydroquinoline-3-carboxylicacidhydrochloride

The FTIR spectrum of the ciprofloxacin was shown in Figure 4.2. A broader stretching vibration present at 3530, indicating the presence of the hydroxyl group of quinolone scaffold.

TABLE 4.3: FTIR Spectral data of Ciprofloxacin

Functional Group	**Observed Wavenumber (cm^{-1})**
-OH	3368
C=O	1700
C=C	1610

Strong absorption band appearing at 1700 cm^{-1} is characteristic of carbonyl (C=O) stretching vibration. Especially, the amide carbonyl, confirming the successful formation of the carbonyl amide linkage.

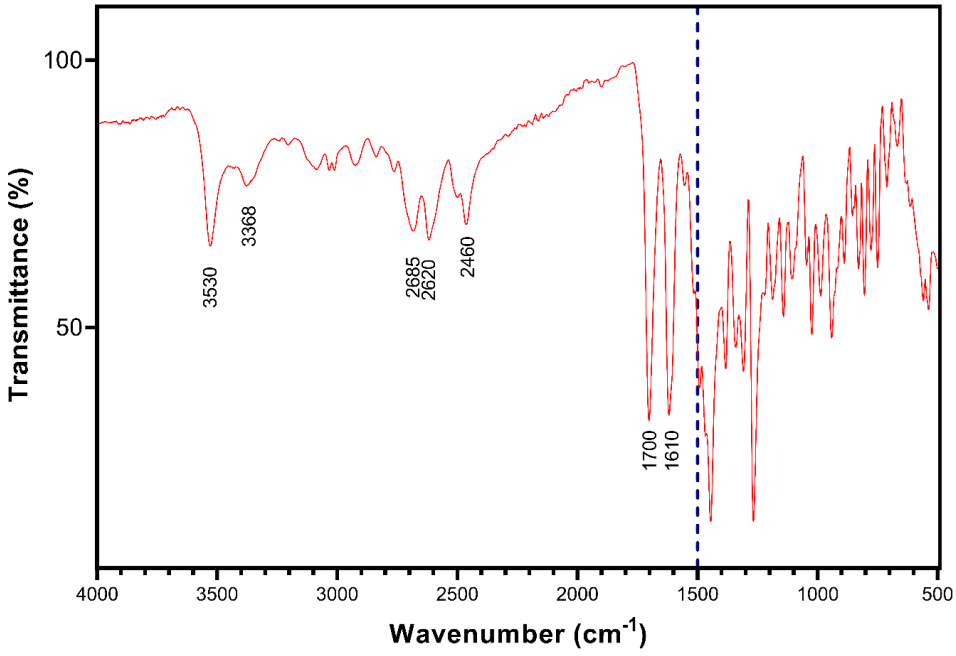

FIGURE 4.2: FTIR Spectra of compound Ciprofloxacin

The aromatic C=C stretch of the quinolone core appear at 1610 cm^{-1} are consistent with the ciprofloxacin aromatic framework [137]. Overall, the FTIR spectrum confirms all key functional groups of ciprofloxacin. The principal FTIR absorption bands for Ciprofloxacin are shown in Table 4.3.

4.2.2 FTIR of 7-(4-(2-((3s,5s,7s)-adamantan-1-ylamino)acetyl)piperazin-1-yl)-1-cyclopropyl-6-fluoro-4-oxo-1,4-dihydroquinoline-3-carboxylicacid(CW1)

The FTIR spectrum of the synthesized compound CW1 was shown in Figure 4.3. A broad absorption peak observed at 3429 cm^{-1} corresponds to the hydroxyl (-OH) group in the quinolone scaffold. In the same region, weaker N-H stretching vibrations present, indicating the presence of the secondary amine linkage formed between the intermediate and the attached moiety [138].

TABLE 4.4: FTIR Spectral data of compound CW1

Functional Group	**Observed Wavenumber (cm^{-1})**
OH/ N-H	3429
C-H	2913
C=O	1733
C=C	1622

Strong absorption band appearing at 1733 cm^{-1} is characteristic of carbonyl (C=O) stretching vibration. Especially, the amide carbonyl, confirming the successful formation of the carbonyl amide linkage. The aromatic C=C stretch of the quinolone core appear at 1622 cm^{-1} are consistent with the ciprofloxacin aromatic framework. The successful incorporation of the amantadine moiety is evidenced by characteristic C-H stretching vibration at 2913 cm^{-1} region, overlapping with other aliphatic signals from the cyclopropyl group [139].

Overall, the FTIR spectrum confirms the successful conjugation with amantadine, clearly showing all key functional groups. The principal FTIR absorption bands for CW1 are shown in Table 4.4.

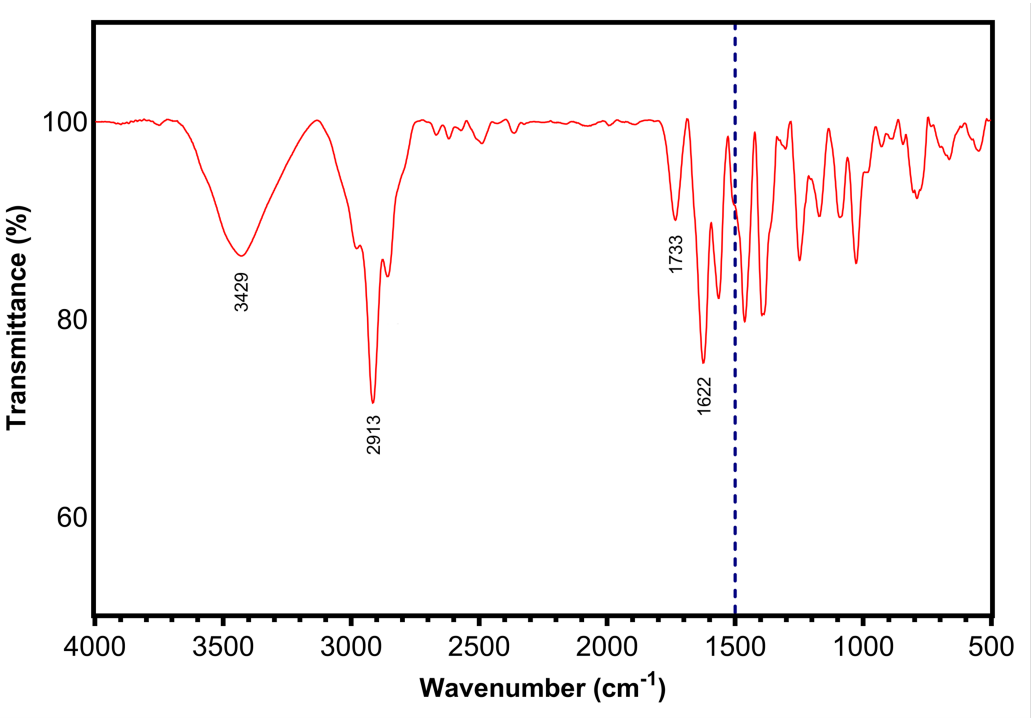

FIGURE 4.3: FTIR Spectra of compound CW1

4.2.3 FTIR of 1-cyclopropyl-7-(4-(2-((3-ethynylphenyl)amino)acetyl)piperazin-1-yl)-6-fluoro-4-oxo-1,4-dihydroquinoline-3-carboxylicacid(CW2)

The FTIR spectrum of compound CW2 was shown in Figure 4.4. It displays sharp absorption band at 3482 which are attributed to -OH and N-H stretching vibration. Absorption band observed at 3355 cm^{-1} belongs to terminal alkyne which confirms successful incorporation of desired compound [140].

The absorption band observed at 2940 cm^{-1} corresponds to aliphatic C-H stretching vibrations, consistent with the presence of the quinolone nucleus [141].

TABLE 4.5: FTIR Spectral data of compound CW2

Functional Group	**Observed Wavenumber (cm^{-1})**
N-H/ -OH	3482
-C≡CH	3355
C-H	2940
C=O	1682
C=C	1600

A strong and sharp absorption band appearing at 1682 cm^{-1} is assigned to the amide carbonyl (C=O) stretching vibration, confirming successful chloroacetylation of the piperazine nitrogen. The absorption band at 1600 cm^{-1} corresponds to aromatic C=C stretching vibrations of the quinolone ring. The FTIR spectrum confirms the successful conjugation with 3-ethynylylaniline, clearly showing all key functional groups. The major FTIR absorption bands of CW2 are summarized in Table 4.5.

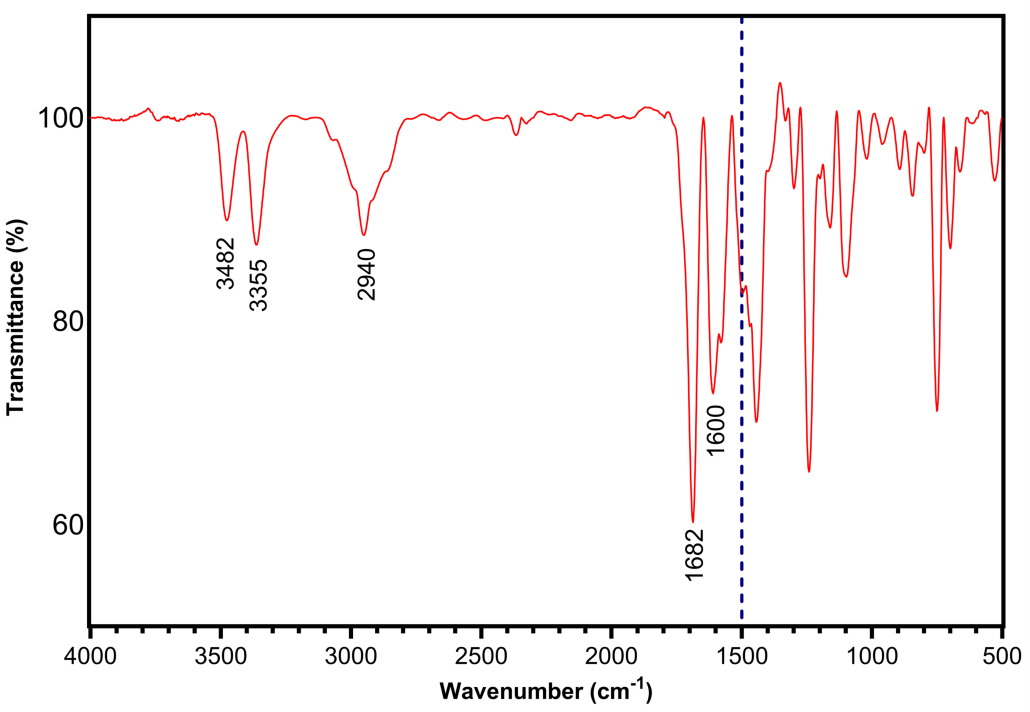

FIGURE 4.4: FTIR Spectra of compound CW2

4.2.4 FTIR of 1-cyclopropyl-7-(4-(2-((4-(N-(4,6-dimethylpyrimidin-2-yl)sulfamoyl)phenyl)amino)acetyl)piperazin-1-yl)-6-fluoro-4-oxo-1,4-dihydroquinoline-3-carboxylicacid(CW3)

The FTIR spectrum of compound CW3 was shown in Figure 4.5. The spectra show broad and intense absorption band at 3218 cm^{-1} which is attributed to the -OH stretching vibration of the carboxylic acid group, and 3400 is assigned to the N-H stretching vibration of the amine. The absorption band appearing at

2983 cm^{-1} is assigned to C-H stretching vibration, confirming the presence of the quinolone nucleus.

TABLE 4.6: FTIR Spectral data of compound CW3

Functional Group	**Observed Wavenumber (cm^{-1})**
N-H/ -OH	3400 & 3218
-CH	2983
C=O	1722
C=C	1608
S=O	1463

A strong absorption band appearing at 1722 cm^{-1} is assigned to the amide carbonyl (C=O) stretching vibration. In addition, a prominent band observed at 1608 cm^{-1} is attributed to C=C stretching vibrations of the aromatic rings. Furthermore, absorption band detected at 1463 cm^{-1} is attributed to the asymmetric and symmetric stretching vibrations of the sulfonyl (S=O) group, respectively. These results provide clear spectroscopic evidence for the successful incorporation of sulfonamide functionality, a key structural feature of CW3. The main FTIR absorption bands for CW3 are shown in Table 4.6.

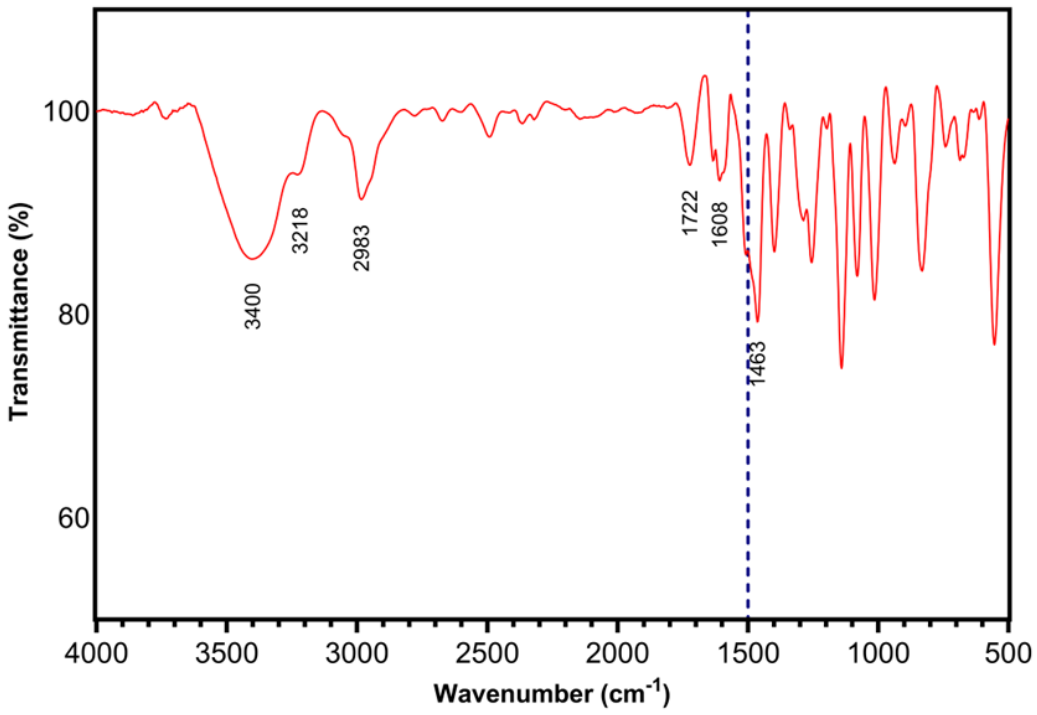

FIGURE 4.5: FTIR Spectra of compound CW3

4.2.5 FTIR of 7-(4-(2-(3-(carboxymethyl)-1H-indol-1-yl)acetyl)piperazin-1-yl)-1-cyclopropyl-6-fluoro-4-oxo-1, 4-dihydroquinoline-3-carboxylicacid(CW4)

The FTIR spectrum of compound CW4 was shown in Figure 4.6. A broad and intense absorption band observed at 3400 cm^{-1} is attributed to the -OH stretching vibration of the quinolone ring.

The absorption band appearing at 2925 cm^{-1} is assigned to -CH stretching vibration, confirming the presence of the quinolone nucleus and the indole ring system.

TABLE 4.7: FTIR Spectral data of compound CW4

Functional Group	**Observed Wavenumber (cm^{-1})**
-OH	3400
-CH stretching	2925
C=O	1715
C=C	1622

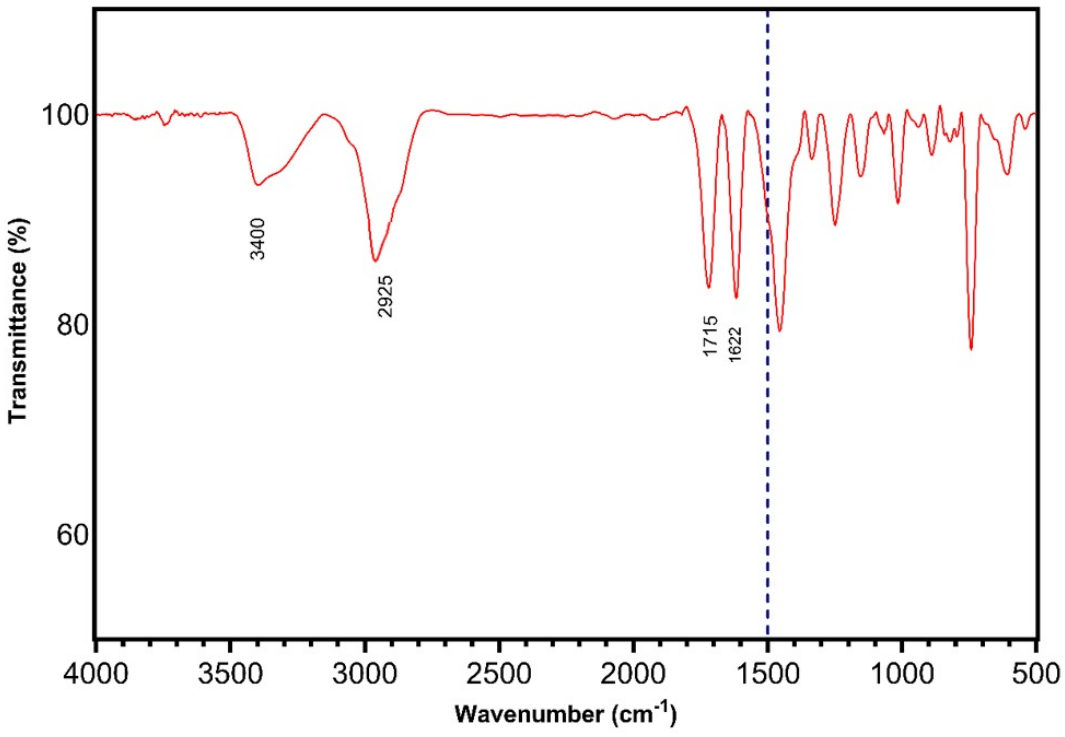

FIGURE 4.6: FTIR Spectra of compound CW4

A strong absorption band seen at 1715 cm^{-1} is characteristic of the amide carbonyl (C=O) stretching vibration. Moreover, a prominent band appearing at 1622 cm^{-1} is attributed to C=C stretching vibration of aromatic rings.

These results provide strong spectroscopic evidence supportive to structural confirmation of the indole-linked fluoroquinolone derivative. The main FTIR absorption bands for CW4 are shown in Table 4.7.

4.2.6 FTIR of 7-(4-(2-(benzo[d]thiazol-2-ylamino)acetyl)piperazin-1-yl)-1-cyclopropyl-6-fluoro-4-oxo-1,4-dihydroquinoline-3-carboxylicacid(CW5)

The FTIR spectrum of compound CW5 was recorded in Figure 4.7. A broad absorption band seen at 3415 cm^{-1} is ascribed to the O-H stretching vibration. While a sharp band present at 2977 cm^{-1} represents C-H stretching vibration of the quinolone ring.

These peaks confirm the presence of both the quinolone nucleus and the benzothiazole ring system.

TABLE 4.8: FTIR Spectral data of compound CW5

Functional Group	**Observed Wavenumber (cm^{-1})**
O-H	3415
C-H	2977
C=O	1720
C=C	1623

A strong and sharp absorption band observed at 1720 cm^{-1} is characteristic of the amide carbonyl (C=O) stretching vibration. The absorption band detected at 1623 cm^{-1} is assigned to C=C stretching vibrations of aromatic rings. These results offer solid evidence supporting the successful synthesis of the benzothiazole-linked fluoroquinolone derivative. The key FTIR absorption bands for CW5 are shown in Table 4.8.

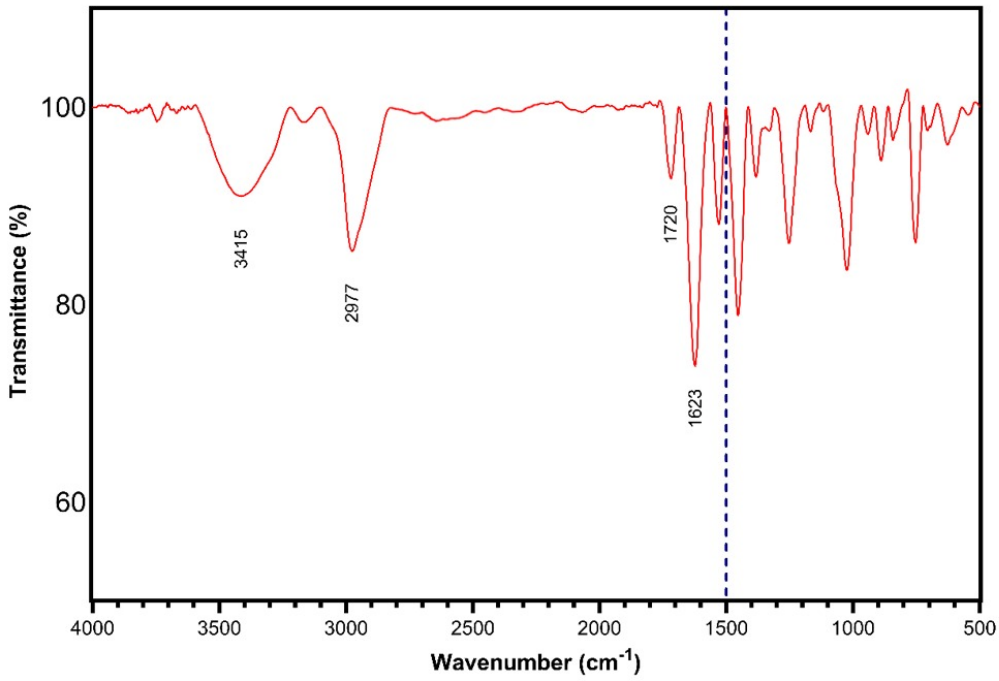

FIGURE 4.7: FTIR Spectra of compound CW5

4.3 *In silico* ADME and Drug-Likeness Evaluation

4.3.1 Physicochemical Properties of Synthesized Derivatives

The physicochemical features of the synthesized derivatives (CW1-CW5) were evaluated using the SwissADME web server, and the calculated parameters are summarized in Table 4.9. These parameters included molecular weight, hydrogen bond donors and acceptors, topological polar surface area (TPSA), lipophilicity, rotatable bonds, molar refractivity, and fraction of sp^3-hybridized carbons ($F.Csp^3$).

The molecular weights of the synthesized derivatives of ciprofloxacin ranged from 488.51 g/mol to 649.69 g/mol. However, CW2 possess the lowest molecular weight, while CW3 exhibited the highest molecular weight (649.69 g/mol). Furthermore, hydrogen bond acceptors ranged from 5 to 9, but hydrogen bond donors ranged

between 2 and 3 across the derivatives. The TPSA values show considerable variability, however, both CW1 and CW2 exhibit similar values of 94.88 $Å^2$, while CW3 exhibited the highest TPSA (175.21 $Å^2$) and CW4 and CW5 displayed intermediate TPSA values of 125.08 $Å^2$ and 136.01 $Å^2$.

The number of rotatable bonds ranged between 7 to 10, with CW3 owning highest molecular flexibility. The fraction of sp^3 carbon atoms ($F.Csp^3$) vary from 0.30 to 0.32 for all compounds except CW1 which show higher value of 0.62 demonstrating a relatively greater degree of saturation in comparison to other compounds. Generally, the physicochemical parameters show structural diversity among the compounds, with variability in size, polarity, and flexibility that might influence their pharmacokinetic behavior.

TABLE 4.9: SwissADME database utilized to calculate Physiochemical properties of compounds

Compound	**Molecular Formula**	**MW (g/mol)**	**F.Csp^3**	**nHA**	**nAHA**	**nHBA**	**nHBD**	**nRB**	**MR**	**TPSA (A2)**
CW1	$C_{29}H_{35}FN_4O_4$	522.61	0.62	38	10	6	2	7	149.72	94.88
CW2	$C_{27}H_{25}FN_4O_4$	488.51	0.30	36	16	5	2	7	141.92	94.88
CW3	$C_{31}H_{32}FN_7O_6S$	649.69	0.32	46	22	9	3	10	176.62	175.21
CW4	$C_{29}H_{27}FN_4O_6$	546.55	0.31	40	19	7	2	8	152.98	125.08
CW5	$C_{26}H_{24}FN_5O_4S$	521.56	0.31	37	19	6	2	7	147.16	136.01

4.3.2 Pharmacokinetic Profile Prediction

Pharmacokinetic properties of the synthesized derivatives were predicted with SwissADME, and the results were presented in Table 4.10. Key parameters evaluated include gastrointestinal (GI) absorption, blood-brain barrier (BBB) permeability, P-glycoprotein (P-gp) substrate status, bioavailability score, and cytochrome P450 (CYP) enzyme inhibition profiles.

CW1, CW2, and CW4 show higher GI absorption, whereas CW3 and CW5 are predicted to have low GI absorption. The bioavailability scores of CW1, CW2, CW4 and CW5 consisted with values ranging from 0.55 to 0.56. However, CW3 presented low bioavailability score of 0.11. All compounds were predicted to be

non-permeable across the blood-brain barrier, suggesting limited central nervous system exposure.

None of the synthesized compounds were predicted to act as P-gp substrates. Regarding metabolic interactions, all compounds were prophesied to inhibit the CYP2C9 and CYP3A4 enzymes. CYP1A2 inhibition was not detected for any compound. CYP2C19 inhibition was predicted for CW1, CW2, CW4, and CW5, while CW3 showed no inhibition of this enzyme. CYP2D6 inhibition was predicted for CW2 and CW4, whereas CW1, CW3, and CW5 were predicted to be non-inhibitors.

TABLE 4.10: The bioavailability evaluations and pharmacokinetics of Schiff base derivatives calculated using the SwissADME database

Compound	**Bioavailability**	**GI absorption**	**BBB permeability**	**P-gp substrate**	**CYP 1A2 Inh**	**CYP 2C19 Inh**	**CYP 2C9 Inh**	**CYP 2D6 Inh**	**CYP 3A4 Inh**	**TPSA (A2)**
CW1	0.55	High	No	Yes	No	Yes	No	Yes	Yes	94.88
CW2	0.56	High	No	Yes	No	Yes	Yes	Yes	Yes	94.88
CW3	0.11	Low	No	Yes	No	No	Yes	No	Yes	175.21
CW4	0.56	High	No	Yes	No	Yes	Yes	Yes	No	125.08
CW5	0.56	Low	No	Yes	No	Yes	Yes	Yes	Yes	136.01

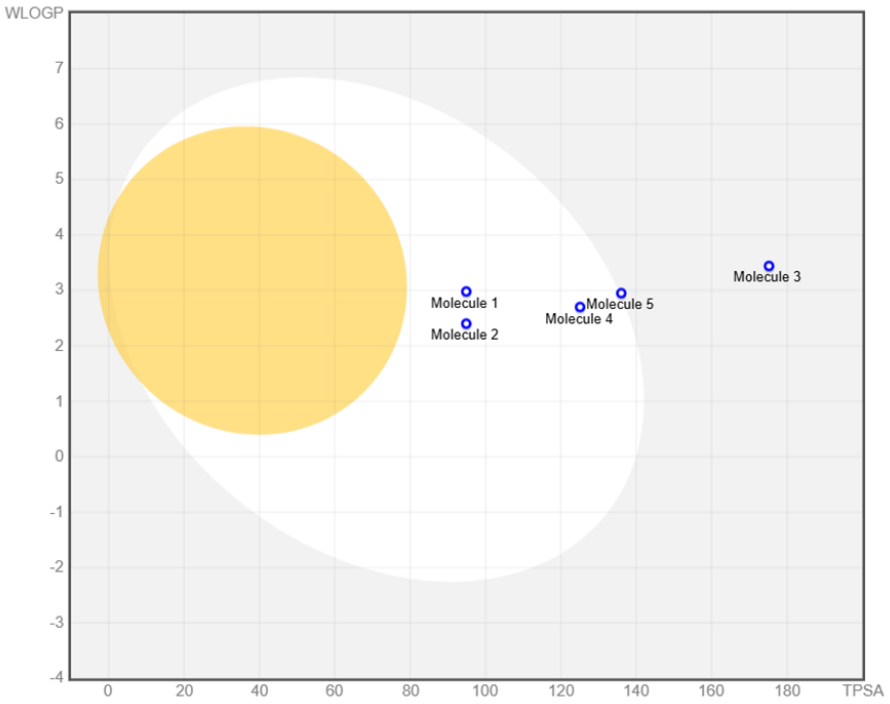

FIGURE 4.8: The boiled egg analysis of the produced derivatives

The BOILED-Egg model shown in Figure 4.8 further reinforced the predicted pharmacokinetic behavior, showing that the compounds mostly fall within regions associated with limited BBB penetration. At the same time, selected derivatives demonstrated favorable GI absorption characteristics.

4.3.3 Drug-Likeness Assessment

Drug-likeness properties of the synthesized compounds were assessed using five commonly applied rule-based filters, including Lipinski, Ghose, Veber, Egan, and Muegge rules. The results of this assessment are summarized in Table 4.11.

CW1, CW2, CW4, and CW5 satisfied the Lipinski criteria, whereas CW3 failed to comply with this rule. All compounds exhibited Ghose filter violations. CW3 compound failed to comply with Veber, Egan, and Muegge criteria, while rest of the compounds obeyed these rules. Overall, CW1, CW2, CW4, and CW5 presented favorable drug-likeness profiles against multiple filters, while CW3 exhibited multiple variations from predictable drug-likeness parameters.

TABLE 4.11: Drug Likeness scores

Compound	**Lipinski**	**Ghose**	**Veber**	**Egan**	**Muege**
CW1	Yes	No	Yes	Yes	Yes
CW2	Yes	No	Yes	Yes	Yes
CW3	No	No	No	No	No
CW4	Yes	No	Yes	Yes	Yes
CW5	Yes	No	Yes	No	Yes

4.3.4 Medicinal Chemistry

Medicinal chemistry profile of the synthesized derivatives was evaluated through SwissADME, focusing on PAINS alerts, Brenk alerts, lead-likeness, and synthetic accessibility. The results are briefly shown in Table 4.12.

None of the derivatives exhibited PAINS alerts, presenting low likelihood of false positive activity in biological assays. Brenk alerts were absent in all compounds, while CW2 presented one alert linked to a triple-bond feature. Neither of the

derivatives satisfied lead-likeness criteria, mainly due to molecular weight values above 350 g/mol. CW3 and CW4 showed additional violations linked to lipophilicity and the number of rotatable bonds. Synthetic accessibility scores ranged between 3.42 to 5.81, presenting moderate synthetic complexity across the derivatives. CW2 exhibited the lowest synthetic accessibility score, while CW1 displayed the highest synthetic accessibility score.

TABLE 4.12: PAINS, Brenk, Lead-likeness, and synthetic accessibility scores of new derivatives

Compound	**Pains**	**Brenk**	**Lead Likeness**	**Synthetic Accessibility**
CW1	0 alert	0 alert	No, 1 violation: MW>350	5.81
CW2	0 alert	1 alert: triple - bond	No, 1 violation: MW>350	3.42
CW3	0 alert	0 alert	No; 2 violations: MW>350, Rotors>7	4.23
CW4	0 alert	0 alert	No; 2 violations: MW>350, Rotors>7	3.71
CW5	0 alert	0 alert	No; 2 violations: MW>350, XLOGP3>3.5	3.71

4.3.5 Lipophilicity

The lipophilicity of the compounds was predicted via five different models including; XlogP3, WlogP, iLogP, MlogP, and SILICOS-IT provided by SwissADME. The predicted values are shown in Table 4.13. iLogP values ranged between 2.64 to 3.66, demonstrating moderate lipophilicity across the compounds. XlogP3 values displayed variability with CW5 demonstrating the highest value. WlogP values were relatively higher, particularly for CW3, which presented the maximum predicted lipophilicity in this model. MlogP values were commonly lower, ranging between 0.60 to 2.57. SILICOS-IT predictions recognized CW5 as the most lipophilic compound and CW3 displayed the lowest value.

TABLE 4.13: SwissADME used to calculate lipophilic parameters of derivatives

Compound	**ILogP**	**XLogP3**	**WLog**	**MLogP**	**SILICOS-IT**
CW1	3.66	1.12	2.98	2.57	3.02
CW2	3.11	3.08	2.40	2.16	3.17

Table 4.13 continued from previous page

Compound	ILogP	XLogP3	WLog	MLogP	SILICOS-IT
CW3	2.92	2.78	3.44	0.60	1.97
CW4	2.64	2.50	2.70	1.68	2.54
CW5	2.72	3.63	2.95	2.05	3.47

4.3.6 Water Solubility Predictions

Water solubility of the compounds was predicted via three computational models: ESOL, Ali, and SILICOS-IT. The results are summarized in Table 4.14. According to the ESOL model, CW1 was classified as soluble, while others were classified as moderately soluble. The Ali model yielded similar classifications, with CW3 and CW5 predicted as poorly soluble. In contrast, the SILICOS-IT model predicted CW3 and CW5 as poorly soluble and the remaining compounds as moderately soluble.

TABLE 4.14: Water solubility prediction, values based on alternative models

Compound	Log S (ESOL)	Solubility Class	Log S (Ali)	Solubility Class	Log S (SILICOS-IT)	Solubility Class
CW1	-3.52	Soluble	-2.71	Soluble	-5.08	Moderately Soluble
CW2	-4.68	Moderately Soluble	-4.74	Moderately Soluble	-5.66	Moderately Soluble
CW3	-5.31	Moderately Soluble	-6.12	Poorly Soluble	-7.89	Poorly Soluble
CW4	-4.63	Moderately Soluble	-4.77	Moderately Soluble	-5.29	Moderately Soluble
CW5	-5.28	Moderately Soluble	-6.17	Poorly Soluble	-6.11	Poorly Soluble

4.4 *In silico* Toxicological Evaluation

4.4.1 Acute Toxicity and GHS Classification

Acute toxicity predictions for the synthesized derivatives were generated using the Pro-Tox 3.0 platform, and the results are presented in Table 4.15. The predicted

LD_{50} values ranged from 4000 to 4336 mg/kg. Based on these values, CW1 and CW3 were classified under GHS toxicity class 5, while others were categorized under class 4. These classifications indicate low to moderate acute toxicity across the series.

TABLE 4.15: Acute Toxicity and Toxicity Class

Compound	**LD_{50} (mg/kg)**	**GHS Toxicity Class**	**Toxicity Interpretation**
CW1	4000	5	May be harmful
CW2	4336	4	Harmful if swallowed
CW3	4000	5	May be harmful
CW4	4336	4	Harmful if swallowed
CW5	4336	4	Harmful if swallowed

4.4.2 Organ-Specific Toxicity Prediction

Organ toxicity predictions are summarized in Table 4.16. All compounds were predicted to be inactive for hepatotoxicity except CW3 which is predicted to be active. While all compounds were predicted to be active for neurotoxicity except CW3 which is predicted inactive. However, respiratory toxicity and nephrotoxicity were predicted to be active for all compounds, while cardiotoxicity was predicted to be inactive across all compounds.

TABLE 4.16: Organ Toxicity Prediction of Synthesized Compounds

Compound	**Hepato toxicity**	**Neuro toxicity**	**Nephro toxicity**	**Respiratory toxicity**	**Cardio toxicity**
CW1	Inactive (0.64)	Active (0.88)	Active (0.76)	Active (0.85)	Inactive (0.85)
CW2	Inactive (0.59)	Active (0.90)	Active (0.77)	Active (0.83)	Inactive (0.83)
CW3	Active (0.54)	Inactive (0.50)	Active (0.60)	Active (0.85)	Inactive (0.80)
CW4	Inactive (0.57)	Active (0.94)	Active (0.79)	Active (0.85)	Inactive (0.84)
CW5	Inactive (0.52)	Active (0.85)	Active (0.67)	Active (0.92)	Inactive (0.82)

4.4.3 Systemic and Genetic Toxicity Prediction

Systemic and genetic toxicity predictions are shown in Table 4.17. CW5 was predicted to be active for carcinogenicity, whereas the remaining compounds were predicted to be inactive. All derivatives were predicted to be inactive for mutagenicity and cytotoxicity.

Clinical toxicity was predicted to be active across all compounds. Immunotoxicity predictions varied, with CW2 showing active immunotoxicity, while the remaining derivatives were predicted to be inactive.

TABLE 4.17: Systemic and Genetic Toxicity

Compound	**Carcino genicity**	**Immuno toxicity**	**Muta genicity**	**Cytotoxicity**	**Clinical Toxicity**
CW1	Inactive (0.63)	Inactive (0.69)	Inactive (0.59)	Inactive (0.73)	Active (0.89)
CW2	Inactive (0.61)	Active (0.90)	Inactive (0.53)	Inactive (0.75)	Active (0.87)
CW3	Inactive (0.61)	Inactive (0.77)	Inactive (0.69)	Inactive (0.67)	Active (0.54)
CW4	Inactive (0.58)	Inactive (0.82)	Inactive (0.59)	Inactive (0.64)	Active (0.82)
CW5	Active (0.89)	Inactive (0.57)	Inactive (0.72)	Inactive (0.70)	Active (0.70)

4.5 Structural Analysis of Target Proteins

Structural analysis was done to evaluate the stability, quality, and suitability of the protein structures for subsequent computational studies. Key parameters, including resolution, R-value, unit cell geometry, and Ramachandran plot statistics were used to evaluate structural assessment.

These parameters are widely accepted indicators of model accuracy and are essential for ensuring meaningful molecular interaction and docking analyses.

4.5.1 OmpF (PDB ID: 4KRA)

The OmpF protein has resolution of 3.32 Åand an R-value of 0.339, demonstrating a well-defined protein structure. The unit cell angles lie at 90° and the unit cell dimensions observed were consistent with reported outer membrane porin structures.

Analysis of Ramachandran plot shown in Figure 4.9 displayed that 98.0% of amino acid residues were placed within the allowed regions of the phi (ϕ) and psi (ψ) angles. This proportion reflects good stereochemical quality and proposes minimal strain in the protein backbone.

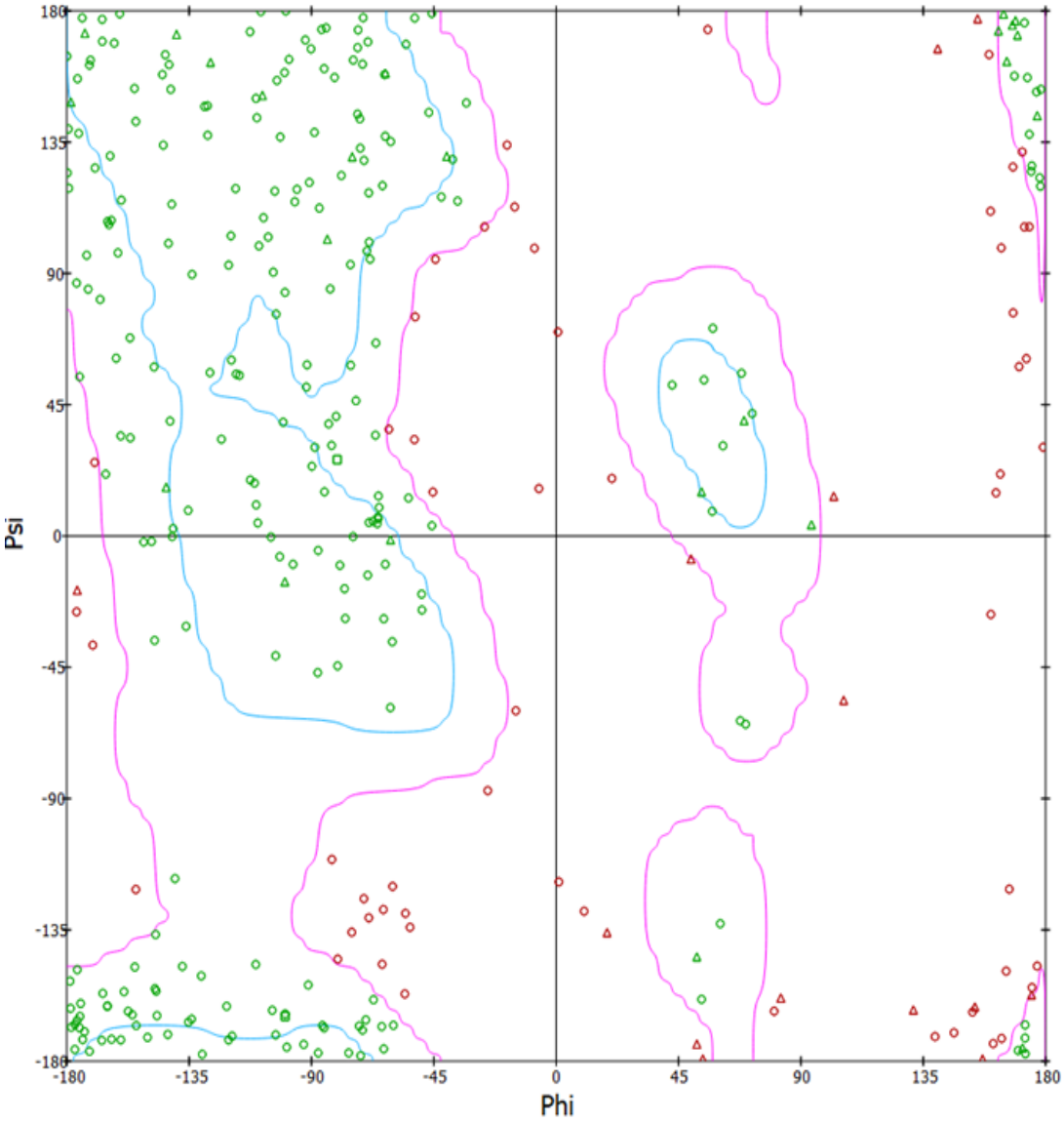

FIGURE 4.9: Structural analysis of OmpF

4.5.2 Topoisomerase II (PDB ID: 5BTC)

The selected protein shows 2.55 Åresolution and an R-value of 0.250, reflecting refined quality. The unit cell geometry with 90° angles, designate consistent crystal packing.

Evaluation of Ramachandran plot in Figure 4.10 displayed 98.0% of residues lie in the permitted regions, confirming favorable backbone conformations and structural stability. This level of conformational precision is particularly important for enzymes such as topoisomerase II, where accurate folding is essential for catalytic function.

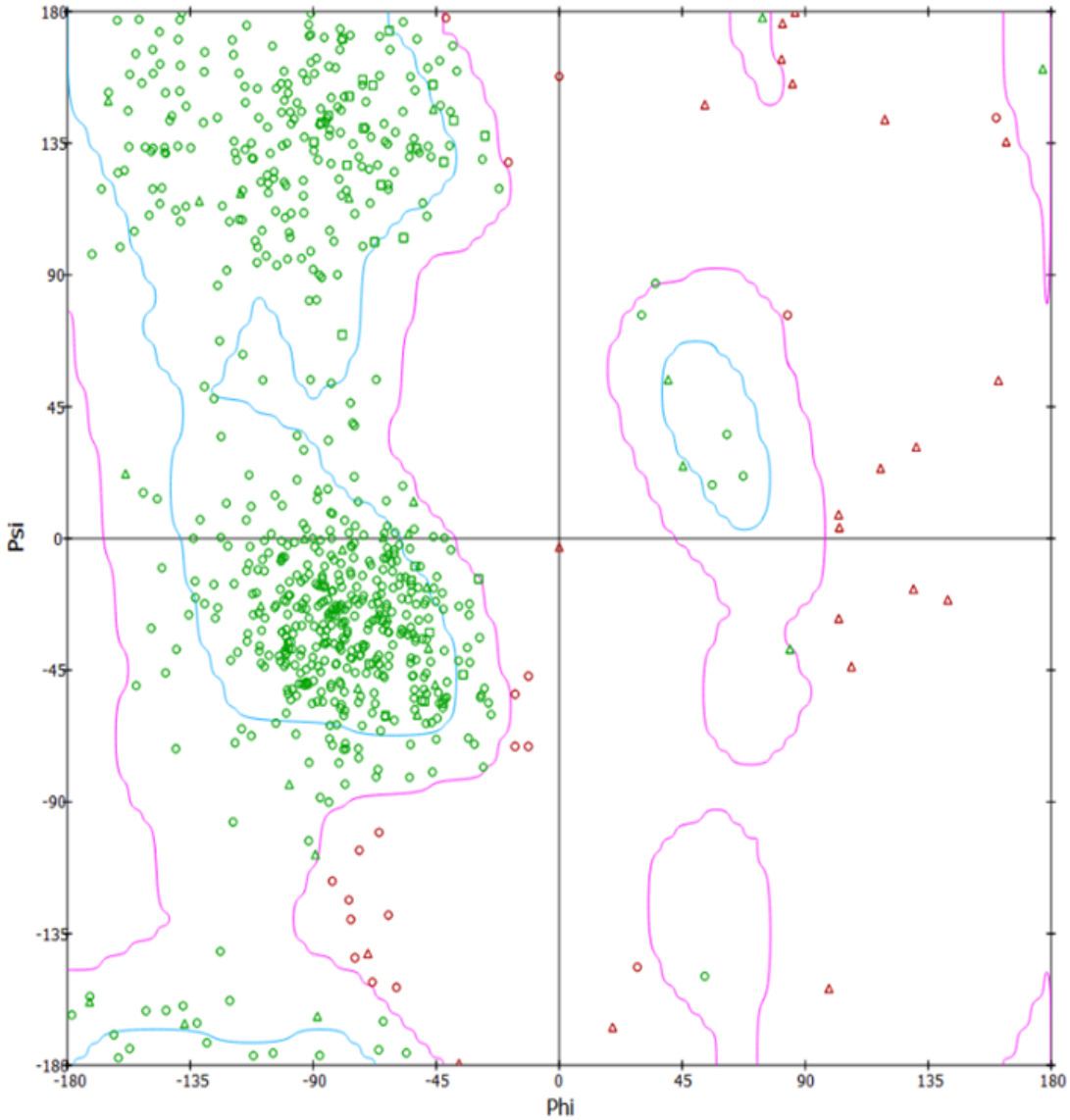

FIGURE 4.10: Structural analysis of Topoisomerase II

4.5.3 Multi-drug Efflux Pump (PDB ID: 8GJL)

The selected protein structure has a resolution of 3.44 Å. The unit cell angles and dimensions were in acceptable limits. Analysis of Ramachandran Figure 4.11 showed that 98.0% of amino acid residues fell within the allowed conformational regions, indicating good stereochemical quality and minimal structural distortion.

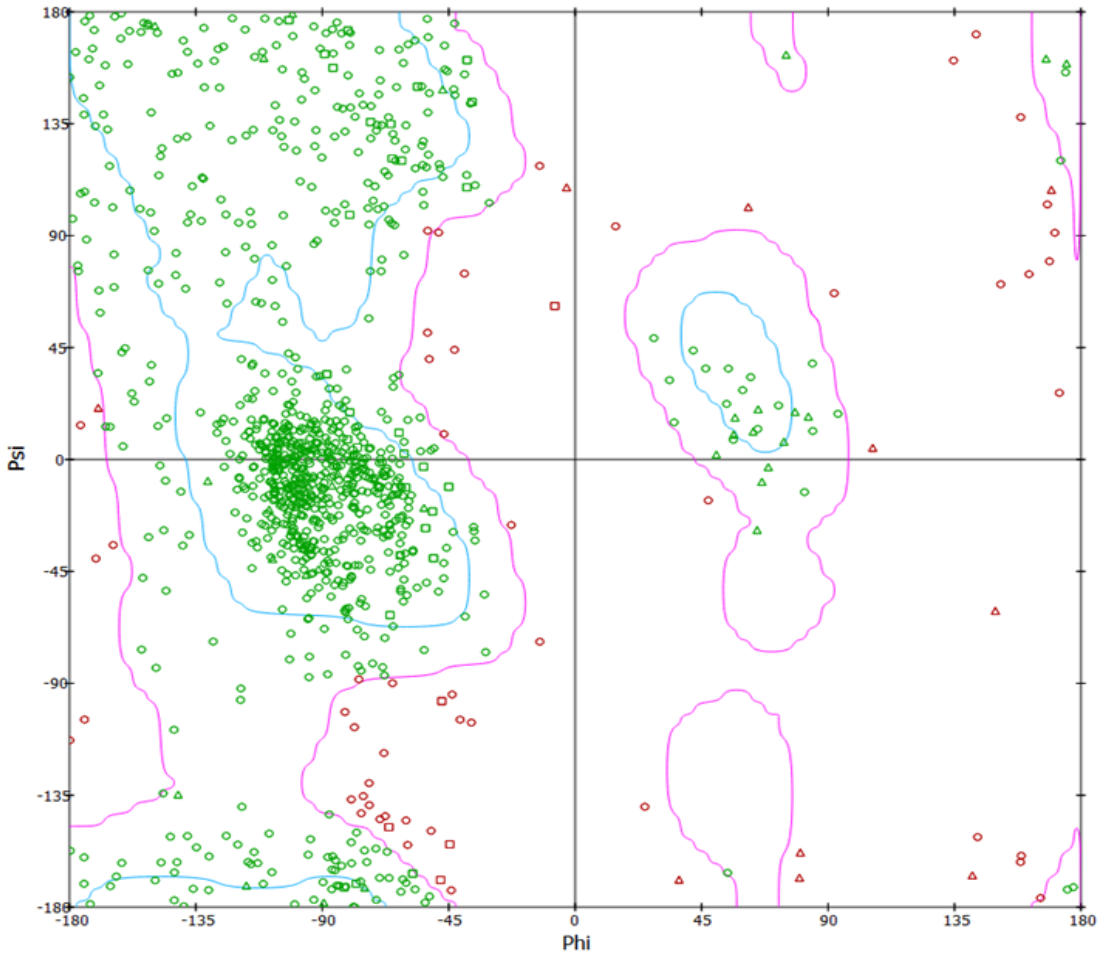

FIGURE 4.11: Structural analysis of Multi-drug Efflux Pump

4.5.4 Assessment of Binding Interaction across Multiple Proteins

Molecular docking was carried out to assess the interaction of synthesized compounds with the bacterial target proteins. Docking simulations were run with AutoDock Vina, and binding affinities were calculated using the estimated binding free energy values (kcal/mol), which indicate the stability of the ligand protein complexes. The docking study revealed precise information about the ligands'

binding mechanisms and interaction patterns within the active regions of target proteins. The produced compounds displayed significant binding affinities against OmpF, Topoisomerase II, and the multidrug efflux pump proteins, as shown in Tables 4.18-4.20. Compared to the reference ciprofloxacin, most compounds had higher binding energies and developed various non-covalent interactions, like π-alkyl, π-π stacking, hydrogen bonding, and van der Waals interactions. These excellent docking results indicate that the synthesized compounds have strong and specific protein-ligand interactions, implying that they could interfere with bacterial permeability, DNA replication, and efflux mechanism.

4.5.4.1 Protein 1: OmpF (4KRA)

Molecular docking was performed to assess the binding of the synthesized compounds against the OmpF protein. The docking scores and interaction profiles revealed that all synthesized compounds exhibited higher binding affinities compared to the standard ciprofloxacin, indicating their enhanced potential to interact with the OmpF active site.

TABLE 4.18: Docking analysis of compounds in OmpF active site: Binding affinity, interaction residues and bond types

Compound	**Binding Affinity (kcal/mol)**	**Bonding Interaction Type**	**Interacting with Amino Acid Residues**	**Bond Type with Ligand**
CW1	-9.8	π-Alkyl, Conventional hydrogen bond, Alkyl, Carbon-hydrogen bond, π-π T-shaped	TYR A:112, TYR A:301, ARG A:268, ASP A:108, SER A:114, PRO A:111, TRP A:309, MET A:109, ALA A:121	Aromatic C-H, Aromatic ring, C=O, OH
CW2	-8.8	π-Alkyl, Conventional hydrogen bond, Alkyl, Carbon-hydrogen bond, π-π T-shaped, Van der Waals	TYR A:301, THR A:299, ARG A:268, ASN A:307, ASP A:108, ARG A:60, ARG A:130, GLY A:120, GLU A:116 TYR A:112, ARG A:20, ALA A:110	Aromatic C-H, Aromatic ring, Alkyl chain, C=O, OH

Continued from previous page

Compound	**Binding Affinity**	**Bonding Interaction Type**	**Interacting with Amino Acid Residues**	**Bond Type with Ligand**
CW3	-8.9	π-Alkyl, Conventional hydrogen bond, π-π T-shaped, π-π stacked, Carbon-hydrogen bond	ARG A:20, TYR A:36, LYS A:16, ALA A:110, ASP A:108, TYR A:112, TRP A:309, TYR A:36, ASN A:307, ARG A:130	Aromatic C-H, Aromatic ring, NH-NH, C=O, OH
CW4	-9.2	π-Alkyl, Conventional hydrogen bond, Alkyl, Carbon-hydrogen bond, Unfavorable donor-donor, π-Cation	SER A:114, TYR A:36, ARG A:20, ARG A:268, ARG A:60, VAL A:18, GLY A:120, ALA A:110, THR A:299, TYR A:301, TRP A:309, ASP A:108, GLU A:116, ARG A:130, PHE A:113, LYS A:16, MET A:109	Aromatic C-H, C=O, OH, Aromatic-alkyl, Alkyl chain
CW5	-9.6	π-Alkyl, Conventional hydrogen bond, Alkyl, Carbon-hydrogen bond, π-π stacked, π-π T-shaped	TYR A:301, GLY A:120, ARG A:268, ASP A:108, TYR A:112, PRO A:111, TRP A:309, MET A:109	Aromatic C-H, Aromatic ring, C=O, NH
Ciprofloxacin	-6.9	Conventional hydrogen bond, π-π T-shaped, Unfavorable donor-donor, Carbon-hydrogen bond, Van der Waals, π-cation	TYR A:36, ARG A:20, TYR A:301, TYR A:112, ASN A:307, ARG A:60 MET A:109, ARG A:20, PRO A:111, LYS A:16, TRP A:309, ASP A:108, ALA A:110, ASN A:307	Aromatic C-H, OH, N-H, N-H···H-N, Aromatic-cation

Molecular docking analysis of all synthesized compounds (CW1-CW5) exhibited strong and favourable binding with the OmpF active site, with docking scores ranging from -8.8 to -9.8 kcal/mol. Among them, CW1 showed the highest binding affinity (-9.8 kcal/mol), while CW2 showed lowest binding affinity (-9.2 kcal/mol), indicating CW1 has highly stable ligand-protein complex.

These compounds consistently interacted with key active site residues such as TYR112, TYR301, ARG268, ASP108, TRP309, MET109, PRO111, and GLY120 through a combination of π-π interactions, π-alkyl contacts, and conventional hydrogen bonding, which collectively contributed to enhanced stabilization within the binding pocket.

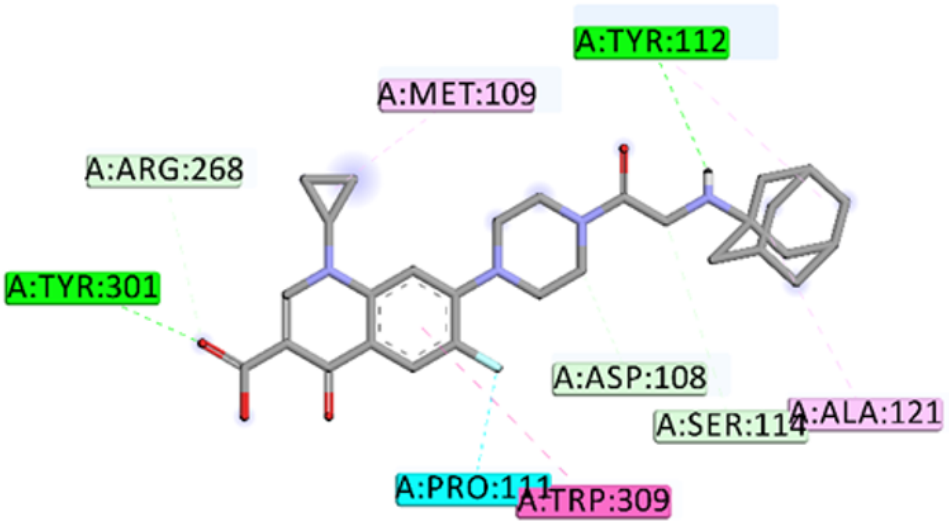

(a - CW1)

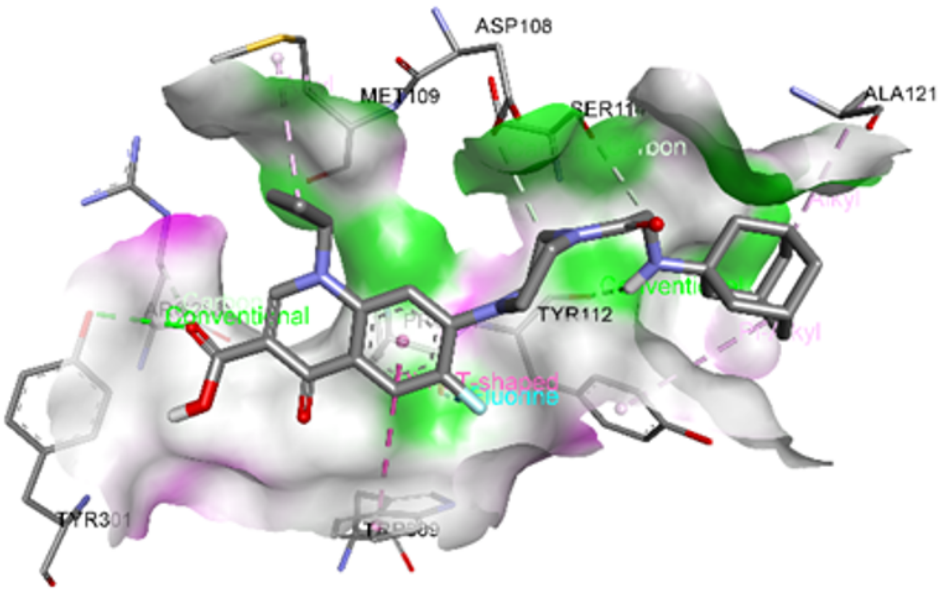

(b - CW1)

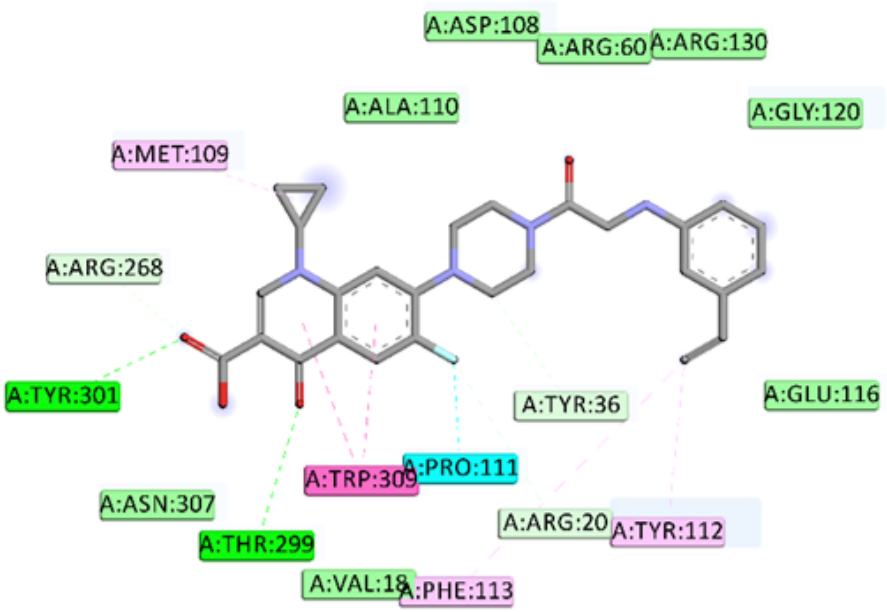
A:ASP:108
A:ARG:60
A:ARG:130
A:ALA:110
A:GLY:120
A:MET:109
A:ARG:268
A:TYR:301
A:TYR:36
A:GLU:116
A:PRO:111
A:TRP:309
A:ASN:307
A:ARG:20
A:TYR:112
A:THR:299
A:VAL:18
A:PHE:113

(a - CW2)

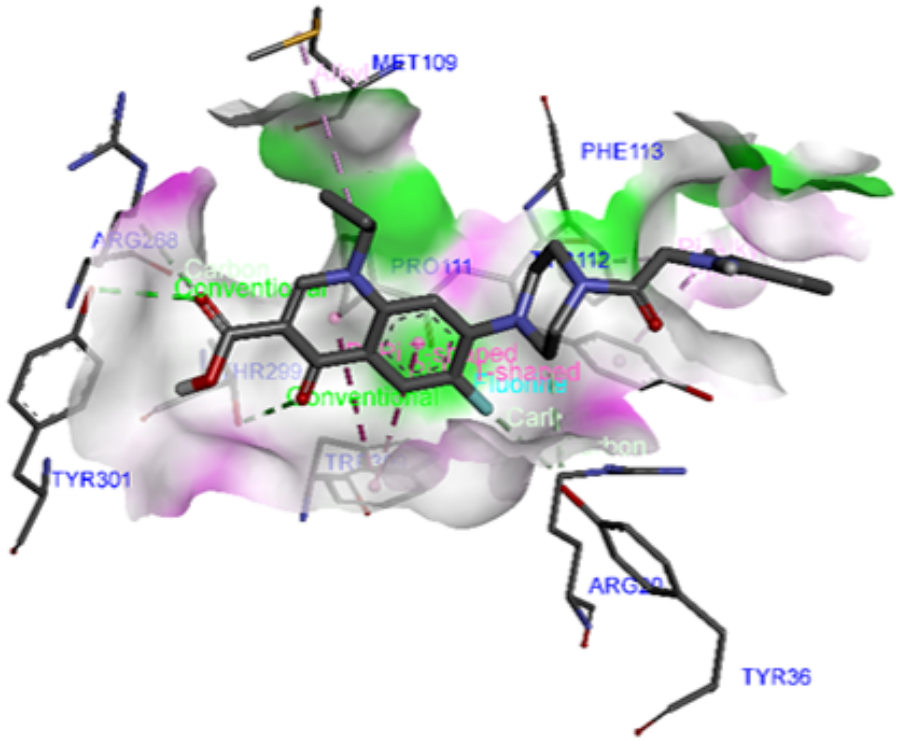
MET109
PHE113
TYR301
TYR36

(b - CW2)

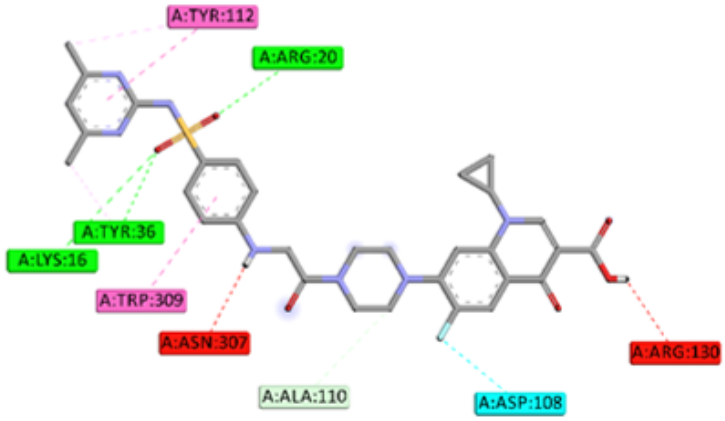

(a - CW3)

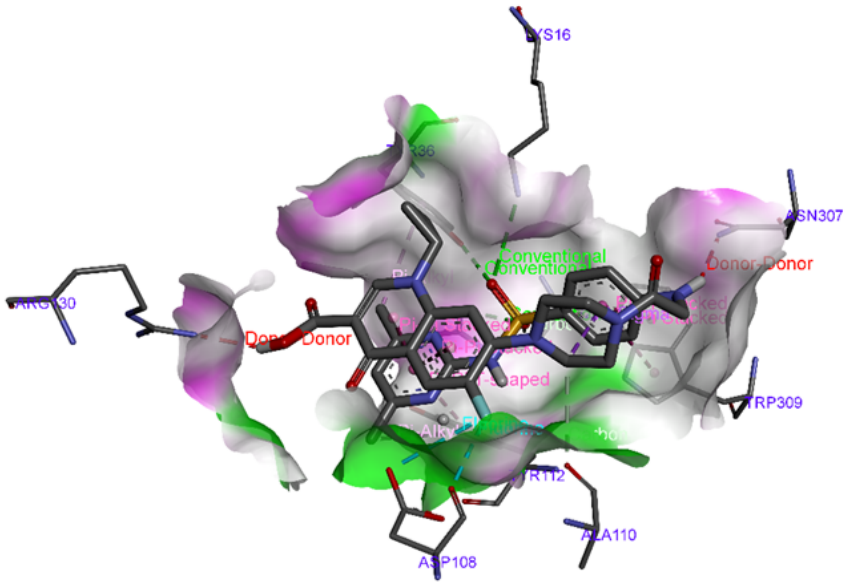

(b - CW3)

FIGURE 4.12: Illustration of molecular docking with compound CW1, CW2 and CW3 against OmpF

In comparison, the reference drug ciprofloxacin showed relatively lower binding affinity (-6.9 kcal/mol), in spite of forming interactions with several important residues including TYR36, ARG20, TYR301, TYR112, TRP309, and ASP108. Whereas ciprofloxacin involved hydrogen bonding, π-π, and π-cation interactions,

the reduced docking score proposes weaker overall stabilization compared to the synthesized compounds. These findings show that the newly designed compounds, mainly CW1 and CW5, own superior binding potential toward OmpF, highlighting their potential as more effective antibacterial candidates than the standard drug.

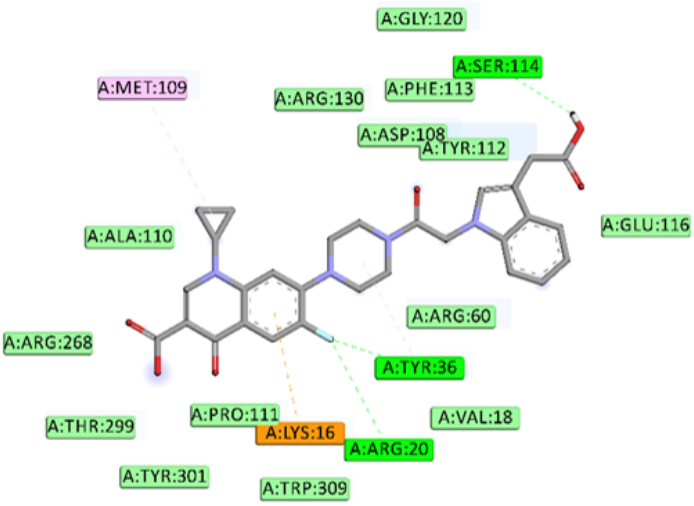

(a - CW4)

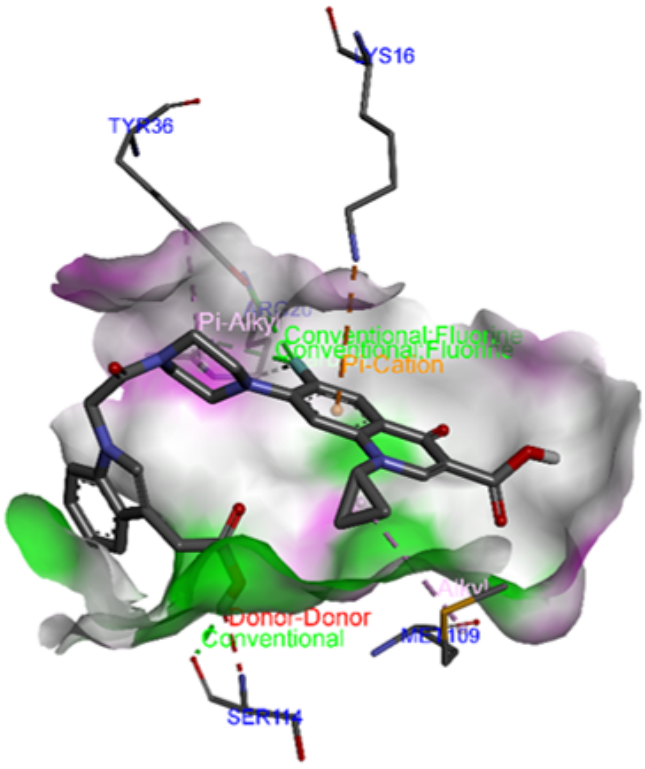

(b - CW4)

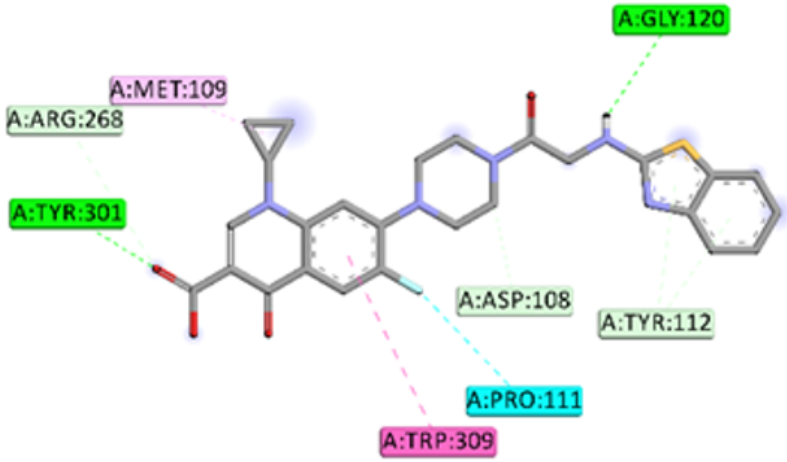

(a - CW5)

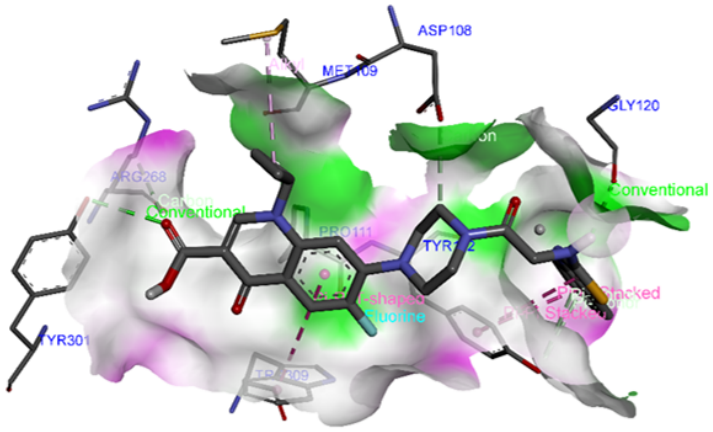

(b - CW5)

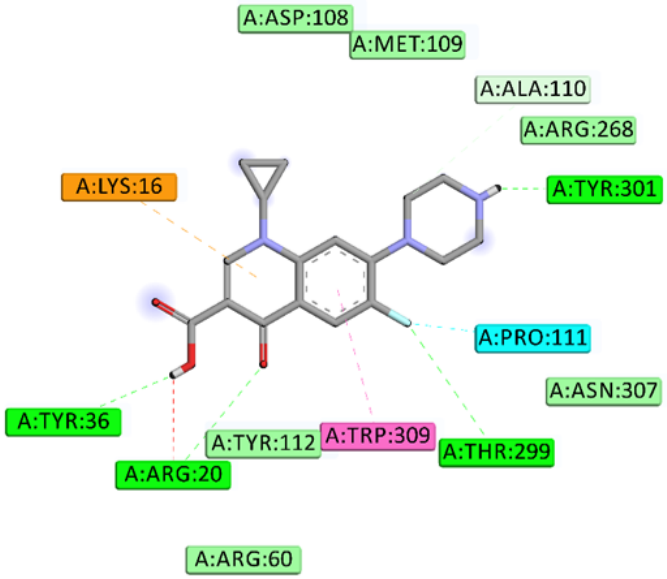

(a - Standard)

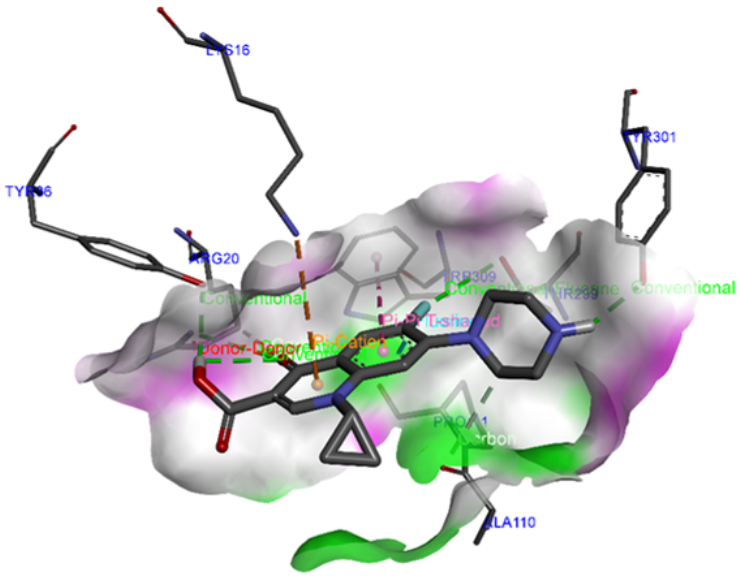

(b - Standard)

FIGURE 4.13: Illustration of molecular docking with compound CW4, CW5 and Standard against OmpF

To study the binding affinities and interaction patterns of the synthesized derivatives within the active site of the Topoisomerase II enzyme, molecular docking was conducted. All of the synthesized compounds showed higher binding affinities than standard ciprofloxacin, according to the docking results, suggesting that they might successfully interact with and inhibit Topoisomerase II.

TABLE 4.19: Docking analysis of compounds in Topoisomerase II active site: Binding affinity, interaction residues, and bond types

Compound	**Binding Affinity (kcal/mol)**	**Bonding Interaction Type**	**Interacting with Amino Acid Residues**	**Bond Type with Ligand**
CW1	-9.4	π-Alkyl, Conventional hydrogen bond, Alkyl, Carbon-hydrogen bond, π-Sigma	ASP A:157, ARG A:587, TYR A:569, ARG A:609, ASN A:602, GLU A:604, GLY A:606, ILE A:607, LEU A:591, ASP A:588, TYR A:156, ASP A:157, ILE A:607, ILE A:601, LYS A:603, LYS A:611, TYR A:610, TYR A:610, LYS A:603	Aromatic C-H, NH, C=O, Aromatic-σ, Aromatic-alkyl

Continued from previous page

Compound	**Binding Affinity**	**Bonding Interaction Type**	**Interacting with Amino Acid Residues**	**Bond Type with Ligand**
CW2	-8.5	π-Alkyl, Conventional hydrogen bond, Alkyl, Carbon-hydrogen bond, Van der Waals, π-Donor hydrogen bond	ASP A:94, SER A:104, GLY A:120, ASN A:121, ASN A:279, SER A:118, GLN A:277, TRP A:103, TYR A:276, VAL A:97, ALA A:126, GLN A:101, MET A:127, SER A:90, PRO A:124, ARG A:98, TYR A:93, PRO A:123	Aromatic C-H, Aromatic alkyl, C=O, π-H, NH,
CW3	-10.3	π-Alkyl, Conventional hydrogen bond, Alkyl, π-Anion, Carbon hydrogen bond	ILE A:607, ARG A:609, ASP A:532, HIS A:87, GLU A:615, ASP A:157, GLU A:459, PRO A:86, PRO A:86	Aromatic C-H, C=O, Aromatic anion, NH
CW4	-9.4	π-Alkyl, Conventional hydrogen bond, Alkyl, Carbon-hydrogen bond	ASP A:157, ARG A:609, GLY A:606, ASP A:605, GLU A:604, GLN A:608	Aromatic C-H, C=O, NH
		π-Cation, π-Anion, π-Sigma, Van der Waals	TYR A:610, ASP A:157, ARG A:159, ILE A:607, LYS A:603, ILE A6:01, LYS A:611, TYR A:569, LEU A:591, ARG A:587, GLU A:615	Aromatic-cation, Aromatic-σ
CW5	-9.4	Alkyl, Conventional hydrogen bond, π-Alkyl, Van der Waals, Carbon-hydrogen bond	ARG A:609, ARG A:587, ASP A:605, ASP A:157, ILE A:607, ILE A:607	Aromatic C-H, Aromatic alkyl, C=O, NH
Ciprofloxacin	-7.3	π-Alkyl, Conventional hydrogen bond, Carbon-hydrogen bond, π-π T-shaped, Van der Waals	ASN A:279, SER A:104, TRP A:103, GLY A:120, TYR A:276, TYR A:276, GLN A:101, PRO A:124, THR A:230, PRO A:275, LEU A:274, VAL A:278, ASN A:121	Aromatic C-H, C=O, NH, Aromatic-aromatic, Aromatic-alkyl

Molecular docking analysis of all synthesized compounds (CW1-CW5) exhibited strong and favourable binding affinities, ranging from -8.5 to -10.3 kcal/mol against Topoisomerase II. Amongst them, CW3 demonstrated the highest binding affinity (-10.3 kcal/mol), indicating the most stable ligand enzyme complex, while CW1, CW4, and CW5 showed comparable and strong binding scores (-9.4 kcal/mol). These compounds consistently formed multiple stabilizing interactions, including conventional hydrogen bonding, π-alkyl, π-cation/anion, and carbon hydrogen interactions, with key active site residues such as ARG609, ASP157, ILE607, ARG587, GLU604, GLY606, TYR610, and LYS603. The involvement of charged, polar, and hydrophobic residues contributed substantially to effective ligand anchoring and stabilization within the Topoisomerase II binding pocket. In contrast, the reference compound ciprofloxacin exhibited a lower binding affinity (-7.3 kcal/mol) despite interacting with several active site residues through hydrogen bonding, π-alkyl, π-π T-shaped, and van der Waals interactions.

Even though ciprofloxacin displayed appropriate lodging within the binding cavity, its weaker docking score recommends reduced overall stabilization linked to the synthesized derivatives. Collectively, these findings indicate that the newly designed compounds, particularly CW3 possess superior binding potential against Topoisomerase II.

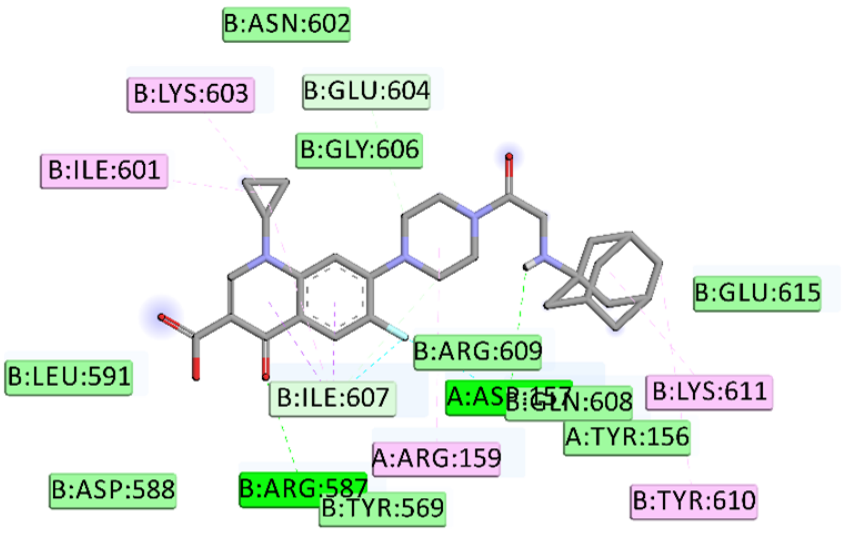

(a - CW1)

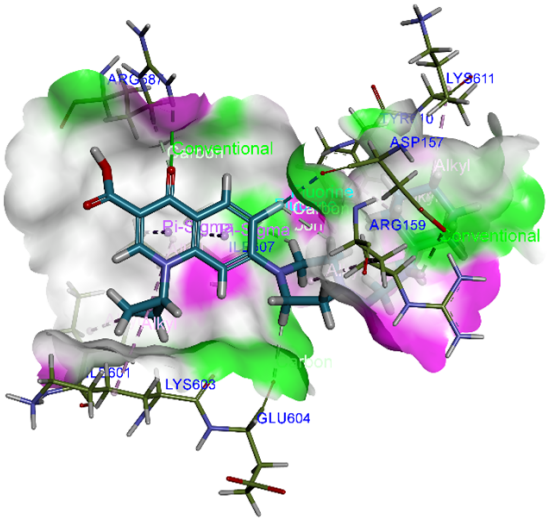

(b - CW1)

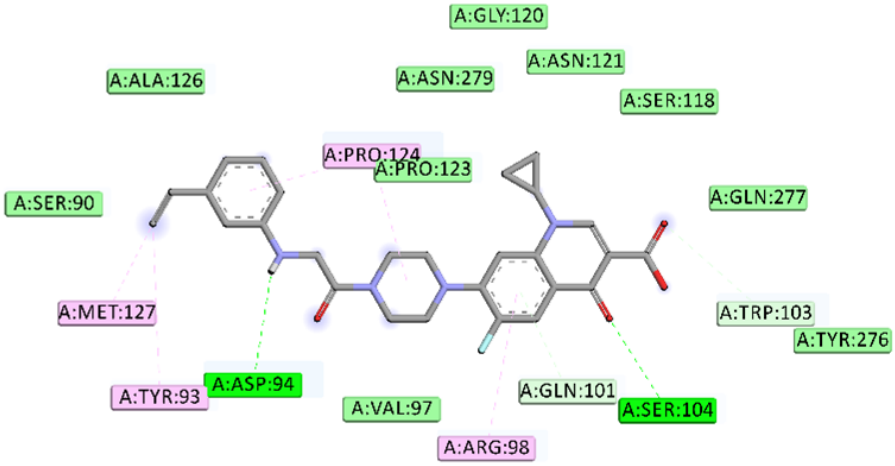

(a - CW2)

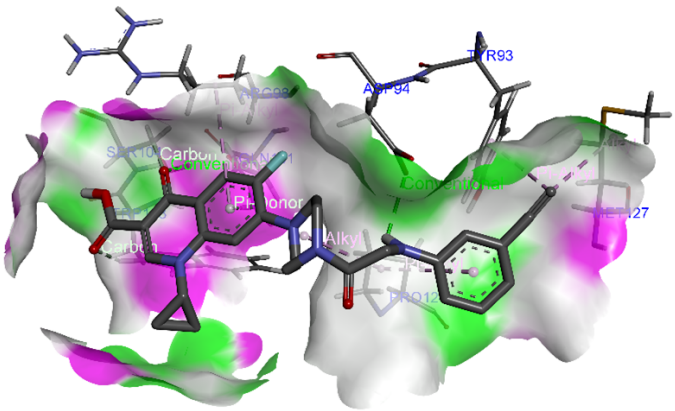

(b - CW2)

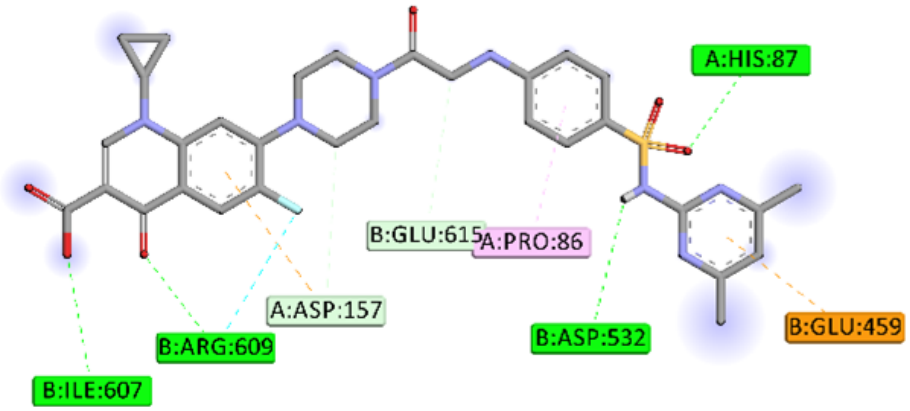

(a - CW3)

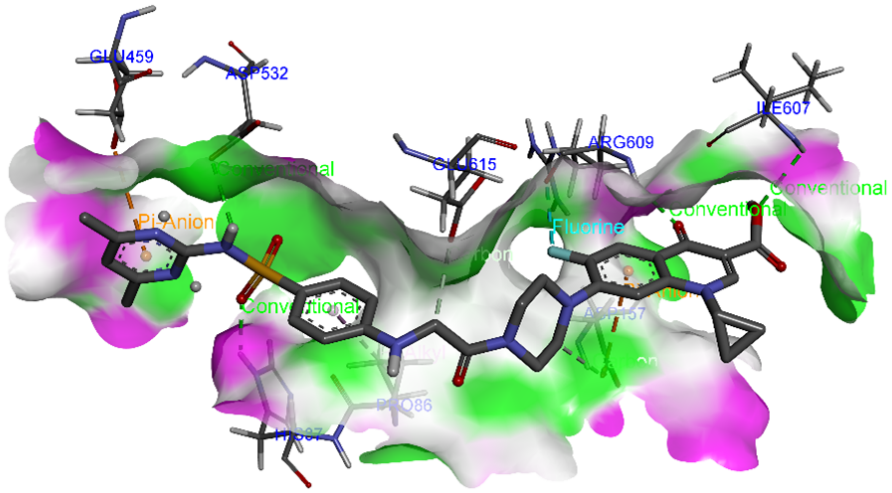

(b - CW3)

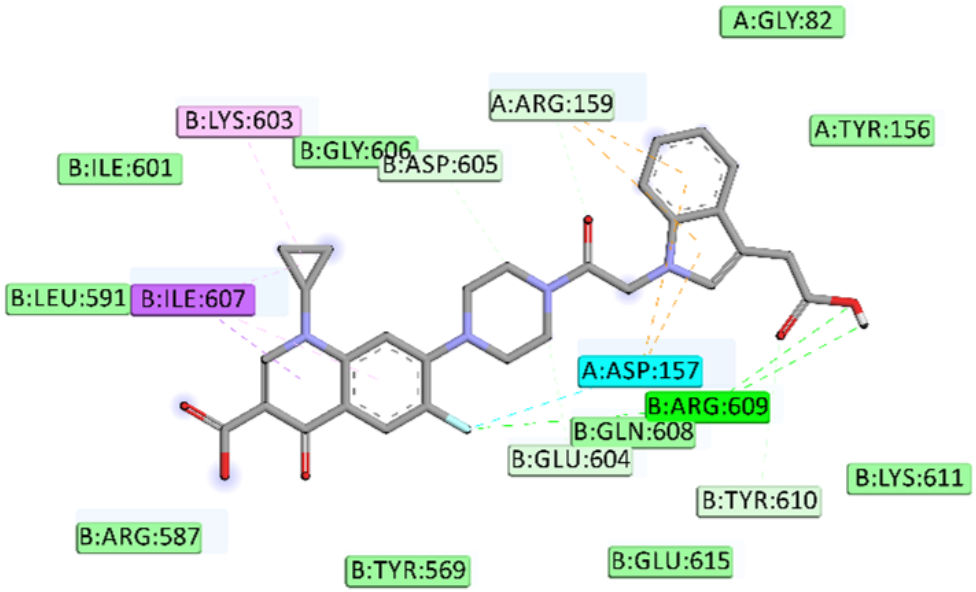

(a - CW4)

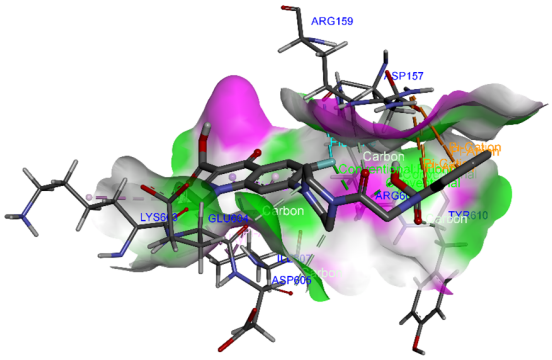

(b - CW4)

FIGURE 4.14: Illustration of molecular docking with compound CW1, CW2, CW3 and CW4 against Topoisomerase II

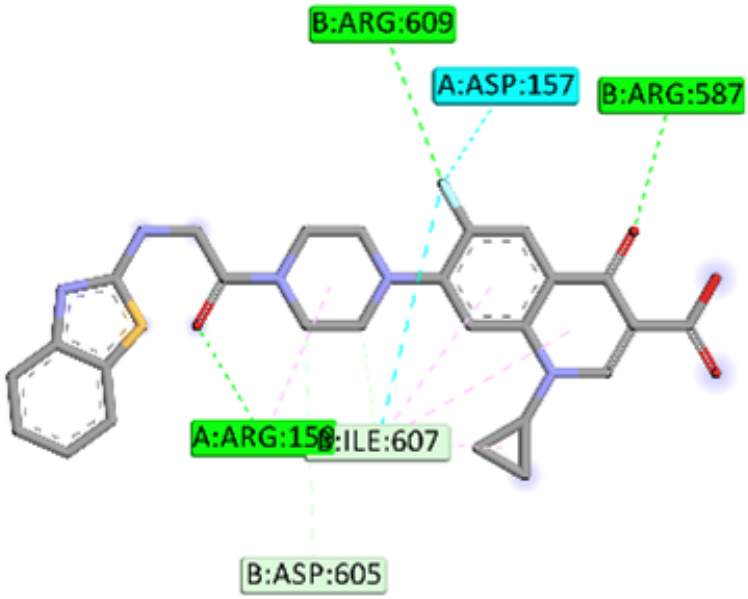

(a - CW5)

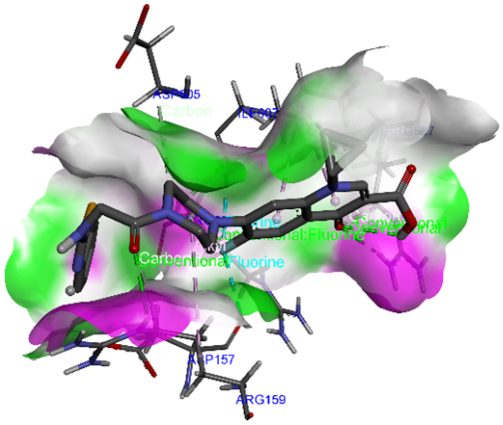

(b - CW5)

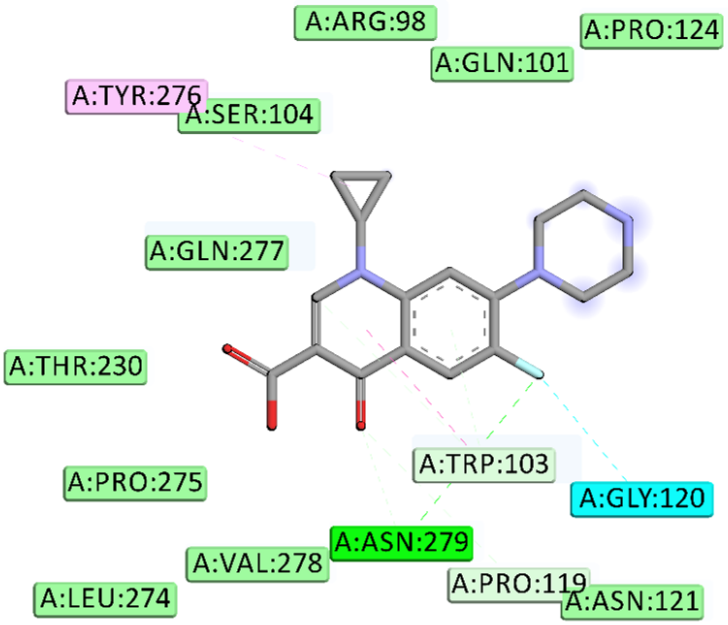

(a - Standard)

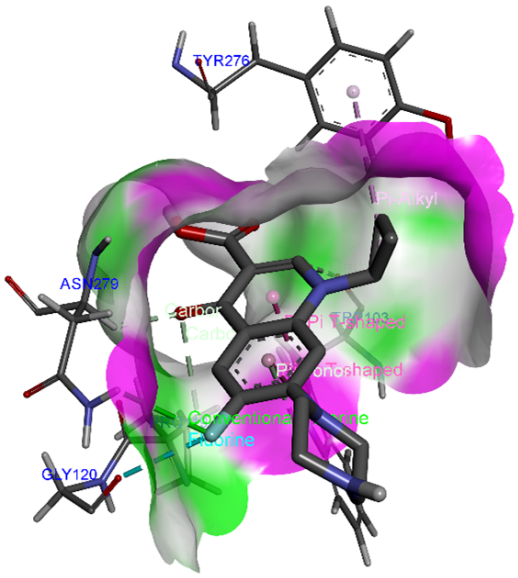

(b - Standard)

FIGURE 4.15: Illustration of molecular docking with compound CW5 and ciprofloxacin against Topoisomerase II

4.5.4.2 Protein 3: Multidrug Efflux Pump

The binding affinities and interaction patterns of the synthetic compounds within the active region of the multidrug efflux pump protein were assessed by molecular

docking. All synthesized compounds showed higher binding affinities than standard ciprofloxacin, according to the docking studies, indicating their potential to disrupt efflux-mediated drug resistance pathways.

TABLE 4.20: Docking analysis of compounds in Multi-drug Efflux Pump active site: Binding affinity, interaction residues, and bond types

Compound	**Binding Affinity (kcal/mol)**	**Bonding Interaction Type**	**Interacting with Amino Acid Residues**	**Bond Type with Ligand**
CW1	-9.7	Alkyl, Conventional hydrogen bond, π-Alkyl, Van der Waals, Carbon-hydrogen bond	SER A:132, SER A:133, TYR A:78, ARG A:130, LEU A:670, TYR A:93, GLN A:45, THR A:43, PRO A:41, ASN A:293, PHE A:613, GLU A:675, SER A:669, SER A:854, GLY A:855	Aromatic C-H, NH, OH, Alkyl chain, Aromatic-alkyl
CW2	-8.7	π-Alkyl, Conventional hydrogen bond, Alkyl, Van der Waals, π-π Stacked, Amide-π stacked, π-Sigma	ALA A:868, GLY A:867, ASN A:917, GLN A:922, GLY A:865, SER A:558 SER A:559, SER A:863, PHE A:553, LYS A:864, LEU A:925, GLU A:860, PHE A:871, GLU A:860, VAL A:861, ILE A:834, ASP A:835, SER A:558,	Alkyl chain, Aromatic-alkyl, C=O, NH, Amide-aromatic
CW3	-10	π-donor hydrogen bond, Conventional hydrogen bond, Van der Waals, π-π stacked, Carbon-hydrogen bond	ALA A:177, SER A:176, THR A:51, TYR A:50, ASN A:180, THR A:49, TYR A:751, TYR A:751, THR A:749, TYR A:50, SER A:176, ASN A:180	Aromatic C-H, C=O, NH, OH, π-donor
CW4	-9.8	Alkyl, Conventional H bond, Carbon-H bond, π-Anion, π-Donor hydrogen bond, π-π T-shaped, π-Alkyl	THR A:43, PRO A:41, TYR A:93, TYR A:78, GLN A:45, SER A:133, ASP A:174, SER A:132, SER A:615, GLU A:675, GLY A:855, ASN A:293, ASP A:174, LEU A:670, SER A:176, LEU A:668, PHE A:613	Aromatic C-H, C=O, OH, Aromatic-ring, NH, Aromatic π system

Continued from previous page

Compound	**Binding Affinity**	**Bonding Interaction Type**	**Interacting with Amino Acid Residues**	**Bond Type with Ligand**
CW5	-8.0	Alkyl, Conventional H bond, π-Donor H bond π-Alkyl	SER A:132, SER A:133, SER A:615, ASN A:293, ILE A:291, LEU A:617, PHE A:610, ASN A:180	Aromatic π system, NH, Aromatic-alkyl
Ciprofloxacin	-7.7	Alkyl, Unfavorable donor-donor	SER A:132, LEU A:668, SER A:134, GLN A:45, ASN A:293, LEU A:670	C=O, N-H, Aromatic C-H

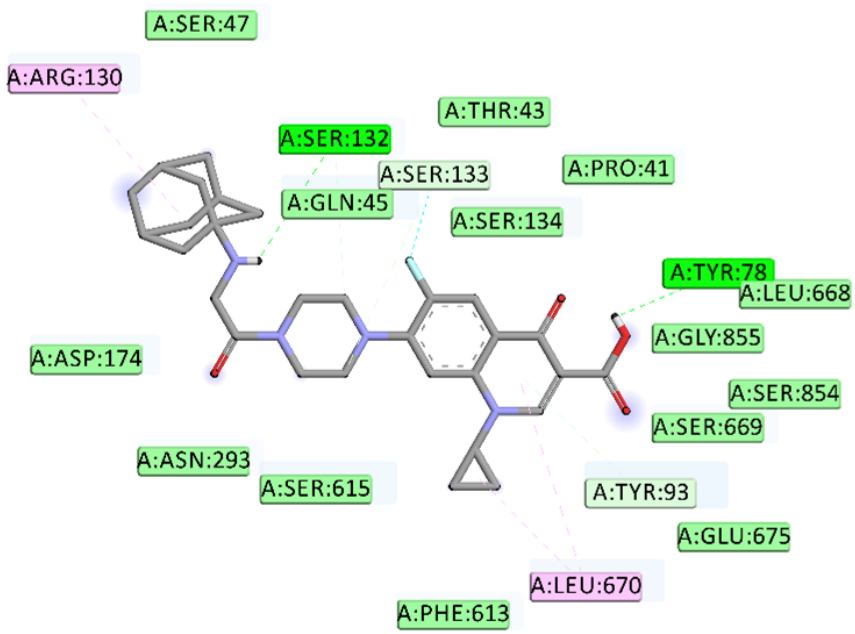

(a - CW1)

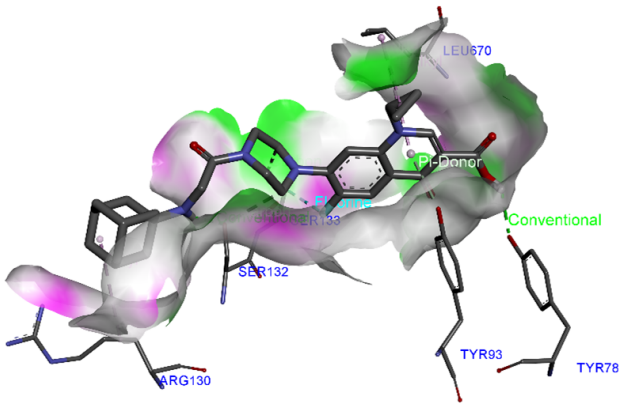

(b - CW1)

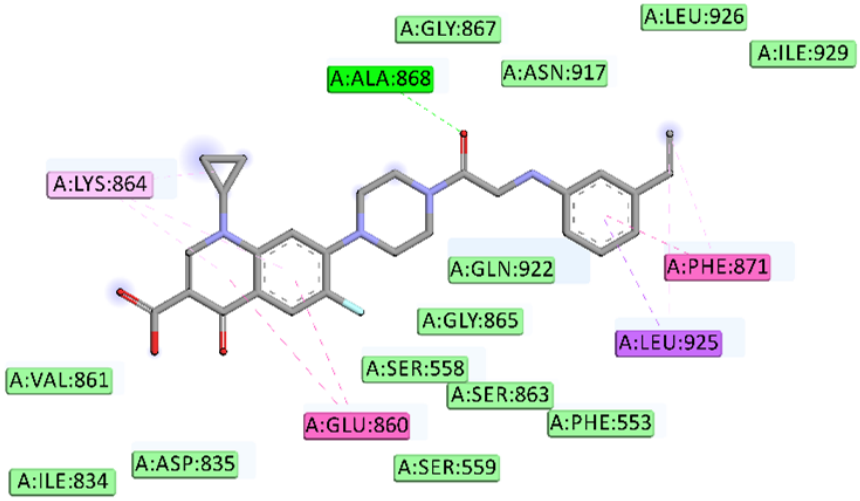

(a - CW2)

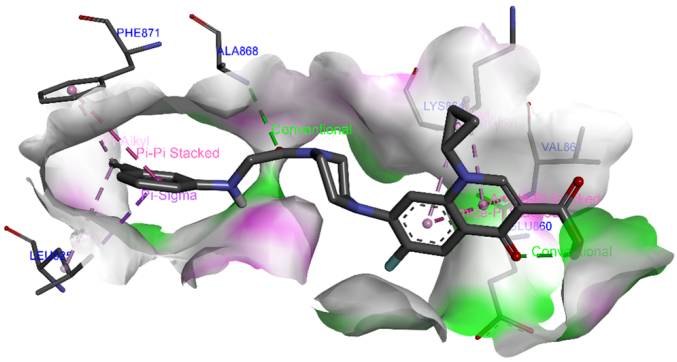

(b - CW2)

FIGURE 4.16: Illustration of molecular docking with compound CW1 and CW2 against Topoisomerase II

Molecular docking against the multidrug efflux pump showed that the synthesized compounds exhibited favourable binding affinities (-8.0 to -10.0 kcal/mol). Amongst them, CW3 showed the strongest binding affinity (-10.0 kcal/mol), where as CW5 showed lowest binding affinity (-8.0 kcal/mol).These synthesized compounds formed multiple stabilizing interactions, like π-alkyl, π-π stacking, van der Waals interactions, π-donor hydrogen bonding, conventional hydrogen bonding with vital residues such as SER132, SER133, ARG130, ASN293, TYR78, TYR93, GLU675, LEU670, GLY855, and PRO41. The involvement of polar, aromatic, and hydrophobic residues contributed significantly to effective ligand anchoring and stabilization within the efflux pump binding pocket.

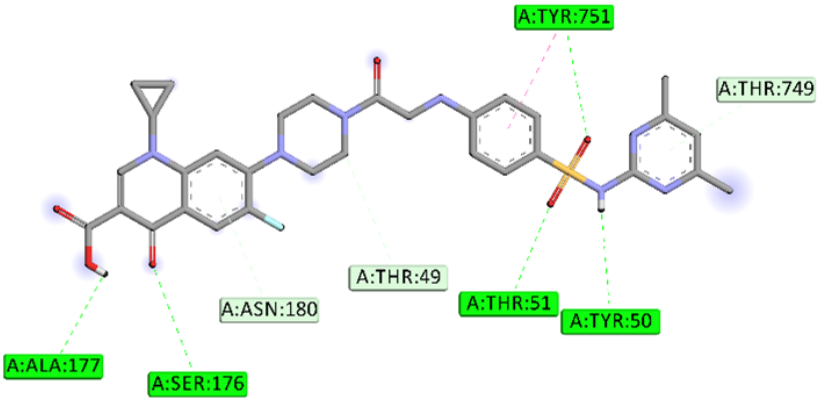

(a - CW3)

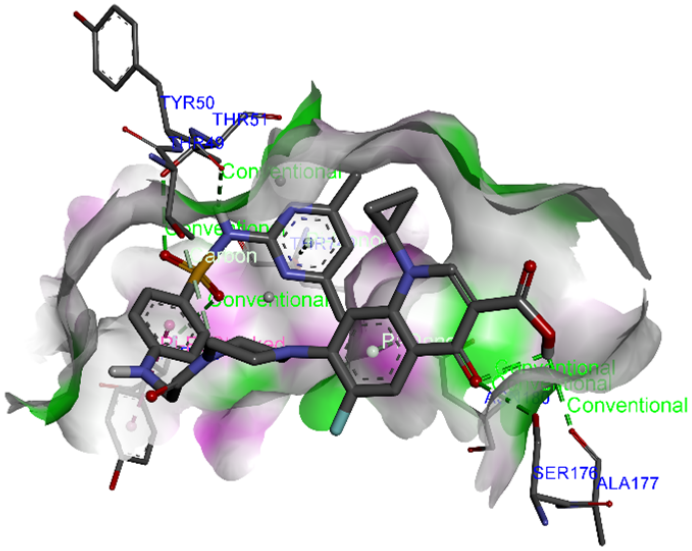

(b - CW3)

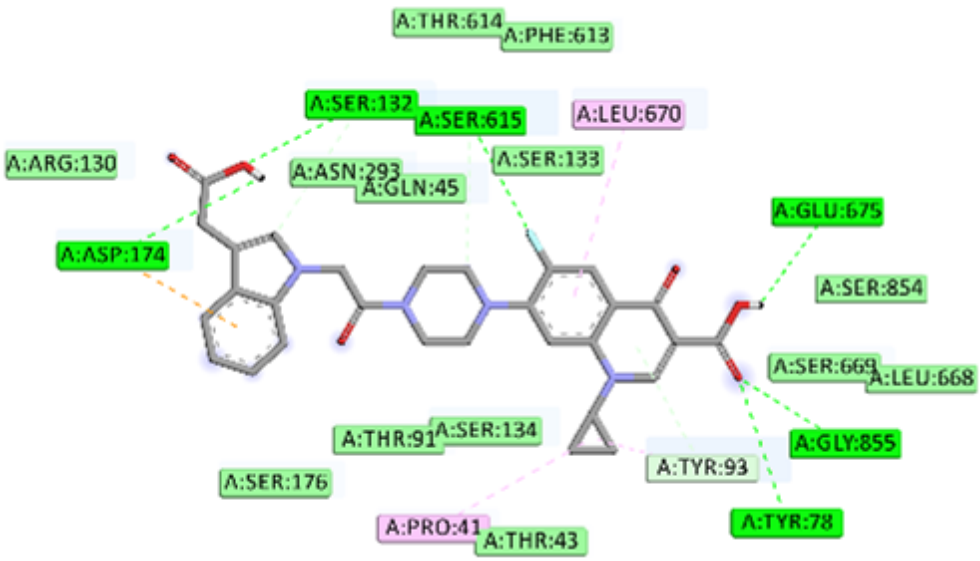

(a - CW4)

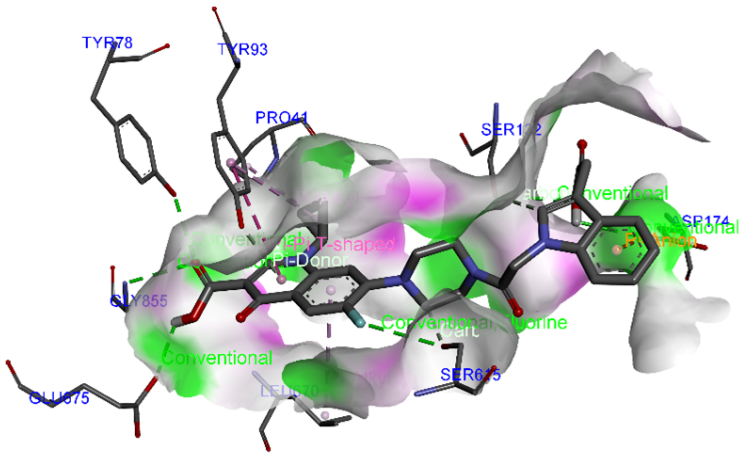

(b - CW4)

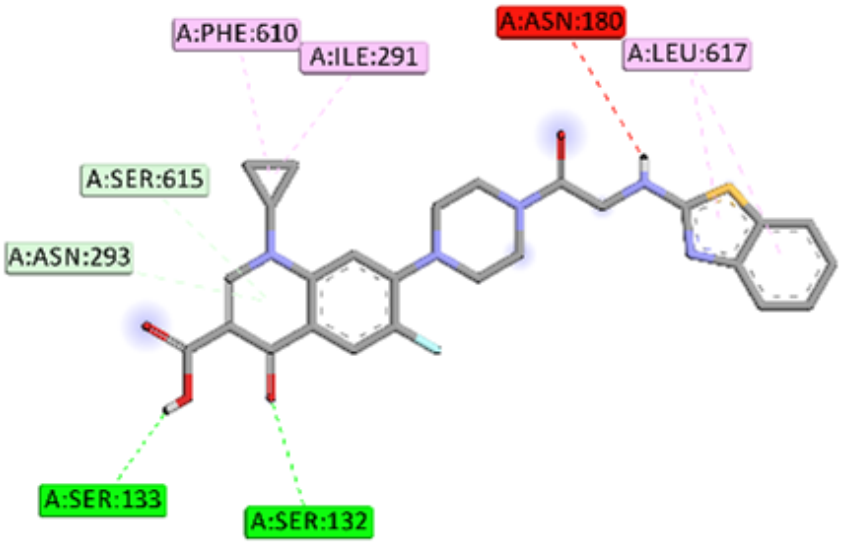

(a - CW5)

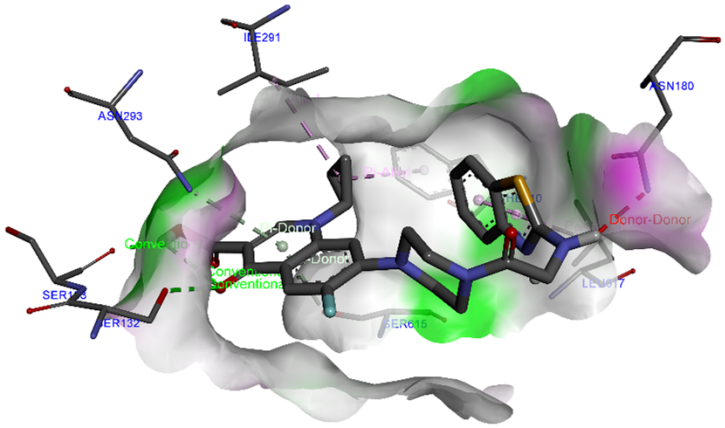

(a - CW5)

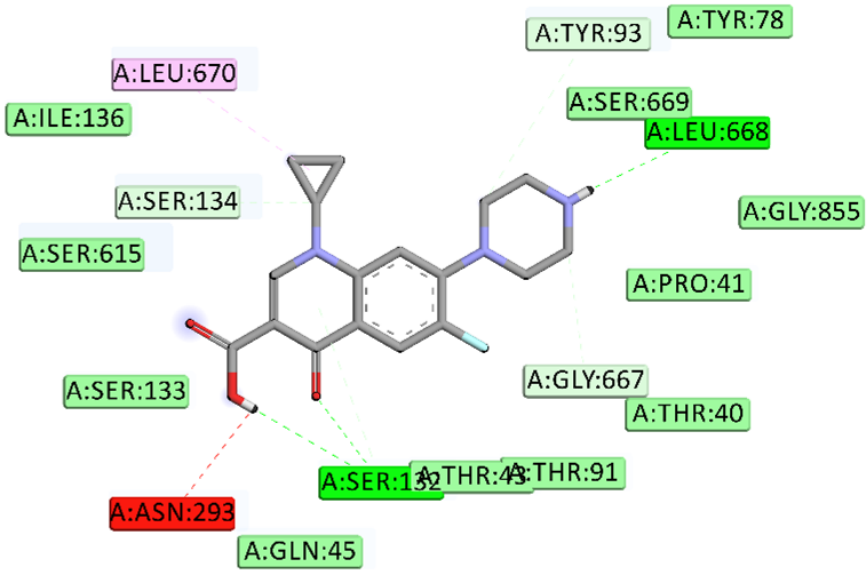

(a - Standard)

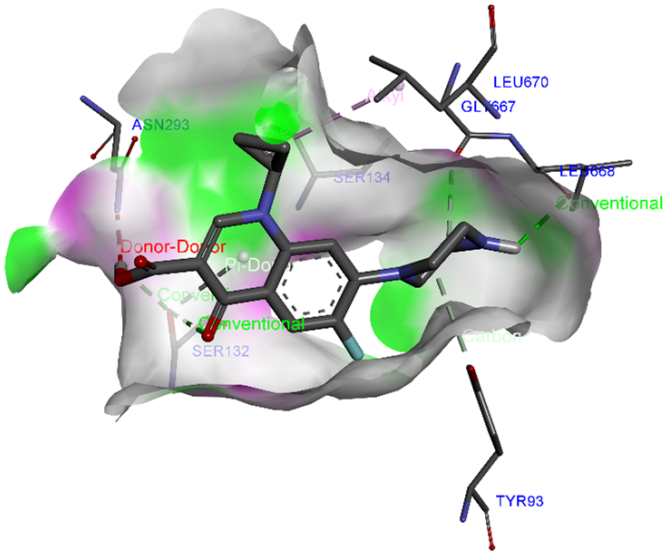

(b - Standard)

FIGURE 4.17: Illustration of molecular docking with compound CW3, CW4, CW5 and ciprofloxacin against Multi-drug Efflux pump

In contrast, the standard ciprofloxacin displayed low binding affinity (–7.7 kcal / mol) in spite of interacting with several overlapping residues through hydrogen bonding and hydrophobic contacts. Though relatively weaker docking score show reduced stabilization within the efflux pump cavity. Together, these findings propose that the synthesized derivatives, particularly CW3 own superior

binding potential against the multi-drug efflux pump compared to the standard drug. Comparative docking results confirmed that all synthesized compounds displayed stronger and more consistent binding affinities toward OmpF, Topoisomerase II, and the multi-drug efflux pump linked with ciprofloxacin. CW1 and CW5 displayed the most favorable interactions with OmpF, whereas CW3 presented the strongest binding against Topoisomerase II and the efflux pump. These improved affinities were led by multiple stabilizing non-covalent interactions, but ciprofloxacin exhibited weaker binding and fewer interactions. Overall, the outcomes highlight the superior multi-target binding potential of the synthesized derivatives, suggesting their promise in overcoming key bacterial resistance mechanisms.

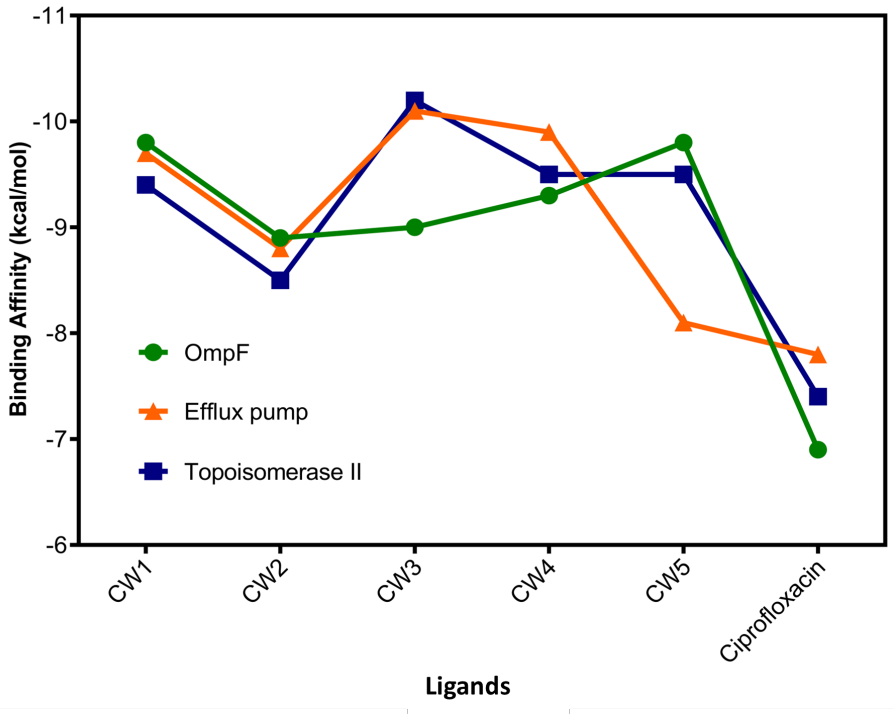

FIGURE 4.18: Illustration of binding affinities of Compounds

The Figure 4.18 illustrate comparison among binding affinities (kcal/mol) of synthesized compounds and standard against protein targets: OmpF, Efflux pump, and Topoisomerase II. Overall, CW3 displayed the strongest binding affinity against efflux pump and topoisomerase II targets, while CW5 displayed strong interaction with OmpF. Ciprofloxacin showed relatively weaker binding, mainly against

OmpF. The graph highlights variability in binding performance of synthesized derivatives comparative to the standard drug.

4.6 Biological Activities

4.6.1 Antibacterial Activity Against Non-Resistant Strains

The antibacterial efficacy of the synthesized compounds was evaluated against both non-resistant and resistant bacterial strains. The results for non-resistant strains are summarized in 4.21 as mean ± standard deviation of triplicate experiments.

All synthesized compounds showed comparable antibacterial activity against the bacterial strains at 0.05 μg/ml concentration, although their effectiveness varied.

TABLE 4.21: Assessment of antibacterial activity of synthesized compounds against non-resistant strains (ZOI mm, ±SD; n=3)

Compound	***E. coli***	***B. subtilis***	***S. aureus***	***P. aeruginosa***	***S. abony***
CW1	31.51±1.34	34.06±1.81	24.85±1.45	23.80±1.49	26.91±1.09
CW2	22.73±1.61	31.41±1.56	20.67±1.83	13.99±1.78	30.93±1.21
CW3	19.70±1.98	36.53±1.36	17.76±0.92	22.78±1.32	33.25±0.95
CW4	24.94±1.79	30.50±2.22	15.82±1.59	18.79±1.04	29.19±1.32
CW5	29.53±1.19	37.16±1.78	28.19±1.61	25.29±1.30	30.49±1.75
Ciprofloxacin	37.02±1.39	40.76±1.08	32.09±2.72	31.05±2.36	38.72±1.45

Against *E. coli*, CW1 showed the highest activity amongst the compounds (31.51 ± 1.34 mm), followed by CW5 (29.53 ± 1.19 mm), however CW3 showed comparatively lower activity (19.70 ± 1.98 mm).

For *B. subtilis*, CW5 demonstrated the strongest antibacterial effect (37.16 ± 1.78 mm), followed by CW3 (36.53 ± 1.36 mm) and CW1 (34.06 ± 1.81 mm). In the case of *S. aureus*, CW5 again showed the highest inhibition (28.19 ± 1.61 mm), while CW4 and CW3 displayed lower activity.

FIGURE 4.19: Zone of inhibition of synthesized compounds against non-resistant bacterial strains

The activity against *P. aeruginosa* was normally reduced compared to other strains, which is consistent with its known intrinsic resistance. Among the compounds, CW5 (25.29 ± 1.30 mm) and CW1 (23.80 ± 1.49 mm) exhibited relatively better activity, whereas CW2 showed the lowest inhibition (13.99 ± 1.78 mm). Against *S. abony*, CW3 demonstrated the highest antibacterial activity (33.25±0.95 mm), followed by CW2 and CW5, indicating comparatively better susceptibility.

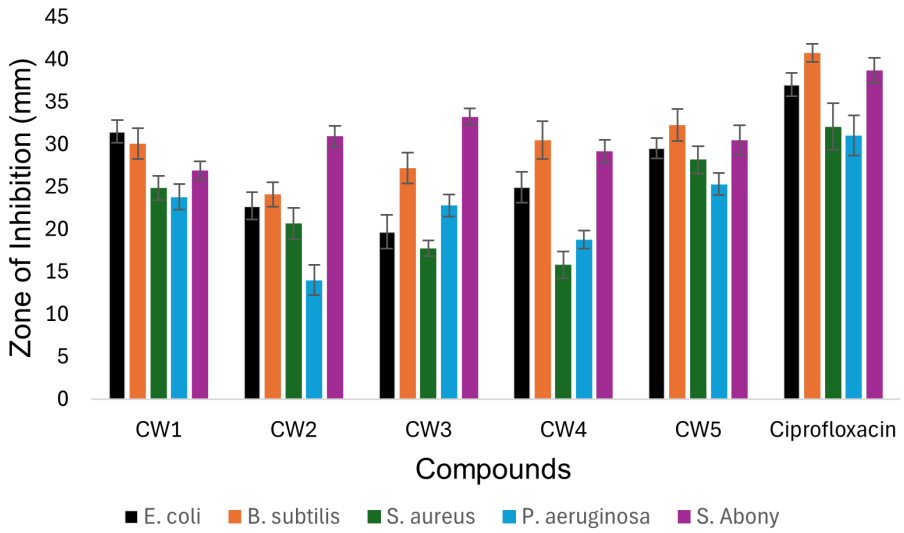

FIGURE 4.20: Illustration of Zone of inhibition by synthesized compounds against non-resistant bacterial strains

The Figure 4.20 illustrates the comparative zone of inhibition of synthesized ciprofloxacin derivatives (CW1–CW5) and standard ciprofloxacin against the tested bacterial strains. ciprofloxacin produced the largest zones of inhibition, ranging from 31.05 ± 2.36 mm against *P. aeruginosa* to 40.76 ± 1.08 mm against *B. subtilis*. However, some compounds, mainly CW5 and CW1, exhibited activity closer to the standard ciprofloxacin against gram-positive bacteria, whereas CW3 displayed notable activity against *S. abony* and *B. subtilis*. Overall, CW5 presented the better antibacterial activity against these strains. These findings indicate that structural alteration of ciprofloxacin influenced antibacterial activity.

4.6.2 Antibacterial Activity Against Resistant Strains

The antibacterial activity of the synthesized ciprofloxacin derivatives was further evaluated against resistant bacterial strains, including *E. coli, A. baumannii*, and *MRSA*. The results are presented as mean ± standard deviation of triplicate experiments in Table 4.22

TABLE 4.22: Assessment of antibacterial activity of synthesized compounds against resistant strains (ZOI mm, ±SD; n=3)

Compound	***E. coli***	***A. Baumannii***	***MRSA***
CW1	28.23±1.43	27.12±0.65	25.81±1.03
CW2	27.51±1.35	26.54±0.92	24.59±1.43
CW3	29.48±1.25	27.85±0.76	26.44±0.68
CW4	26.89±1.05	26.27±1.33	22.61±0.85
CW5	30.7±1.02	30.68±0.73	27.36±1.27
Ciprofloxacin	26.81±1.57	24.21±1.69	21.8±1.6

Against resistant *E. coli*, CW5 exhibited the highest antibacterial activity with a zone of inhibition of 30.7 ± 1.02 mm, followed by CW3 (29.48 ± 1.25 mm) and CW1 (28.23 ± 1.43 mm). CW2 (27.51 ± 1.35 mm) and CW4 (26.89 ± 1.05 mm) showed comparatively lower but still considerable activity. Notably, all synthesized compounds demonstrated activity comparable to or higher than ciprofloxacin (26.81 ± 1.57 mm).

In the case of resistant *A. baumannii*, CW5 again showed the strongest inhibition (30.68 ± 0.73 mm), followed by CW3 (27.85 ± 0.76 mm) and CW1 (27.12 ± 0.65 mm). CW2 (26.54 ± 0.92 mm) and CW4 (26.27 ± 1.33 mm) exhibited slightly lower activity among the derivatives. Importantly, all synthesized compounds displayed significantly higher antibacterial activity than ciprofloxacin (24.21 ± 1.69 mm) against this strain.

Similarly, against *MRSA*, CW5 demonstrated the highest antibacterial effect (27.36 ± 1.27 mm), followed by CW3 (26.44 ± 0.68 mm) and CW1 (25.81 ± 1.03 mm). CW2 (24.59 ± 1.43 mm) and CW4 (22.61 ± 0.85 mm) showed comparatively reduced inhibition; however, all compounds remained more active than ciprofloxacin (21.8 ± 1.6 mm).

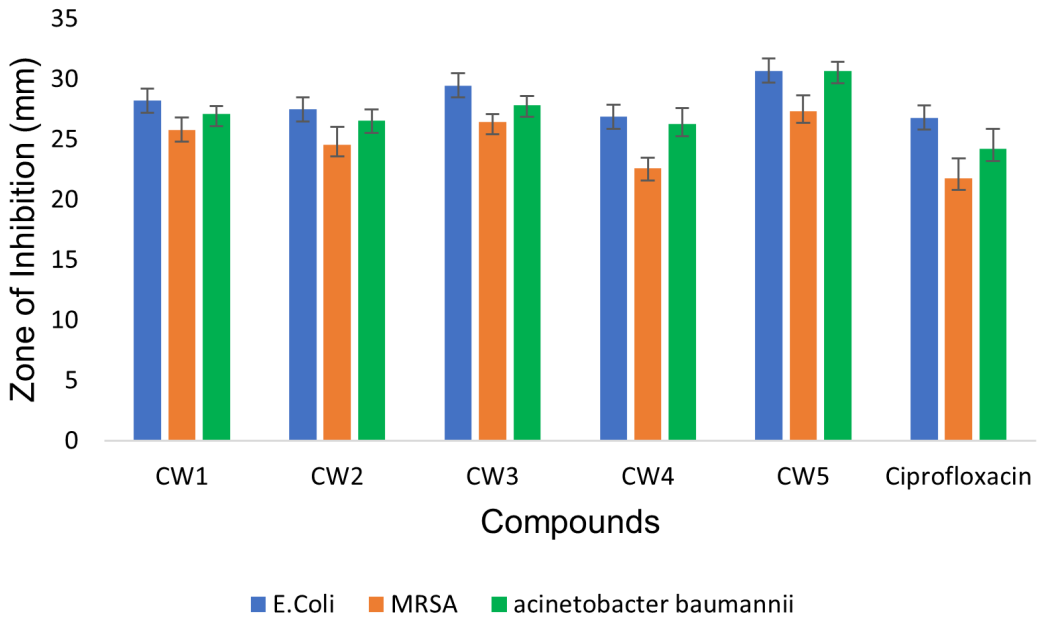

FIGURE 4.21: Illustration of Zone of inhibition by synthesized compounds against resistant bacterial strains

Overall, the synthesized ciprofloxacin derivatives exhibited strong antibacterial activity against resistant bacterial strains, with several compounds demonstrating superior efficacy compared to the standard drug. Among them, CW5 consistently emerged as the most potent compound across all tested resistant strains, followed by CW3 and CW1. These findings indicate that structural modification

of ciprofloxacin not only preserved antibacterial activity but also enhanced effectiveness against resistant pathogens, highlighting the potential of these derivatives as promising candidates for combating antimicrobial resistance.

A comparison between non-resistant and resistant bacterial strains revealed that the synthesized ciprofloxacin derivatives retained significant antibacterial activity across both categories.

While the compounds exhibited strong activity against non-resistant strains, their efficacy against resistant strains remained comparable and, in several cases, even superior to the standard ciprofloxacin.

Notably, CW5 consistently demonstrated the highest antibacterial activity against both non-resistant and resistant strains, followed by CW3 and CW1, indicating that these derivatives maintained their effectiveness despite the presence of resistance mechanisms.

This suggests that structural modification of the ciprofloxacin scaffold may contribute to overcoming bacterial resistance, potentially by enhancing interaction with target sites or reducing susceptibility to common resistance pathways.

Overall, these findings highlight the potential of the synthesized derivatives as promising candidates for the development of new antibacterial agents targeting antimicrobial resistance.

4.6.3 Antifungal Activity

The antifungal effectiveness of the synthesized derivatives assessed against *Aspergillus niger*, *Aspergillus flavus* and *Candida albican* through disk diffusion method. To ensure reproducibility, every experiment was conducted in triplicate under standardized setting.

The synthesized compounds were evaluated at predetermined concentrations. The fungal growth inhibition was observed by measuring the presence or absence of clear regions around the disks following incubation period.

FIGURE 4.22: Illustration of Antifungal activity against synthesized compounds

The results revealed that none of the compounds produced detectable ZOI against any of the fungal strains, demonstrating lack of antifungal activity under the experimental conditions. Likewise, the standard drug included in the assay did not exhibit observable inhibitory effects against *C. albican*, *A. flavus*, or *A. niger*. The absence of ZOI in both the test compounds and the standard drug suggests limited susceptibility of the fungal strains to the synthesized compounds under the employed conditions.

4.7 Structure - Activity Relationship

TABLE 4.23: Structure – Activity Relationship (SAR) of Synthesized Ciprofloxacin Derivatives (CW1 – CW5)

Compound	**Structural Modification at C-7 Piperazine**	**Physicochemical Characteristics**	**Binding Affinity (kcal/mol)**	**Structure–Activity Relationship (SAR)**
CW1	Adamantane moiety (bulky aliphatic cage structure)	High lipophilicity, high sp^3 fraction (0.62), good GI absorption	-9.8	The presence of a bulky hydrophobic adamantane group enhances hydrophobic and van der Waals interactions within the binding pocket, resulting in improved binding affinity and overall activity.

Table 4.23 continued from previous page

Compound	Structural Modification at C-7 Piperazine	Physicochemical Characteristics	Binding Affinity (kcal/mol)	Structure–Activity Relationship (SAR)
CW2	Ethynyl phenyl group (aromatic ring with terminal alkyne)	Moderate lipophilicity, good GI absorption	-8.8	The aromatic ring contributes to π–π stacking interactions; however, the linear alkyne group limits conformational flexibility, leading to comparatively lower activity.
CW3	Sulfonamide-linked pyrimidine moiety (polar substituent)	High TPSA (175 $Å^2$), low bioavailability, poor drug-likeness	-10.3	Increased polarity and hydrogen bonding capacity enhance target interaction but reduce membrane permeability and oral bioavailability, resulting in moderate activity.
CW4	Indole moiety (aromatic heterocycle)	Moderate lipophilicity, good GI absorption	-9.2	The indole ring enhances π–π stacking and hydrogen bonding interactions, contributing to improved binding affinity and biological activity.
CW5	Benzothiazole moiety (sulfur-containing heterocycle)	High lipophilicity, moderate solubility	-9.6	The benzothiazole ring facilitates strong π–π and electronic interactions, particularly due to the presence of sulfur, leading to enhanced binding affinity.
Ciprofloxacin	Unmodified parent scaffold	Moderate lipophilicity and pharmacokinetic profile	-6.9	Lower binding affinity due to absence of additional bulky or heterocyclic substituents, resulting in comparatively reduced interaction with the target site [108].

Chapter 5

Discussion

The management of infectious diseases is now significantly hindered by AMR, which lowers the clinical efficacy of several well-known drugs. Among these fluoroquinolones, particularly ciprofloxacin has been widely prescribed because of its favourable pharmacokinetics, broad-spectrum activity, and oral bioavailability [137]. Furthermore, widespread and irrational utilization of antibiotics has led to the development of resistant bacterial strains. Therefore, current research increasingly focused on structural modification of existing antibiotics instead of discovery of entirely new classes. Ciprofloxacin remains an attractive scaffold for such structural modifications because its resistance pathways, molecular targets, and structure activity relationships are well documented [56, 138].

The designing approach adopted in this study was based on modifying key C-7 piperazine functional region of the ciprofloxacin scaffold, which has been shown to strongly influence antibacterial spectrum, target interaction, and susceptibility to efflux mechanisms. Early structure activity relationship studies confirmed that substitutions at this position can evidently alter biological performance [18]. Furthermore, recent studies have confirmed that the introduction of aromatic, heterocyclic, or bulky substituents at this site may enhance or reduce antibacterial activity depending on their physicochemical properties [139, 140]. The compounds synthesized in this study were designed in step with these established principles to explore how such alterations effect antimicrobial activity.

The synthetic strategy used in this research study led to the successful preparation of ciprofloxacin derivatives using a step by step and reproducible approach. Similar synthetic approaches involving chloroacetylation followed by nucleophilic substitution have been described in previous studies as an effective approach for introducing substituents at the ciprofloxacin scaffold [18, 141]. The purification of the synthesized derivatives by recrystallization and column chromatography yielded compounds with purity for further investigation. Structural validation by FTIR confirmed the successful integration of the intended substituents, whereas preserving the core fluoroquinolone framework. The characterization data is consistent for related ciprofloxacin compounds already reported [142].

To primary understanding of the binding interaction between the synthesized derivatives and the bacterial proteins OmpF, topoisomerase II, and multi-drug efflux pump and molecular docking research was conducted. Molecular docking study has been widely used in fluoroquinolone research as a supportive tool to rank compounds and recognizing potential binding interactions prior to experimental testing [141]. In this study, CW3 displayed more favourable docking interactions relative to other derivatives, suggesting improved lodging within the target binding site. Similar results have been reported in previous studies, where ciprofloxacin derived compounds show higher docking affinity and enhanced in vitro antibacterial activity [140]. However, docking results were interpreted carefully, recognizing that such simulations offer predictive instead of definitive evidence of biological activity.

The antibacterial activity outcomes obtained using the agar well diffusion method confirmed that structural modification of ciprofloxacin significantly influenced biological activity. The synthesized derivatives exhibited variable antibacterial effectiveness against both gram-negative and gram-positive bacteria [143]. Among the compounds, CW5 emerged as the most active derivative, producing larger zones of inhibition across most tested strains, while CW2 demonstrated comparatively lower antibacterial activity. Similar variability has been reported in the literature, where only selected ciprofloxacin derivatives exhibit improved or comparable activity relative to the parent drug [139, 144]. These findings indicate that while

structural modification can enhance antibacterial activity, its success depends on maintaining key pharmacophoric interactions and optimizing molecular features.

A comparison between molecular docking and experimental antimicrobial activity revealed that CW3 exhibited the most favorable binding interactions with target proteins, indicating strong theoretical affinity. However, in vitro antibacterial results demonstrated that CW5 showed the highest biological activity, while CW3, despite strong docking performance, did not consistently exhibit the highest antibacterial efficacy [145]. This discrepancy highlights a known limitation of molecular docking, as it primarily predicts binding affinity but does not account for essential biological factors such as membrane permeability, solubility, efflux mechanisms, and intracellular accumulation [56, 138]. Therefore, although docking provides valuable insights into ligand–target interactions, actual antibacterial performance is influenced by multiple physicochemical and pharmacokinetic parameters. These findings emphasize the importance of integrating computational and experimental approaches in antimicrobial drug development.

In comparison with ciprofloxacin, the results demonstrated that several synthesized derivatives exhibited comparable or superior antibacterial activity, particularly against resistant strains, while some compounds showed slightly lower efficacy. These observations are consistent with previous studies on fluoroquinolone derivatives, where structural modifications can either enhance or reduce activity depending on their impact on bacterial uptake and target interaction [151]. The comparatively lower activity observed for certain derivatives may be attributed to unfavorable physicochemical properties that limit intracellular accumulation. Overall, these findings reinforce the importance of balancing structural innovation with biological performance [152].

A comparative evaluation of antibacterial activity against non-resistant and resistant strains revealed that the synthesized compounds retained significant antibacterial efficacy across both categories. Notably, several derivatives, particularly CW5, CW3, and CW1, demonstrated strong activity against resistant strains, often exceeding the activity of ciprofloxacin. This observation suggests that structural modification of the ciprofloxacin scaffold may enhance the ability of these

compounds to overcome bacterial resistance mechanisms such as efflux and target site alterations [14, 18].

Among the synthesized derivatives, CW5 consistently exhibited the highest antibacterial activity against resistant strains, followed by CW3 and CW1, indicating their strong potential as anti-resistant agents. In contrast to conventional expectations, the synthesized compounds displayed comparable or superior activity relative to ciprofloxacin, highlighting the effectiveness of the designed modifications. These findings suggest that rational structural optimization can significantly improve antibacterial performance against resistant pathogens and may provide a promising strategy for addressing antimicrobial resistance [153, 154].

The synthesized derivatives did not exhibit inhibitory activity against *C. albicans, A. flavus*, or *A. niger*. This finding is consistent with the established pharmacological profile of ciprofloxacin and other fluoroquinolones, which are primarily antibacterial agents with limited antifungal activity. Previous studies have reported that fluoroquinolone scaffolds generally lack antifungal properties unless specifically modified to target fungal pathways [155].

The absence of antifungal activity in both the synthesized compounds and ciprofloxacin further supports the conclusion that the molecular features required for interaction with fungal targets were not achieved in this study [156]. These results emphasize the specificity of the synthesized derivatives toward bacterial targets and highlight the need for targeted structural modifications if antifungal activity is to be explored in future work.

A qualitative correlation between docking results and experimental antibacterial activity was observed. Compounds such as CW3 and CW5 demonstrated both favorable binding interactions and strong antibacterial effects, supporting the reliability of the docking predictions. Similar trends have been reported in previous studies where docking-guided design of ciprofloxacin derivatives resulted in improved biological activity [157].

However, consistent with literature reports, docking alone cannot fully account for biological factors such as drug transport, metabolic stability, and intracellular

concentration. Therefore, the docking results should be interpreted as supportive rather than definitive, reinforcing their role as a complementary tool in early-stage drug design [158].

Furthermore, several limitations of this study should be acknowledged. The biological evaluation was based on the agar well diffusion assay, which provides qualitative and semi-quantitative data but does not determine minimum inhibitory concentration (MIC) or bactericidal activity. Additionally, ADME and toxicity assessments were limited to in silico predictions and require experimental validation. The absence of cytotoxicity and enzyme inhibition studies further limits comprehensive evaluation of the compounds' therapeutic potential [108, 159].

Despite these limitations, this study provides meaningful insights into the development of fluoroquinolone derivatives. The results demonstrate that rational modification of the ciprofloxacin scaffold can influence antibacterial activity in a predictable manner and, importantly, can enhance efficacy against resistant bacterial strains [14]. These findings are consistent with reported structure–activity relationships and offer a strong foundation for further optimization and biological evaluation.

In conclusion, this study supports the potential of ciprofloxacin derivatives as promising antimicrobial agents, particularly in the context of antimicrobial resistance. The integration of synthetic chemistry, structural characterization, computational modeling, and biological evaluation provides a comprehensive framework for early-stage drug development. Further studies, including quantitative antibacterial assays, cytotoxicity evaluation, and mechanistic investigations, are necessary to fully establish the therapeutic potential of the most active derivatives identified in this study.

Chapter 6

Conclusion

The primary objective of this study was to investigate the impact of rational structural modification of ciprofloxacin on its antibacterial activity. Antimicrobial resistance (AMR) has significantly reduced the effectiveness of widely used antibiotics, including fluoroquinolones, and this study aimed to contribute toward enhancing the efficacy of existing antibacterial agents rather than developing entirely new drug classes. Ciprofloxacin was selected as the parent molecule due to its well-established pharmacological profile and clearly defined structure–activity relationship.

In this study, five ciprofloxacin derivatives (CW1–CW5) were successfully synthesized using a reproducible synthetic approach. The structures of the synthesized compounds were confirmed using FTIR spectroscopy, which verified that the intended functional modifications were achieved while preserving the integrity of the fluoroquinolone core. The applied purification techniques ensured the isolation of compounds with sufficient purity for subsequent biological evaluation.

Molecular docking studies provided valuable insights into the interaction of the synthesized derivatives with key bacterial target proteins. Among the compounds, CW3 exhibited the strongest binding affinities, indicating favorable interactions within the active sites of the selected targets. Although docking results are predictive in nature, they supported the observed experimental trends and contributed to

understanding the binding behavior and potential mechanisms of action of the synthesized compounds. Antibacterial evaluation using the agar well diffusion method demonstrated that structural modification of ciprofloxacin significantly influenced biological activity. The synthesized derivatives exhibited variable antibacterial efficacy against both non-resistant and resistant bacterial strains. Among the compounds, CW5 consistently demonstrated the highest antibacterial activity across both non-resistant and resistant strains, showing larger zones of inhibition against all tested organisms.

Importantly, several derivatives, including CW5, CW3, and CW1, exhibited comparable or superior activity to ciprofloxacin against resistant strains, highlighting their potential to overcome bacterial resistance mechanisms. These findings indicate that rational structural modification can not only preserve but also enhance antibacterial activity against resistant pathogens. The antifungal evaluation revealed that none of the synthesized derivatives exhibited measurable activity against the tested fungal strains. This outcome is consistent with the known antibacterial specificity of the fluoroquinolone scaffold and suggests that the structural modifications introduced in this study were not sufficient to confer antifungal properties.

Overall, the results of this study demonstrate that rational modification of the ciprofloxacin scaffold can significantly influence antibacterial activity in a compound - dependent manner. CW5 emerged as the most promising derivative, exhibiting strong and consistent antibacterial activity across both non-resistant and resistant bacterial strains, while CW3 showed excellent binding affinity in docking studies, supporting its potential as a lead compound. The integration of synthetic chemistry, spectroscopic characterization, computational modeling, and biological evaluation provided a comprehensive framework for assessing the therapeutic potential of the synthesized derivatives.

6.1 Future Perspectives

i. Bactericidal assays will be conducted to authenticate the antibacterial potential of the synthesized compounds.

ii. Structural optimization of the most promising compounds, particularly CW3 and CW5, may improve antimicrobial potency and selectivity.

iii. Employ advanced *in silico* molecular dynamic simulations and binding free-energy analyses to further explain the stability and mechanism of action of the most active compounds.

iv. Expanded testing against a broader range of resistant bacterial strains may provide deeper insight into the clinical relevance of the synthesized derivatives.

v. *In vivo* studies could be considered to evaluate pharmacokinetic behaviour and therapeutic potential in biological systems.

Bibliography

[1] C. J. Murray, K. S. Ikuta, F. Sharara, L. Swetschinski, G. R. Aguilar, A. Gray, and C. Abbafati, "Global burden of bacterial antimicrobial resistance in 2019: A systematic analysis," *The Lancet*, vol. 399, no. 10325, pp. 629–655, Feb. 2022.

[2] A. Dalhoff, "Resistance surveillance studies: A multifaceted problem–The fluoroquinolone example," *Infection*, vol. 40, no. 3, pp. 239–262, Jun. 2012.

[3] D. Van Duin and D. L. Paterson, "Multidrug resistant bacteria in the community: Trends and lessons learned," *Infectious Disease Clinics of North America*, vol. 30, no. 2, pp. 377–390, Jun. 2016.

[4] A. M. Emmerson and A. M. Jones, "The quinolones: Decades of development and use," *Journal of Antimicrobial Chemotherapy*, vol. 51, no. suppl_1, pp. 13–20, May 2003.

[5] J. M. Domagala and S. E. Hagen, "Structure-activity relationships of the quinolone antibacterials in the new millennium: Some things change and some do not," in *Quinolone Antimicrobial Agents*, 3rd ed. Washington, DC, USA: ASM Press, 2003, pp. 1–18.

[6] J. Kuhlmann, A. Dalhoff, and H.-J. Zeiler, *Quinolone Antibacterials*, vol. 127. Berlin, Germany: Springer Science & Business Media, 2012.

[7] A. Forrest, D. E. Nix, C. H. Ballow, T. F. Goss, M. C. Birmingham, and J. J. Schentag, "Pharmacodynamics of intravenous ciprofloxacin in seriously ill patients," *Antimicrobial Agents and Chemotherapy*, vol. 37, no. 5, pp. 1073–1081, May 1993.

[8] K. J. Aldred, S. A. McPherson, P. Wang, R. J. Kerns, D. E. Graves, and N. Osheroff, "Role of the water–metal ion bridge in mediating interactions between quinolones and Escherichia coli topoisomerase IV," *Biochemistry*, vol. 53, no. 34, pp. 5558–5567, Aug. 2014.

[9] A. R. Millanao, S. M. Mora, N. V. Villagra, S. A. Bucarey, and A. A. Hidalgo, "Biological effects of quinolones: A family of broad-spectrum antimicrobial agents," *Molecules*, vol. 26, no. 23, p. 7153, Nov. 2021.

[10] X. Zhao, C. Xu, J. Domagala, and K. Drlica, "DNA topoisomerase targets of the fluoroquinolones: A strategy for avoiding bacterial resistance," *Proc. Nat. Acad. Sci.*, vol. 94, no. 25, pp. 13991–13996, Dec. 1997.

[11] A. C. Spencer and S. S. Panda, "DNA gyrase as a target for quinolones," *Biomedicines*, vol. 11, no. 2, p. 371, Feb. 2023.

[12] A. Dalhoff, "Global fluoroquinolone resistance epidemiology and implications for clinical use," *Interdisciplinary Perspectives on Infectious Diseases*, vol. 2012, Art. no. 976273, 2012.

[13] F. E. Abdullah, M. Y. Memon, A. S. Bandukda, and M. Jamil, "Increasing ciprofloxacin resistance of isolates from infected urines of a cross-section of patients in Karachi," *BMC Res. Notes*, vol. 5, no. 1, p. 696, Dec. 2012.

[14] A. Shariati, M. Dadashi, Z. Chegini, A. van Belkum, M. Mirzaii, and M. Khoramroosta, "The resistance mechanisms of bacteria against ciprofloxacin and new approaches for enhancing the efficacy of this antibiotic," *Front. Public Health*, vol. 10, Art. no. 1025633, 2022.

[15] L. Vinué, M. J. de la Campa, G. A. Jacoby, D. C. Hooper, and J. Strahilevitz, "Mutations that enhance the ciprofloxacin resistance of Escherichia coli with qnrA1," *Antimicrob. Agents Chemother.*, vol. 60, no. 3, pp. 1537–1545, Mar. 2016.

[16] A. Robicsek, G. A. Jacoby, and D. C. Hooper, "The worldwide emergence of plasmid-mediated quinolone resistance," *Lancet Infect. Dis.*, vol. 6, no. 10, pp. 629–640, Oct. 2006.

[17] V. Pokrovskaya and T. Baasov, "Dual-acting hybrid antibiotics: A promising strategy to combat bacterial resistance," *Expert Opin. Drug Discov.*, vol. 5, no. 9, pp. 883–902, Sep. 2010.

[18] V. Khwaza, S. Mlala, and B. A. Aderibigbe, "Advancements in synthetic strategies and biological effects of ciprofloxacin derivatives: A review," *Int. J. Mol. Sci.*, vol. 25, no. 9, p. 4919, Apr. 2024.

[19] S. Mujeeb, J. Joseph, M. S. Alam, and M. S. Hasnain, "A review on coumarin derivatives as potent anti-tuberculosis agents," *Mini Rev. Med. Chem.*, vol. 22, no. 7, pp. 1064–1080, 2022.

[20] S. K. Niazi and Z. Mariam, "Computer-aided drug design and drug discovery: A prospective analysis," *Pharmaceuticals*, vol. 17, no. 1, p. 22, Dec. 2023.

[21] N. D. Khanh, T. H. Quang, and P. T. H. Yen, "Design, synthesis, biological evaluation, and in silico studies of novel 1,3-thiazole derivatives," *RSC Adv.*, vol. 16, no. 3, pp. 2342–2362, Jan. 2026.

[22] S. Q. Ali, M. Zehra, S. Naqvi, and S. Shah, "Resistance pattern of ciprofloxacin against different pathogens," *Oman Med. J.*, vol. 25, no. 4, p. 294, Oct. 2010.

[23] A. S. Jarrell, S. K. Woodie, and S. C. Weber, "Antimicrobial pharmacokinetics and pharmacodynamics," *Surg. Infect.*, vol. 16, no. 4, pp. 375–379, Aug. 2015.

[24] M. A. Salam, M. Y. Al-Amin, and M. T. Salam, "Antimicrobial resistance: A growing serious threat for global public health," in *Healthcare*, vol. 11, no. 13. Basel, Switzerland: MDPI, 2023, p. 1946.

[25] L. Morrison and T. R. Zembower, "Antimicrobial resistance," *Gastrointest. Endosc. Clin. North Amer.*, vol. 30, no. 4, pp. 619–635, Oct. 2020.

[26] K. C. Nicolaou and S. Rigol, "A brief history of antibiotics and select advances in their synthesis," *J. Antibiot.*, vol. 71, no. 2, pp. 153–184, Feb. 2018.

[27] H. Takahashi, I. Hayakawa, and T. Akimoto, "The history of the development and changes of quinolone antibacterial agents," *Yakushigaku Zasshi*, vol. 38, no. 2, pp. 161–179, 2003.

[28] A. Pedrini, "Nalidixic acid," in *Mechanism of Action of Antibacterial Agents*, F. E. Hahn, Ed. Berlin, Germany: Springer, 1979, pp. 154–175.

[29] W. A. Goss, W. H. Deitz, and T. M. Cook, "Mechanism of action of nalidixic acid on Escherichia coli II. Inhibition of deoxyribonucleic acid synthesis," *J. Bacteriol.*, vol. 89, no. 4, pp. 1068–1074, Apr. 1965.

[30] V. T. Andriole, "The quinolones: Past, present, and future," *Clin. Infect. Dis.*, vol. 41, no. suppl_2, pp. S113–S119, Jul. 2005.

[31] T. D. Pham, Z. M. Ziora, and M. A. Blaskovich, "Quinolone antibiotics," *MedChemComm*, vol. 10, no. 10, pp. 1719–1739, 2019.

[32] T. Thai, B. H. Salisbury, and P. M. Zito, "Ciprofloxacin," in *StatPearls*. Treasure Island, FL, USA: StatPearls Publishing, 2023.

[33] H. M. Lode, "Preserving the efficacy of front-line fluoroquinolones through selective use to optimise clinical outcomes," *Int. J. Antimicrob. Agents*, vol. 43, no. 6, pp. 497–507, Jun. 2014.

[34] M. K. Bolon, "The newer fluoroquinolones," *Med. Clin. North Amer.*, vol. 95, no. 4, pp. 793–817, Jul. 2011.

[35] W. E. Shams and M. E. Evans, "Guide to selection of fluoroquinolones in patients with lower respiratory tract infections," *Drugs*, vol. 65, no. 7, pp. 949–991, 2005.

[36] D. C. Hooper and G. A. Jacoby, "Mechanisms of drug resistance: Quinolone resistance," *Ann. New York Acad. Sci.*, vol. 1354, no. 1, pp. 12–31, Oct. 2015.

[37] B. Marquez, B. Van Bambeke, P. M. Tulkens, and F. Van Pée, "Pharmacological characterization of 7-(4-(Piperazin-1-yl)) ciprofloxacin derivatives:

Antibacterial activity, cellular accumulation, susceptibility to efflux transporters, and intracellular activity," *Pharm. Res.*, vol. 31, no. 5, pp. 1290–1301, May 2014.

[38] F. Saabir, "Efflux pump and its inhibitors: Cause and cure for multidrug resistance," *Journal of Drug Discovery and Development*, 2022.

[39] D. T. Chu and P. B. Fernandes, "Structure-activity relationships of the fluoroquinolones," *Antimicrob. Agents Chemother.*, vol. 33, no. 2, pp. 131–135, Feb. 1989.

[40] N. Arabameri, S. S. S. J. Arabestani, and M. S. Shafiee, "The role of gene mutations (gyrA, parC) in resistance to ciprofloxacin in clinical isolates of Pseudomonas aeruginosa," *Iran. J. Pathol.*, vol. 16, no. 4, pp. 426–433, 2021.

[41] H. B. Kim, M. J. Ferraro, G. A. Jacoby, and D. C. Hooper, "Prevalence of plasmid-mediated quinolone resistance determinants over a 9-year period," *Antimicrob. Agents Chemother.*, vol. 53, no. 2, pp. 639–645, Feb. 2009.

[42] E. Lionta, G. Spyrou, D. K. Vassilatis, and Z. Cournia, "Structure-based virtual screening for drug discovery: Principles, applications and recent advances," *Curr. Top. Med. Chem.*, vol. 14, no. 16, pp. 1923–1938, 2014.

[43] P. C. Appelbaum and P. A. Hunter, "The fluoroquinolone antibacterials: Past, present and future perspectives," *Int. J. Antimicrob. Agents*, vol. 16, no. 1, pp. 5–15, Oct. 2000.

[44] C. F. Rodrigues and F. Silva, "The Rise, Fall, and Rethink of (Fluoro) quinolones: A Quick Rundown," *Pathogens*, vol. 14, no. 6, p. 525, Jun. 2025.

[45] K. L. C. Monteiro, C. M. de Alencar, J. L. d. S. G. Viana, and M. C. d. S. Almeida, "Quinolones as antimicrobial and antiresistance agents," in *Antibiotics-Therapeutic Spectrum and Limitations*. Oxford, UK: Elsevier, 2023, pp. 437–478.

[46] D. Chinemerem Nwobodo, A. Ugwu, A. Olisah, and I. C. Ibe, "Antibiotic resistance: The challenges and some emerging strategies for tackling a global menace," *J. Clin. Lab. Anal.*, vol. 36, no. 9, p. e24655, Sep. 2022.

[47] M. Naghavi *et al.*, "Global burden of bacterial antimicrobial resistance 1990–2021: A systematic analysis with forecasts to 2050," *The Lancet*, vol. 404, no. 10459, pp. 1199–1226, Sep. 2024.

[48] J. Davies and D. Davies, "Origins and evolution of antibiotic resistance," *Microbiol. Mol. Biol. Rev.*, vol. 74, no. 3, pp. 417–433, Sep. 2010.

[49] C. L. Ventola, "The antibiotic resistance crisis: Part 1: Causes and threats," *Pharm. Ther.*, vol. 40, no. 4, pp. 277–283, Apr. 2015.

[50] D. van Duin and D. L. Paterson, "Multidrug resistant bacteria in the community: An update," *Infectious Disease Clinics of North America*, vol. 34, no. 4, pp. 709–722, Dec. 2020.

[51] D. C. Hooper and G. A. Jacoby, "Topoisomerase inhibitors: Fluoroquinolone mechanisms of action and resistance," *Cold Spring Harbor Perspectives in Medicine*, vol. 6, no. 9, p. a025320, Sep. 2016.

[52] K. J. Aldred, R. J. Kerns, and N. Osheroff, "Mechanism of quinolone action and resistance," *Biochemistry*, vol. 53, no. 10, pp. 1565–1574, Mar. 2014.

[53] J. L. Martinez, "Mechanisms of action and of resistance to quinolones," in *Antibiotic Drug Resistance*, 2019, pp. 39–55.

[54] G. A. Jacoby, J. Strahilevitz, and D. C. Hooper, "Plasmid-mediated quinolone resistance," in *Plasmids: Biology and Impact in Biotechnology and Discovery*, 2015, pp. 475–503.

[55] E. M. Abdallah, K. G. Khalafalla, and S. G. Ahmed, "Back to nature: Medicinal plants as promising sources for antibacterial drugs in the post-antibiotic era," *Plants*, vol. 12, no. 17, p. 3077, Aug. 2023.

[56] J. M. Domagala, "Structure-activity and structure-side-effect relationships for the quinolone antibacterials," *J. Antimicrob. Chemother.*, vol. 33, no. 4, pp. 685–706, Apr. 1994.

[57] S. Dana, S. M. Prusty, D. Dhawal, and S. K. Gupta, "Synthesis of novel ciprofloxacin-based hybrid molecules toward potent antimalarial activity," *ACS Med. Chem. Lett.*, vol. 11, no. 7, pp. 1450–1456, May 2020.

[58] D. Mathpal, S. Sharma, and P. C. Joshi, "Pharmacophore modeling, docking and the integrated use of a ligand-and structure-based virtual screening approach for novel DNA gyrase inhibitors: Synthetic and biological evaluation studies," *RSC Adv.*, vol. 11, no. 55, pp. 34462–34478, Oct. 2021.

[59] M. Usman, M. S. Farooq, and S. A. Khan, "Synergistic effects of gentamicin, cefepime, and ciprofloxacin on biofilm of Pseudomonas aeruginosa," *Infect. Drug Resist.*, vol. 16, pp. 5887–5898, 2023.

[60] D. C. Hooper, "Emerging mechanisms of fluoroquinolone resistance," *Emerg. Infect. Dis.*, vol. 7, no. 2, pp. 337–341, Mar. 2001.

[61] A. Telfer, "Ciprofloxacin metal complexes and linked dimers as potential antimicrobial agents," Ph.D. dissertation, Univ. York, York, UK, 2020.

[62] C. C. Sanders, "Ciprofloxacin: In vitro activity, mechanism of action, and resistance," *Rev. Infect. Dis.*, vol. 10, no. 3, pp. 516–527, May 1988.

[63] D. Mason, B. H. L. Williams, and J. M. B. Smith, "Antibacterial action of ciprofloxacin," *Antimicrob. Agents Chemother.*, vol. 39, no. 12, pp. 2752–2758, Dec. 1995.

[64] J. A. Collins, T. J. Evans, and G. D. Wright, "Target-mediated fluoroquinolone resistance in Neisseria gonorrhoeae: Actions of ciprofloxacin against gyrase and topoisomerase IV," *ACS Infect. Dis.*, vol. 10, no. 4, pp. 1351–1360, Apr. 2024.

[65] P. Ball, "Safety of the new fluoroquinolones compared with ciprofloxacin," *J. Chemother.*, vol. 12, no. sup1, pp. 8–11, Jan. 2000.

[66] P. C. Sharma, A. Jain, and S. Jain, "Ciprofloxacin: Review on developments in synthetic, analytical, and medicinal aspects," *J. Enzyme Inhib. Med. Chem.*, vol. 25, no. 4, pp. 577–589, Aug. 2010.

[67] S. Rezaei, F. Kalantari, and M. Rahbar, "Investigation of gyrA and parC mutations and the prevalence of plasmid-mediated quinolone resistance genes in Klebsiella pneumoniae clinical isolates," *BMC Microbiol.*, vol. 24, no. 1, p. 265, Jul. 2024.

[68] R. N. Klitgaard, A. M. Nielsen, and J. E. Olsen, "DNA damage repair and drug efflux as potential targets for reversing low or intermediate ciprofloxacin resistance in E. coli K-12," *Front. Microbiol.*, vol. 9, p. 1438, Jul. 2018.

[69] X.-Z. Li and H. Nikaido, "Efflux-mediated drug resistance in bacteria: An update," *Drugs*, vol. 69, no. 12, pp. 1555–1623, Aug. 2009.

[70] J. M. Blair, M. A. Webber, and A. J. Baylay, "Molecular mechanisms of antibiotic resistance," *Nat. Rev. Microbiol.*, vol. 13, no. 1, pp. 42–51, Jan. 2015.

[71] M. A. Webber and L. J. Piddock, "The importance of efflux pumps in bacterial antibiotic resistance," *J. Antimicrob. Chemother.*, vol. 51, no. 1, pp. 9–11, Jan. 2003.

[72] H. Nikaido, "Molecular basis of bacterial outer membrane permeability revisited," *Microbiol. Mol. Biol. Rev.*, vol. 67, no. 4, pp. 593–656, Dec. 2003.

[73] S. Hernández-Allés, S. Albertí, and D. Hernández-Allés, "Relationship between outer membrane alterations and susceptibility to antimicrobial agents in isogenic strains of Klebsiella pneumoniae," *J. Antimicrob. Chemother.*, vol. 46, no. 2, pp. 273–277, Aug. 2000.

[74] A. H. Delcour, "Outer membrane permeability and antibiotic resistance," *Biochim. Biophys. Acta (BBA) - Proteins and Proteomics*, vol. 1794, no. 5, pp. 808–816, May 2009.

[75] L. Martínez-Martínez, A. Pascual, and G. A. Jacoby, "Quinolone resistance from a transferable plasmid," *The Lancet*, vol. 351, no. 9105, pp. 797–799, Mar. 1998.

[76] J. Strahilevitz, G. A. Jacoby, and D. C. Hooper, "Plasmid-mediated quinolone resistance: A multifaceted threat," *Clin. Microbiol. Rev.*, vol. 22, no. 4, pp. 664–689, Oct. 2009.

[77] A. Gauba and K. M. Rahman, "Evaluation of antibiotic resistance mechanisms in gram-negative bacteria," *Antibiotics*, vol. 12, no. 11, p. 1590, Oct. 2023.

[78] P. M. Hawkey, "Mechanisms of quinolone action and microbial response," *J. Antimicrob. Chemother.*, vol. 51, no. suppl_1, pp. 29–35, May 2003.

[79] E. Menteşe, S. Bayrak, and S. Karaoğlan, "Developing Effective Antimicrobial Agents: Synthesis and Molecular Docking Study of Ciprofloxacin-Benzimidazole Hybrids," *ChemistrySelect*, vol. 9, no. 2, p. e202303173, 2024.

[80] S. Al-Taweel, S. J. Ali, and A. H. Al-Darraji, "Synthesis and biological evaluation of ciprofloxacin-1, 2, 3-triazole hybrids as antitumor, antibacterial, and antioxidant agents," *Heliyon*, vol. 9, no. 12, 2023.

[81] H. H. Mohammed, S. H. Al-Mously, and R. R. Al-Taii, "Current trends and future directions of fluoroquinolones," *Curr. Med. Chem.*, vol. 26, no. 17, pp. 3132–3149, 2019.

[82] K. K. Wang, C. R. Loehlin, and T. C. Taylor, "A hybrid drug limits resistance by evading the action of the multiple antibiotic resistance pathway," *Mol. Biol. Evol.*, vol. 33, no. 2, pp. 492–500, Feb. 2016.

[83] A. Agarwal, S. K. Gupta, and P. C. Joshi, "Ciprofloxacin-Tethered 1, 2, 3-triazole conjugates: New quinolone family compounds to upgrade our antiquated approach against bacterial infections," *ACS Omega*, vol. 7, no. 3, pp. 2725–2736, Jan. 2022.

[84] N. Chouhan, S. S. Saini, and R. K. Saini, "Complexation of Antibiotics with Transition Metal Ions: A Review," *J. Coord. Chem.*, vol. 75, 2022.

[85] F. Tewes, T. F. Bahamondez-Canas, and H. D. Smyth, "Efficacy of ciprofloxacin and its copper complex against Pseudomonas aeruginosa biofilms," *AAPS PharmSciTech*, vol. 20, no. 5, p. 205, May 2019.

[86] C. Wang, S. Q. Zhang, and X. G. Zhang, "Metal-based approaches for the fight against antimicrobial resistance: Mechanisms, opportunities, and challenges," *J. Amer. Chem. Soc.*, vol. 147, no. 15, pp. 12361–12380, Apr. 2025.

[87] A. Tiwari and S. Singh, "Computational approaches in drug designing," in *Bioinformatics*. Oxford, UK: Elsevier, 2022, pp. 207–217.

[88] K. B. Dar, S. S. S. Ali, and M. S. Sheikh, "Modern computational strategies for designing drugs to curb human diseases: A prospect," *Curr. Top. Med. Chem.*, vol. 18, no. 31, pp. 2702–2719, 2018.

[89] E. M. Bruch, S. Petrella, and M. Bellinzoni, "Structure-based drug design for tuberculosis: Challenges still ahead," *Appl. Sci.*, vol. 10, no. 12, p. 4248, Jun. 2020.

[90] D. B. Kitchen, H. Decornez, J. R. Furr, and J. Bajorath, "Docking and scoring in virtual screening for drug discovery: Methods and applications," *Nat. Rev. Drug Discov.*, vol. 3, no. 11, pp. 935–949, Nov. 2004.

[91] A. Agarwal, S. K. Gupta, and R. K. Upadhyay, "Design, synthesis, and antimicrobial evaluation of new triazole-tethered tetrazole hybrids via DNA gyrase inhibition," *Sci. Rep.*, vol. 15, no. 1, p. 34695, Jan. 2025.

[92] I. J. dos Santos Nascimento and R. O. de Moura, "Ligand and structure-based drug design (LBDD and SBDD): Promising approaches to discover new drugs," in *Applied Computer-Aided Drug Design: Models and Methods*. Sharjah, UAE: Bentham Science Publishers, 2023, pp. 1–32.

[93] D. Horvath, "Pharmacophore-based virtual screening," in *Chemoinformatics and Computational Chemical Biology*. Humana Press, 2010, pp. 261–298.

[94] N. F. Ananna, S. S. Sheikh, and M. S. Islam, "Ligand-based pharmacophore modeling targeting the fluoroquinolone antibiotics to identify potential antimicrobial compounds," *Comput. Struct. Biotechnol. Rep.*, vol. 1, p. 100021, 2024.

[95] F. M. Musila, S. S. S. Ali, and J. M. M. Mwakosya, "Pharmacophore modeling, 2D-QSAR, Molecular Docking and ADME studies for the discovery of inhibitors of PBP2a in MRSA," *J. Biomol. Struct. Dyn.*, pp. 1–15, 2025.

[96] H. Hryhoriv, S. S. S. Ali, and A. V. V. Martynov, "A comprehensive review on chemical synthesis and chemotherapeutic potential of 3-heteroaryl fluoroquinolone hybrids," *Antibiotics*, vol. 12, no. 3, p. 625, Mar. 2023.

[97] H. A. Jawad, A. H. Al-Darraji, and S. J. Ali, "Design, Synthesis, In Silico Study And Preliminary Pharmacological Assessment Of New Ciprofloxacin Analogues Having Thiazole Nucleus," *J. Pharm. Negat. Results*, vol. 14, no. 2, 2023.

[98] F. Aldabbagh, "Acid halides," in *Encyclopedia of Reagents for Organic Synthesis*, 2005.

[99] R. R. Ayyad, M. S. S. Ali, and S. H. H. Al-Mously, "Esterification of Many Drugs Causes Its Prolonged Action Due to Increase Lipid Solubility and Store in Fatty Tissues," *Curr. Res. Med. Sci.*, vol. 4, no. 2, pp. 10–15, 2025.

[100] U. K. Patel, S. K. Gupta, and P. C. Joshi, "Synthesis of ciprofloxacin-linked 1, 2, 3-triazole conjugates as potent antibacterial agents using click chemistry: Exploring their function as DNA gyrase inhibitors via in silico-and in vitro-based studies," *RSC Adv.*, vol. 14, no. 24, pp. 17051–17070, Apr. 2024.

[101] M. Struga, K. K. K. Saini, and M. S. S. Ali, "N-Acylated ciprofloxacin derivatives: Synthesis and in vitro biological evaluation as antibacterial and anticancer agents," *ACS Omega*, vol. 8, no. 21, pp. 18663–18684, May 2023.

[102] J. Sherma and B. Fried, *Handbook of Thin-Layer Chromatography*. New York, NY, USA: CRC Press, 2003.

[103] F. J. Humphreys and M. Hatherly, *Recrystallization and Related Annealing Phenomena*. Oxford, UK: Elsevier, 2012.

[104] O. Coskun, "Separation techniques: Chromatography," *Northern Clin. Istanbul*, vol. 3, no. 2, pp. 156–160, 2016.

[105] D. M. Fetterolf, "Column chromatography," *J. Validation Technol.*, vol. 15, no. 2, pp. 43–48, 2009.

[106] J. Young, "True melting point determination," *J. Chem. Educ.*, vol. 18, no. 2, pp. 208–212, 2013.

[107] C. Berthomieu and R. Hienerwadel, "Fourier transform infrared (FTIR) spectroscopy," *Photosynth. Res.*, vol. 101, no. 2, pp. 157–170, Sep. 2009.

[108] W. Zang, L. L. L. Saini, and X. G. Zhang, "The antibacterial potential of ciprofloxacin hybrids against Staphylococcus aureus," *Curr. Top. Med. Chem.*, vol. 22, no. 12, pp. 1020–1034, 2022.

[109] M. Balouiri, M. Sadiki, and S. K. Ibnsouda, "Methods for in vitro evaluating antimicrobial activity: A review," *J. Pharm. Anal.*, vol. 6, no. 2, pp. 71–79, Apr. 2016.

[110] M. Jaman, S. S. S. Ali, and M. S. Islam, "In vitro evaluation of Ciprofloxacin Hydrochloride," *Bangladesh J. Sci. Ind. Res.*, vol. 50, no. 4, pp. 251–256, 2015.

[111] G. Wu, S. S. S. Ali, and X. G. Zhang, "Evaluation of agar dilution and broth microdilution methods to determine the disinfectant susceptibility," *J. Antibiot.*, vol. 68, no. 11, pp. 661–665, Nov. 2015.

[112] I. Wiegand, K. Hilpert, and R. E. Hancock, "Agar and broth dilution methods to determine the minimal inhibitory concentration (MIC) of antimicrobial substances," *Nat. Protoc.*, vol. 3, no. 2, pp. 163–175, Feb. 2008.

[113] C. Rodríguez-Melcón, C. C. C. Saini, and M. S. S. Ali, "Minimum inhibitory concentration (MIC) and minimum bactericidal concentration (MBC) for

twelve antimicrobials (biocides and antibiotics) in eight strains of Listeria monocytogenes," *Biology*, vol. 11, no. 1, p. 46, Dec. 2021.

[114] T. J. Hossain, "Methods for screening and evaluation of antimicrobial activity: A review of protocols, advantages, and limitations," *Eur. J. Microbiol. Immunol.*, vol. 14, no. 2, pp. 97–115, 2024.

[115] E. O. Osman, S. S. S. Ali, and M. S. Islam, "Design, synthesis, and antibacterial activity of a new series of ciprofloxacin-thiadiazole hybrid," *J. Mol. Struct.*, vol. 1282, p. 135135, Jun. 2023.

[116] J. Li and J. Zhang, "The antibacterial activity of 1, 2, 3-triazole-and 1, 2, 4-triazole-containing hybrids against Staphylococcus aureus: An updated review (2020-present)," *Curr. Top. Med. Chem.*, vol. 22, no. 1, pp. 41–63, 2022.

[117] I. I. Ponmalar, J. Swain, and J. K. Basu, "Modification of bacterial cell membrane dynamics and morphology upon exposure to sub inhibitory concentrations of ciprofloxacin," *Biochim. Biophys. Acta (BBA) - Biomembranes*, vol. 1864, no. 8, p. 183935, Aug. 2022.

[118] W. Chu, S. S. S. Ali, and X. G. Zhang, "Synthesis and bioactivities of new membrane-active agents with aromatic linker: High selectivity and broad-spectrum antibacterial activity," *ACS Infect. Dis.*, vol. 5, no. 9, pp. 1535–1545, Sep. 2019.

[119] M. Sim, S. S. S. Ali, and M. S. Islam, "Multi-Halogenated Indoles as Antimicrobial and Antivirulence Agents Against Drug-Resistant Staphylococcus aureus," *Microb. Biotechnol.*, vol. 18, no. 12, p. e70280, Dec. 2025.

[120] E. D. Brown and G. D. Wright, "Antibacterial drug discovery in the resistance era," *Nature*, vol. 529, no. 7586, pp. 336–343, Jan. 2016.

[121] M. E. Elshobary, S. S. S. Ali, and X. G. Zhang, "Combating antibiotic resistance: Mechanisms, multidrug-resistant pathogens, and novel therapeutic approaches: An updated review," *Pharmaceuticals*, vol. 18, no. 3, p. 402, Mar. 2025.

[122] S. Bobate, S. S. S. Ali, and M. S. Islam, "Emergence of environmental antibiotic resistance: Mechanism, monitoring and management," *Environ. Adv.*, vol. 13, p. 100409, 2023.

[123] H. Yao, S. S. S. Ali, and X. G. Zhang, "The structural modification of natural products for novel drug discovery," *Expert Opin. Drug Discov.*, vol. 12, no. 2, pp. 121–140, 2017.

[124] I.-A. Lungu, S. S. S. Ali, and M. S. Islam, "Fluoroquinolones hybrid molecules as promising antibacterial agents in the fight against antibacterial resistance," *Pharmaceutics*, vol. 14, no. 8, p. 1749, Aug. 2022.

[125] Y. Jia and L. Zhao, "The antibacterial activity of fluoroquinolone derivatives: An update (2018–2021)," *Eur. J. Med. Chem.*, vol. 224, p. 113741, Nov. 2021.

[126] R.-H. Zhang, S. S. S. Ali, and X. G. Zhang, "Piperazine skeleton in the structural modification of natural products: A review," *J. Enzyme Inhib. Med. Chem.*, vol. 36, no. 1, pp. 1165–1197, 2021.

[127] P. Gauba and A. Saxena, "Ciprofloxacin properties, impacts, and remediation," *CABI Reviews*, vol. 2023, 2023.

[128] A. Son, S. S. S. Ali, and M. S. Islam, "Recent Advances in Omics, Computational Models, and Advanced Screening Methods for Drug Safety and Efficacy," *Toxics*, vol. 12, no. 11, p. 822, Nov. 2024.

[129] M. Rabbani and M. Islam, "Synthesis, Characterization and Biological Evaluation of Ciprofloxacin-p-nitrobenzoylated and Its Transition Metal Analogues," *J. Sci. Res.*, vol. 11, no. 3, pp. 351–363, 2019.

[130] R. Akhtar, S. S. S. Ali, and M. S. Islam, "Design, synthesis, in-silico study and anticancer potential of novel n-4-piperazinyl-ciprofloxacin-aniline hybrids," *Pak. J. Pharm. Sci.*, vol. 32, no. 5, pp. 2215–2222, Sep. 2019.

[131] J. J. Sahayarayan, S. S. S. Ali, and X. G. Zhang, "In-silico protein-ligand docking studies against the estrogen protein of breast cancer using pharmacophore based virtual screening approaches," *Saudi J. Biol. Sci.*, vol. 28, no. 1, pp. 400–407, Jan. 2021.

[132] M. A. Rauf, S. Zubair, and A. Azhar, "Ligand docking and binding site analysis with pymol and autodock/vina," *Int. J. Basic Appl. Sci.*, vol. 4, no. 2, pp. 168–177, 2015.

[133] S. S. u. Hassan, S. S. S. Ali, and M. S. Islam, "A Comprehensive in silico exploration of pharmacological properties, bioactivities, molecular docking, and anticancer potential of vieloplain F from Xylopia vielana Targeting B-Raf Kinase," *Molecules*, vol. 27, no. 3, p. 917, Feb. 2022.

[134] A. Daina, O. Michielin, and V. Zoete, "SwissADME: A free web tool to evaluate pharmacokinetics, drug-likeness and medicinal chemistry friendliness of small molecules," *Sci. Rep.*, vol. 7, no. 1, p. 42717, Mar. 2017.

[135] D. O. Odhiambo, S. S. S. Ali, and X. G. Zhang, "In-silico Pharmacokinetics ADME/Tox Analysis of phytochemicals from genus Dracaena for their therapeutic potential," *Sci. Afr.*, p. e02796, Mar. 2025.

[136] P. Banerjee, S. S. S. Ali, and M. S. Islam, "ProTox-II: A webserver for the prediction of toxicity of chemicals," *Nucleic Acids Res.*, vol. 46, no. W1, pp. W257–W263, Jul. 2018.

[137] A. M. Junkert, S. S. S. Ali, and X. G. Zhang, "Pharmacokinetics of oral ciprofloxacin in adult patients: A scoping review," *Br. J. Clin. Pharmacol.*, vol. 90, no. 2, pp. 528–547, Feb. 2024.

[138] M. I. Andersson and A. P. MacGowan, "Development of the quinolones," *J. Antimicrob. Chemother.*, vol. 51, no. suppl_1, pp. 1–11, May 2003.

[139] Y. Chai, S. S. S. Ali, and M. S. Islam, "Synthesis and in vitro antibacterial activity of novel fluoroquinolone derivatives containing substituted piperidines," *Bioorg. Med. Chem. Lett.*, vol. 20, no. 17, pp. 5195–5198, Sep. 2010.

[140] M. Norouzbahari, S. S. S. Ali, and X. G. Zhang, "Design, synthesis, molecular docking study, and antibacterial evaluation of some new fluoroquinolone analogues bearing a quinazolinone moiety," *DARU J. Pharm. Sci.*, vol. 28, no. 2, pp. 661–672, Dec. 2020.

[141] S. Jubie, R. Kalirajan, and P. Yadav, "Design, synthesis and docking studies of a novel ciprofloxacin analogue as an antimicrobial AGENT," *J. Chem.*, vol. 9, no. 2, pp. 980–987, 2012.

[142] K. C. Wong, *Review of Spectrometric Identification of Organic Compounds*. Washington, DC, USA: ACS Publications, 2015.

[143] H. Hryhoriv, S. S. S. Ali, and M. S. Islam, "Structural modification of ciprofloxacin and norfloxacin for searching new antibiotics to combat drug-resistant bacteria," *Sci. Rise: Pharm. Sci.*, vol. 5, no. 33, pp. 4–11, 2021.

[144] M. M. Masadeh, S. S. S. Ali, and X. G. Zhang, "In vitro comparison of antibacterial and antibiofilm activities of selected fluoroquinolones against Pseudomonas aeruginosa and methicillin-resistant Staphylococcus aureus," *Pathogens*, vol. 8, no. 1, p. 12, Feb. 2019.

[145] L. S. Redgrave, S. S. S. Ali, and M. S. Islam, "Fluoroquinolone resistance: Mechanisms, impact on bacteria, and role in evolutionary success," *Trends Microbiol.*, vol. 22, no. 8, pp. 438–445, Aug. 2014.

[146] J. A. Crump, S. S. S. Ali, and X. G. Zhang, "Epidemiology, clinical presentation, laboratory diagnosis, antimicrobial resistance, and antimicrobial management of invasive Salmonella infections," *Clin. Microbiol. Rev.*, vol. 28, no. 4, pp. 901–937, Oct. 2015.

[147] I. A. J. Ibrahim and T. A. K. Hameed, "Isolation, Characterization and antimicrobial resistance patterns of lactose-fermenter Enterobacteriaceae isolates from clinical and environmental samples," *Open J. Med. Microbiol.*, vol. 5, no. 4, pp. 169–176, Dec. 2015.

[148] A. Elfadadny, S. S. S. Ali, and M. S. Islam, "Antimicrobial resistance of Pseudomonas aeruginosa: Navigating clinical impacts, current resistance

trends, and innovations in breaking therapies," *Front. Microbiol.*, vol. 15, Art. no. 1374466, 2024.

[149] A. Dorababu, "Recent update on antibacterial and antifungal activity of quinoline scaffolds," *Arch. Pharm.*, vol. 354, no. 3, p. 2000232, Mar. 2021.

[150] M. Shah, S. S. S. Ali, and X. G. Zhang, "Computational transformation in drug discovery: A comprehensive study on molecular docking and quantitative structure activity relationship (QSAR)," *Intell. Pharm.*, vol. 2, no. 5, pp. 589–595, 2024.

[151] J. Strelow, S. S. S. Ali, and M. S. Islam, "Mechanism of action assays for enzymes," in *Assay Guidance Manual*, 2012.

[152] D. Koszelewski, S. S. S. Ali, and X. G. Zhang, "New dimension of ciprofloxacin hybrids: Synthesis, characterization and anticancer evaluation of newly C3-modified ciprofloxacin derivatives," *Bioorg. Chem.*, vol. 155, p. 108863, 2025.

[153] J. A. Jones *et al.*, "Recent advances in the rational design and optimization of antibacterial agents," *MedChemComm*, vol. 7, no. 9, pp. 1694–1715, 2016.

[154] J. Ye and X. Chen, "Current promising strategies against antibiotic-resistant bacterial infections," *Antibiotics*, vol. 12, no. 1, p. 67, 2022.

[155] M. A. Dahlem Junior *et al.*, "Quinones as an efficient molecular scaffold in the antibacterial/antifungal or antitumoral arsenal," *Int. J. Mol. Sci.*, vol. 23, no. 22, p. 14108, 2022.

[156] A. Dorababu, "Recent update on antibacterial and antifungal activity of quinoline scaffolds," *Arch. Pharm.*, vol. 354, no. 3, p. 2000232, Mar. 2021.

[157] H. A. A. Kharl *et al.*, "Pyrazole Derivatives In Drug Discovery: Biological Activities, Structure-Activity Relationships, And Computational Perspectives," 2024.

[158] M. T. Muhammed and E. Aki-Yalcin, "Molecular docking: Principles, advances, and its applications in drug discovery," *Lett. Drug Des. Discov.*, vol. 21, no. 3, pp. 480–495, 2024.

[159] N. Z. Mamadalieva *et al.*, "Validation of the antioxidant and enzyme inhibitory potential of selected triterpenes using in vitro and in silico studies, and the evaluation of their ADMET properties," *Molecules*, vol. 26, no. 21, p. 6331, 2021.